Preprint *July 31, 1996*

Energy Levels of Light Nuclei
$A = 20$

D.R. Tilley[a,b], C.M. Cheves[a,c], J.F. Guillemette[a,c],
S. Raman[d] and H.R. Weller[a,c]

[a] *Triangle Universities Nuclear Laboratory, Durham, NC 27708-0308*
[b] *Department of Physics, North Carolina State University, Raleigh, NC 27695-8202*
[c] *Department of Physics, Duke University, Durham, NC 27708-0305*
[d] *Oak Ridge National Laboratory, Oak Ridge, TN 37831*

Abstract: This is a preliminary version the $A = 20$ evaluation which we plan to submit to Nuclear Physics in the fall of 1996. Your comments on this draft will be greatly appreciated.

(References closed September 15, 1995)

This work is supported by the US Department of Energy, Office of High Energy and Nuclear Physics, under: Contract No. DEFG05-88-ER40441 (North Carolina State University); Contract No. DEFG05-91-ER40619 (Duke University).

^{20}n, ^{20}He, ^{20}Li, ^{20}Be

(Not observed)

See (77CE1A, 83ANZQ, 86AN07, 87SI1E).

^{20}B

(Not observed)

The mass excess of ^{20}B is predicted to be 69.08 MeV (74TH01). ^{20}B is then unstable with respect to breakup into $^{19}\mathrm{B} + \mathrm{n}$ by 0.9 MeV: see ^{19}B in (95TI1C) and (78AJ03, 83ANZQ) and see the work on effective interactions for the (0p1s0d) nuclear shell-model space (92WA22).

^{20}C

(Not illustrated)

^{20}C has been observed in heavy ion projectile fragmentation reactions (87GI05, 90MU06, 91MU19) and in proton-induced target-fragmentation reactions (87VI1D, 88MU08, 92WO1G). The atomic mass excess is 37.560 ± 0.200 MeV (93AU05). It is then stable with respect to $^{19}\mathrm{C} + \mathrm{n}$ and $^{18}\mathrm{C} + 2\mathrm{n}$ by 3.3 and 3.9 MeV, respectively. β-delayed neutron emission has been observed (87GI05, 90MU06, 91MU19).

The half life and neutron emission probability have been measured to be $\tau_{1/2} = 16^{+14}_{-7}$ ms, $P_\mathrm{n} = 50 \pm 30$ (89LE16) and $\tau_{1/2} = 14^{+6}_{-5}$ ms, $P_\mathrm{n} = 72 \pm 14$ (90MU06).

Shell model calculations for exotic light nuclei are described in (88PO1E, 93PO11). Shell model interactions constructed for the 0p1s0d nuclear shell model space are reported in (92WA22). Self-consistent calculations of light nuclei using the density functional method are reported in (90LO11). Microscopic calculations of beta-decay half-lives for $6 \leq Z \leq 108$ neutron-rich nuclei are reported in (90ST08). See also (87SN1A, 93SA16, 94HA39).

^{20}N

(Not illustrated)

^{20}N is particle stable. Its atomic mass excess is 21.770 ± 0.050 MeV (93AU05). It has been observed in heavy-ion transfer (89OR03) and projectile fragmentation reactions (88DU1C, 87GI05, 88MU08, 90MU06, 91OR01) and in target fragmentation reactions (88WO09, 91RE02, 92WO1G). See also the review (88VI1D). Mass

measurements were reported in (89OR03, 87GI05, 91OR01, 88WO09, 92WO1G). Measurements of beta-delayed neutron emission are described in (88DU1C).

The half-life of ^{20}N is 70 ± 40 ms (88DU1C), 100^{+30}_{-20} ms (88MU08, 90MU06), 142 ± 19 ms (91RE02).

The delayed neutron probability is $53^{+11}_{-7}\%$ (88MU08, 90MU06), $66.1 \pm 5.0\%$ (91RE02). See also (87BAZI, 87DE1O, 87DUZU, 87SI1E, 89HU1E, 92RE1I, 93REZX).

A review of the production of nuclei far from stability is presented in (89VO1F). Production mechanisms are discussed in (88BA1J). Predictions of beta-decay half-lives are described in (90ST08). Results of shell model calculations related to exotic light nuclei are discussed in (92WA22, 93PO11). Bulk properties have been calculated with relativistic mean field theory in (93PA14).

^{20}O

(Figs. 20.1 and 20.5)

GENERAL: See Table 20.0.5

1. ^{20}O(β^-)^{20}F $\qquad Q_{\rm m} = 3.814$

^{20}O decays with a half-life of 13.51 ± 0.05 s to the 1^+ states ^{20}F* (1.06, 3.49) with branching ratios (99.973 ± 0.003) and $(0.027 \pm 0.003)\%$, $\log f_0 t = 3.740 \pm 0.006$ and 3.65 ± 0.06, respectively (87AL06). Upper limits for the branching to other states of ^{20}F are shown in Table II of (87AL06). See also (85BR29).

2. ^{18}O(t, p)^{20}O $\qquad Q_{\rm m} = 3.082$

$Q_0 = 3082.4 \pm 1.3$ keV (85AN17). See also (82AN12).

Observed proton groups are displayed in Tables 20.1 and 20.1.2. ^{20}O* (4.07) decays to ^{20}O* (0, 1.67) with branchings of (26 ± 4) and $(74 \pm 4)\%$. The p-γ angular correlations lead to $J = 2$; the strength of the transition favors $\pi = +$, [δ(E2/M1) $= -0.18 \pm 0.08$ for the $2^+ \rightarrow 2^+$ transition.] ^{20}O*(4.46) and ^{20}O*(5.39) decay primarily via ^{20}O*(1.67); the direct ground-state decay is $< 4\%$ for the first and $< 7\%$ for the second of these states. The angular correlations are essentially isotropic, favoring $J^\pi = 0^+$. The transition ^{20}O*(5.39 $\rightarrow$ 4.07) is not observed: the upper limit is 8%. See also (78AJ03, 83AJ01). For a discussion of $A = 20$ isobaric states see (82AN12, 85AN17).

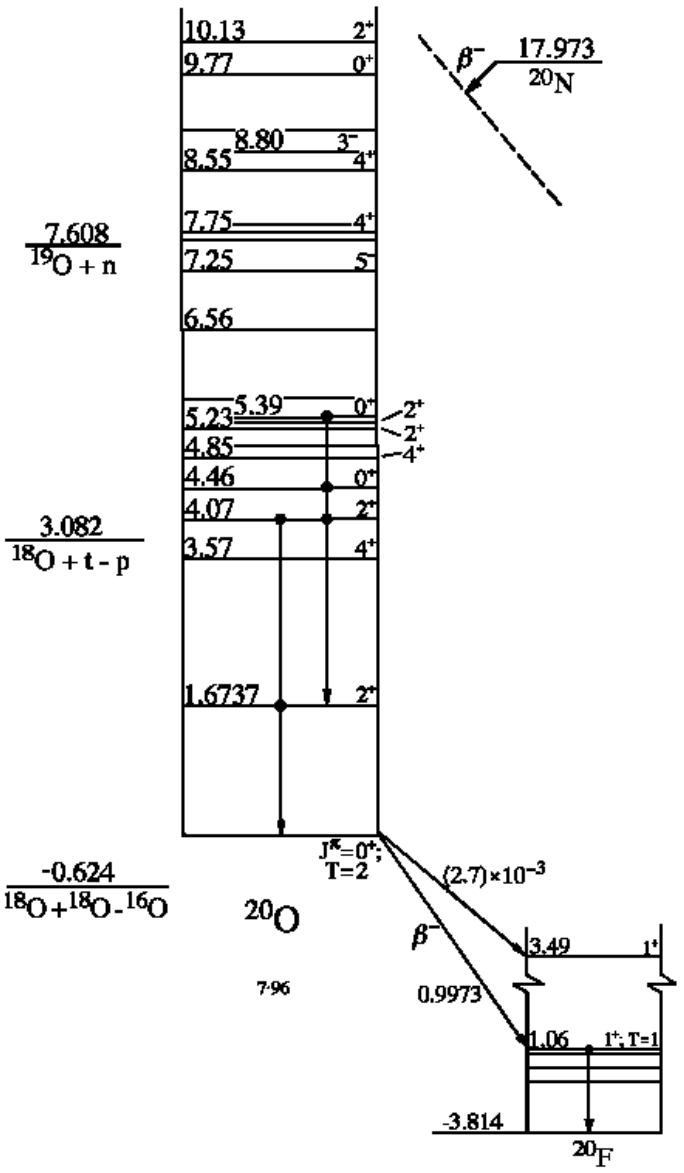

Figure 1: Energy levels of ^{20}O. In these diagrams, energy values are plotted vertically in MeV, based on the ground state as zero. Uncertain levels or transitions are indicated by dashed lines; levels which are known to be particularly broad are cross-hatched. Values of total angular momentum J, parity, and isobaric spin T which appear to be reasonably well established are indicated on the levels; less certain assignments are enclosed in parentheses. For reactions in which ^{20}O is the compound nucleus, some typical thin-target excitation functions are shown schematically, with the yield plotted horizontally and the bombarding energy vertically. Bombarding energies are indicated in laboratory coordinates and plotted to scale in c.m. coordinates. Excited states of the residual nuclei involved in these reactions have generally not been shown; where transitions to such excited states are known to occur, a brace is sometimes used to suggest reference to another diagram. For reactions in which the present nucleus occurs as a residual product, excitation functions have not been shown. Further information on the levels illustrated, including a listing of the reactions in which each has been observed, is contained in the master table, entitled "Energy levels of ^{20}O".

Table 20.0.5
^{20}O – General

Reference	Description
	Models
87BL18	Gogny's effective inter. used to calc. gnd. & excited states of specific spin-isospin order
87CH1J	Nucl. struc. calcs. using mixed-config. shell model: effective & surface δ-interactions
87CO31	Simple parametrization for low energy octupole modes of sd-shell nuclei
87KR08	Discontinuity in ground state band plot of even-even nuclei is traced to p-n interaction
87LI1F	Double delta & surface delta interactions used to calc. low-lying spectra of $^{17-22}$O
88BR11	Semi-empirical effective interactions for the 1s-0d shell
88HI05	Effect on GT strength of config. mixing and p-n correl. in even-even sd-shell nucl.
90SK04	$A = 18$ nuclei, effective interaction in the sd shell (also calc. $A = 20$ energy spectra)
90ZH01	Nuclear structure studies of double Gamow-Teller and double beta decay strength
91MA41	Finite nuclei calculations with realistic potential models (Bonn, Paris, Argonne)
91WA11	Composite particle representation theory calcs. for $A = 20$ states compared to shell model
92JI04	Bonn potential used to evaluate energy spectra of some light sd-shell nuclei
93AM08	6p-2h core excitations in ^{20}O
93PO11	Shell-model calcs. of several properties of exotic light nuclei ($A = 4$–30)
	Complex reactions
Review:	
88JO1B	Exp. & theor. liquid drop & microscopic study of heavy ion radioactivity
Other articles:	
87MU03	Evaporation model calc. of the emission of clusters by excited compound nuclei
88BL11	Systematics of cluster-radioact.-decay constants from microscop. calcs. compared to data
88IV02	Microscopic approach to the rates of radioactive decay by emission of heavy clusters
89SA10	Total cross sections of reactions induced by neutron-rich light nuclei
90GU02	Particle stability of O & Ne isotopes in the reaction 44 MeV/nucleon ^{48}Ca + Ta
	Other topics
Reviews:	
89RA16	Predxns. from systematics & tabulation of B(E2; $0_1^+ \rightarrow 2_1^+$) values for even-even nucl.
89SP01	Reduced electric-octupole transition probabilities, B(E3; $0_1^+ \rightarrow 3_1^-$), for even-even nucl.
90TH1E	Summary of topics presented at Workshop on Primordial Nucleosynthesis
Other articles:	
87LI1F	Double delta & surface delta interactions used to calc. low-lying spectra of $^{17-22}$O
90ZH01	Nuclear structure studies of double Gamow-Teller and double beta decay strength
	Ground state properties
Review:	
89RA17	Compilation of exp. data on nuclear moments for ground & excited states of nucl.

Table 20.0.5 (continued)
^{20}O – General

Reference	Description
	Ground state properties (continued)
Other articles:	
87BL18	Gogny's-plus-tensor inter. for gnd. & excited states with specific spin-isospin order
89SA10	Total cross sections of reactions induced by neutron-rich light nuclei
90LO11	Self-consistent calcs. of light neutron-rich nuclei using density-functional method
93PA14	Relativistic mean field theory; calc. binding energy, rms radii, deformation parameters
93PA19	Continuation of 93PA14: effects of pairing correlations
94CI02	Nuclear SU3 scheme used to calc. specific heat and shape transitions in light sd nuclei

Table 20.1.0
Energy Levels of ^{20}O

E_x (MeV ± keV)	J^π; T	τ	Decay	Reactions
0	0^+; 2	$\tau_{1/2} = 13.51 \pm 0.05$ s	β^-	1, 2, 3, 4
1.67368 ± 0.15	2^+	$\tau_m = 10.5 \pm 0.4$ ps $g = -0.352 \pm 0.015$	γ	2, 3, 4
3.570 ± 7	4^+		(γ)	2, 3, 4
4.072 ± 4	2^+		γ	2, 4
4.456 ± 5	0^+		γ	2, 4
4.850 ± 15	4^+		(γ)	2
5.002 ± 6			(γ)	2
5.234 ± 5	2^+		(γ)	2
5.304 ± 6	2^+		(γ)	2
5.387 ± 6	0^+		γ	2
5.614 ± 3	(3^-)		(γ)	2
6.555 ± 8	(2)		(γ)	2
7.252 ± 8	5^-		(γ)	2
7.622 ± 7	$3^- + 4^-$			2
7.754 ± 5	4^+			2, 3
7.855 ± 6	(5^-)			2, 3
8.554 ± 8	4^+			2
8.804 ± 9	3^-			2, 3
8.962 ± 21	(0^+)			2
9.770 ± 8	0^+			2
10.125 ± 11	2^+			2, 3

Table 20.1.2
Energy Levels of ^{20}O from ^{18}O(t, p)^{20}O [a])

E_x (keV)	L	J^π
0.0	0	0^+
1674 ± 3 [b])	2	2^+
3570 ± 7	4	4^+
4072 ± 4	2	2^+
4456 ± 5 [c])	0	0^+
4850 ± 15	4	4^+
5002 ± 6		
5234 ± 5	2	2^+
5304 ± 6 [c])	2	2^+
5387 ± 6	0	0^+
5614 ± 3	(3)	(3^-)
6555 ± 8		(2)
7252 ± 8	5	5^-
7622 ± 7	$3 + 4$	$3^- + 4^+$
7754 ± 5	4	4^+
7855 ± 6	(5)	(5^-)
8554 ± 8	4	4^+
8804 ± 9	3	3^-
8962 ± 21	(0)	(0^+)
9770 ± 8 [d])	0	0^+
10125 ± 11	2	2^+

[a]) (79LA18): $E_t = 15$ MeV. See also Table 20.3 in (78AJ03) and (79FO17, 79PI01).
[b]) E_γ leads to $E_x = 1673.68 \pm 0.15$ keV (73WA1A).
[c]) 6p-2h structure: see (79LA04, 79LA18).
[d]) This strong state suggests that $(fp)^2$ excitations are important (79LA18).

3. ^{18}O(α, 2p)^{20}O $\quad Q_{\rm m} = -16.732$

See (83AJ01).

4. ^{18}O(^{18}O, ^{16}O)^{20}O $\quad Q_{\rm m} = -0.624$

See (83AJ01).

^{20}F

(Figs. 20.2 and 20.5)

GENERAL: See table 20.1.5.

$\mu = +2.094(2)$ nm (78LEZA)
$Q = 0.070(13)$ b (78LEZA)

Table 20.1.5
^{20}F – General

Reference	Description
	Model calculations
88BR11	Semi-empirical effective interactions for the 1s-0d shell
88ET01	Analysis of magnetic dipole transitions between sd-shell states
90DE34	^{20}F & ^{20}Na nuclei and the ^{19}Ne(p, γ)^{20}Na reaction in a microscopic three-cluster model
90SH12	Extreme collective limits for the magnetic moments of odd-odd nuclei
90SK04	$A = 18$ nuclei, effective interaction in the sd shell (also calc. $A = 20$ energy spectra)
91BO45	Democratic mapping used to calc. low-lying states of sd- and fp-shell nuclei
91MA41	Calculations of sd-shell nuclei with realistic potential models (Bonn, Paris, Argonne)
91PI09	Differential cross section data analyzed using microscopic model; ^{20}F levels deduced
91WA11	Composite Particle Representation Theory calcs. for $A = 20$ states compared to shell model
92BE14	Nuclear level densities and spin cut-off factors deduced from microscopic theory
92JI04	Bonn potential used to evaluate energy spectra of some light sd-shell nuclei using G-matrix
92WA22	Effective interactions for the 0p1s0d nuclear shell-model space
93PO11	Shell-model calcs. of properties of exotic (and normal) light nuclei (A = 4–30)
	Special States
90DE34	^{20}F & ^{20}Na nuclei and the ^{19}Ne(p, γ)^{20}Na reaction; a possible 1^- state in ^{20}Na, ^{20}F
93BR12	Nature of the ^{20}Na 2646-keV level and the stellar reaction rate for ^{19}Ne(p, γ)^{20}Na

Table 20.1.5 (continued)
^{20}F – General

Reference	Description
	Electromagnetic transitions
Review:	
93EN03	Strengths of γ-ray transitions in $A = 5$–44 nuclei
Other articles:	
88ET01	Analysis of magnetic dipole transitions between sd-shell states
90DE34	^{20}F & ^{20}Na nuclei and the ^{19}Ne(p, γ)^{20}Na reaction in a microscopic three-cluster model
	Astrophysics
Review:	
88AP1A	Neutrino diffusion, primordial nucleosynthesis and the r-process
90TH1E	Summary of topics presented at Workshop on Primordial Nucleosynthesis
93SO13	Methods for producing unstable nuclei & their relevance to major explosive stellar processes
Other articles:	
90MA1Z	Nuclear reaction uncertainties in standard and non-standard cosmologies
92CA1J	Quasi-static evolution of ONeMg cores, explosive ignition densities & the collapse explosion
93BR12	Nature of the ^{20}Na 2646-keV level and the stellar reaction rate for ^{19}Ne(p, γ)^{20}Na
	Complex reactions
87BA1T	Spin-isospin excitations in nuclei with relativistic heavy ions
87BU07	Projectile-like fragments from ^{20}Ne + ^{197}Au — counting simultaneously emitted neutrons
87EL14	Isovector excitations in nuclei with composite projectiles: (^{3}He, t), (d, ^{2}He) & heavy ions
87MU03	Study of the emission of clusters by excited compound nuclei
89SA10	Total cross sections of reactions induced by neutron-rich light nuclei
89YO02	Quasi-elastic & deep inelastic transfer in ^{16}O + ^{197}Au for $E < 10$ MeV/u
	Other topics
88RO19	Predictions for observation of ^{20}F(Λ) levels using ^{20}Ne(γ, K$^+$) reaction
89GE10	Threshold pion-nucleus amplitudes as predicted by current algebra
90DE45	Searches for admixture of massive neutrinos into the electron flavour
93NA08	Charge-symmetry-breaking N-N interaction in 1s0d-shell nucl. from ρ^0–ω and π^0–η mixing
	Ground state properties
Reviews:	
89RA17	Compilation of exp. data on nuclear moments for ground & excited states of nuclei
92PY1A	Nuclear quadrupole moments for $Z = 1$–20: precise calcs. on atoms & small molecules
Other articles:	
89SA10	Total cross sections of reactions induced by neutron-rich light nuclei
90SH12	Extreme collective limits for the magnetic moments of odd-odd nuclei
93RO22	Determination of k_0- and Q_0-factors of short-lived nuclides

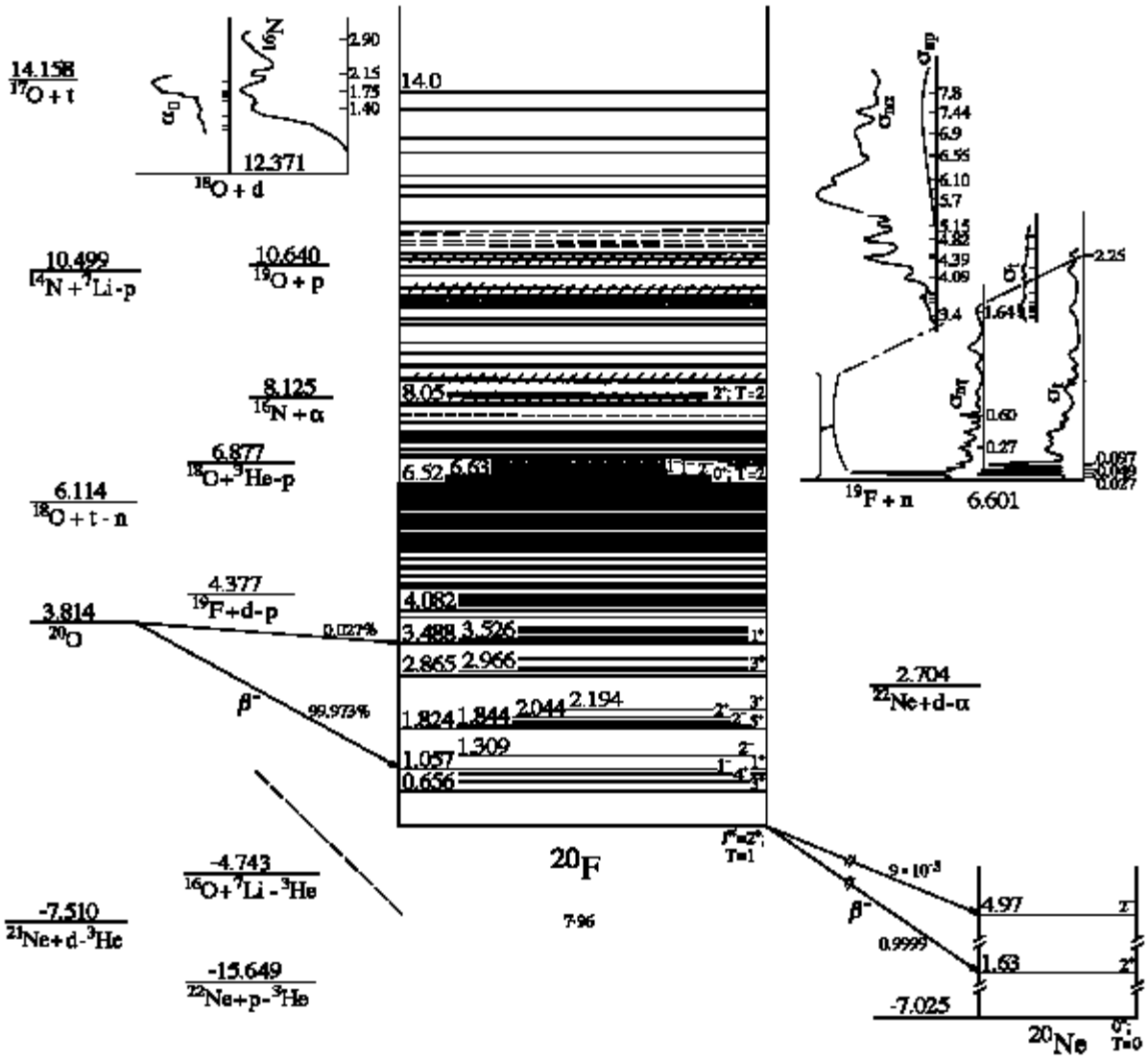

Figure 2: Energy levels of ^{20}F. For notation see Fig. 1.

Table 20.2
Energy Levels of ^{20}F [a])

E_x (MeV ± keV)	J^π; T	τ [b]) or Γ	Decay	Reactions [c])
0	2^+; 1	$\tau_{1/2} = 11.163 \pm 0.008$ s	β^-	1, 2, 4, 5, 6, 7, 9, 10, 11, 14, 16, 17, 17.5, 19, 20
0.65602 ± 0.03	3^+	$\tau_m = 440 \pm 30$ fs	γ	5, 6, 7, 9, 10, 11, 14, 17, 17.5, 19
0.82273 ± 0.03	4^+	$\tau_m = 79 \pm 6$ ps	γ	5, 6, 7, 9, 10, 11, 14, 17, 17.5, 19
0.98359 ± 0.03	1^-	$\tau_m = 1.96 \pm 0.09$ ps	γ	5, 6, 7, 9, 10, 11, 14, 15, 16, 17, 17.5, 19
1.056848 ± 0.004	1^+	$\tau_m = 7.4 \pm 1.6$ fs	γ	6, 7, 9, 10, 11, 14, 15, 16, 17, 17.5, 19
1.30919 ± 0.03	2^-	$\tau_m = 1.87 \pm 0.09$ ps	γ	5, 6, 7, 9, 11, 14, 16, 17, 17.5, 19
1.8238 ± 1.6	5^+	$\tau_m \leq 65$ fs	γ	2, 5, 6, 7, 9, 10, 14, 17.5, 19
1.84380 ± 0.03	2^-	$\tau_m = 66 \pm 5$ fs	γ	2, 7, 9, 11, 14, 17
1.97083 ± 0.04	(3^-)	$\tau_m = 0.61 \pm 0.09$ ps	γ	2, 5, 6, 7, 9, 11, 14, 17.5, 19
2.04398 ± 0.03	2^+	$\tau_m = 3.9 \pm 0.7$ fs	γ	2, 5, 6, 7, 9, 11, 14, 17, 17.5, 19
2.19430 ± 0.03	3^+	$\tau_m = 4.1 \pm 1.2$ fs	γ	2, 5, 6, 7, 9, 10, 11, 14, 17, 17.5, 19
2.86486 ± 0.10	(3^-)	$\tau_m = 29 \pm 4$ fs	γ	5, 6, 7, 9, 11, 14, 17.5, 19
2.96611 ± 0.03	3^+	$\tau_m = 5.2 \pm 1.1$ fs	γ	5, 6, 7, 9, 11, 14, 16.6, 17.5, 19
2.9680 ± 1.5	(4^-)		γ	5, 6, 7, 9, 14, 17.5, 19
3.17169 ± 0.14	$(0^-,\ 1^+)$		γ	5, 6, 7, 9, 11, 14, 17.5, 19
3.48841 ± 0.03	1^+	$\tau_m = 11.7 \pm 0.7$ fs	γ	5, 6, 7, 9, 11, 14, 15, 17.5, 19
3.52631 ± 0.04	(0^+)	$\tau_m = 5.5 \pm 0.6$ fs	γ	9, 11, 14, 17.5
3.58654 ± 0.03	(2)	$\tau_m = 1.1 \pm 0.6$ fs	γ	5, 6, 7, 9, 11, 14, 17.5
3.58980 ± 0.04	(3)			5, 6, 7, 9, 11, 14, 17.5
3.669 ± 3	(4^+)		(γ)	5, 6, 9
3.68017 ± 0.04	(2)	$\tau_m = 22.1 \pm 2.3$ fs	γ	6, 7, 9, 11, 14, 17.5, 19
3.7610 ± 2.0	(≥ 3)		γ	5, 6, 7, 9, 14, 17.5, 19
3.96507 ± 0.04	(1^+)	$\tau_m = 6.9 \pm 2.1$ fs	γ	5, 6, 7, 9, 11, 14, 17.5, 19
4.08217 ± 0.04	(1^+)	$\tau_m = 3.6 \pm 0.7$ fs	γ	5, 6, 7, 8, 9, 11, 14, 17.5, 19
4.1993 ± 2.7	≥ 3		(γ)	5, 6, 14
4.2081 ± 2.6	≥ 3		(γ)	7, 9, 14, 19
4.27709 ± 0.04	$(1^+,\ 2^+)$	$\tau_m = 7 \pm 4$ fs	γ	5, 6, 7, 9, 11, 14, 19
4.3120 ± 2.6	(0^+)	$\tau_m = 5.1 \pm 0.6$ fs	(γ)	14
4.37147 ± 0.11		$\tau_m < 4$ fs	γ	6, 7, 11, 14, 19
4.509 ± 3			(γ)	5, 6, 7, 14

Table 20.2 (continued)
Energy Levels of ^{20}F [a])

E_x (MeV ± keV)	J^π; T	τ [b]) or Γ	Decay	Reactions [c])
4.518 ± 4			(γ)	6, 7, 9, 19
4.5846 ± 3.0			(γ)	5, 6, 7, 14
4.59172 ± 0.07			γ	9, 11, 14, 19
4.722 ± 12			(γ)	9
4.7312 ± 2.9			(γ)	6, 7, 14, 19
4.744 ± 12			(γ)	5, 9
4.7648 ± 2.7			(γ)	6, 7, 9, 14, 19
4.89276 ± 0.17			γ	5, 6, 11, 14, 19
4.8994 ± 2.8			(γ)	7, 9, 14
5.0415 ± 3.1			(γ)	6, 7, 9, 14, 19
5.0668 ± 3.1			(γ)	5, 6, 7, 14
5.130 ± 3			(γ)	5, 6, 7, 9, 14, 19
5.2261 ± 0.4		$\tau_m = 1.4 \pm 1.1$ fs	(γ)	6, 7, 9, 11, 14, 19
5.255 ± 15			(γ)	5
5.28279 ± 0.17		$\tau_m = 3.3 \pm 1.3$ fs	γ	6, 9, 11, 14, 19
5.31917 ± 0.04		$\tau_m = 4.9 \pm 1.1$ fs	γ	5, 6, 7, 9, 11, 14, 19
5.3461 ± 3.3			(γ)	7, 9, 14
5.352 ± 3			(γ)	6, 14
5.407 ± 3			(γ)	5, 6, 7, 9, 14, 19
5.4521 ± 3.8			(γ)	5, 6, 7, 9,14, 19
5.4572 ± 3.2			(γ)	7, 14
5.46589 ± 0.17			γ	7, 11, 14
5.55534 ± 0.04		$\tau_m = 6.0 \pm 1.5$ fs	γ	7, 9, 11, 14, 19
5.574 ± 6			(γ)	6, 7, 9, 19
5.588 ± 2			(γ)	14
5.62313 ± 0.06			γ	6, 7, 9, 11, 14, 19
5.645 ± 12			(γ)	9
5.661 ± 12			(γ)	9
5.710 ± 6			(γ)	9, 14, 19
5.725 ± 10			(γ)	6
5.7649 ± 3.4			(γ)	5, 6, 7, 9, 14, 19
5.795 ± 14			(γ)	7, 9
5.8101 ± 0.4			(γ)	6, 11, 14, 19
5.93613 ± 0.03	2^-	$\tau_m < 2$ fs	γ	5, 9, 11, 14, 19

Table 20.2 (continued)
Energy Levels of ^{20}F [a])

E_x (MeV ± keV)	J^π; T	τ [b]) or Γ	Decay	Reactions [c])
5.93910 ± 0.10			γ	5, 9, 11, 14, 19
5.951 ± 4			(γ)	7
6.007 ± 14			(γ)	5, 9
6.01778 ± 0.03	2^-	$\tau_m = 3.3 \pm 1.2$ fs	γ	6, 7, 11, 14
6.04498 ± 0.08			γ	7, 9, 11, 14, 19
6.065 ± 14			(γ)	9
6.079 ± 14			(γ)	9
6.095 ± 14			(γ)	9
6.111 ± 14			(γ)	9
6.136 ± 14			(γ)	9
6.154 ± 14			(γ)	5, 6, 9, 19
6.189 ± 14			(γ)	6, 7, 9
6.213 ± 14			(γ)	7, 9, 19
6.251 ± 14			(γ)	9, 19
6.287 ± 14			(γ)	9
6.2991 ± 0.3			(γ)	6, 11, 19
6.335 ± 14			(γ)	6, 9, 19
6.355 ± 14			(γ)	5, 6, 9, 19
6.391 ± 14			(γ)	6, 9, 19
6.413 ± 14			(γ)	6, 9, 19
6.444 ± 14			(γ)	9, 19
6.458 ± 14			(γ)	5, 9
6.481 ± 14			(γ)	6, 9, 19
6.509 ± 14			(γ)	9
6.519 ± 3	0^+; $T = 2$		γ	17
6.578 ± 14			(γ)	6, 9, 19
6.6270 ± 0.3	2^-	$\Gamma_{cm} = 0.31 \pm 0.02$ keV	γ, n	11, 12
6.6426 ± 0.3	(3, 4)	$\Gamma_{cm} < 0.08$ keV	γ, n	11
6.6475 ± 0.4	1^-	$\Gamma_{cm} = 1.59 \pm 0.10$ keV	γ, n	11, 12
6.6934 ± 0.6	1^-	$\Gamma_{cm} = 13.8 \pm 0.8$ keV	γ, n	6, 11, 12
6.7661 ± 0.9	(2^-, 3, 4^+)	$\Gamma_{cm} \leq 0.6$ keV	γ, n	6, 11, 16.6, 19
6.825 ± 5			n	6, 12, 19
6.8567 ± 1.0	2	$\Gamma_{cm} = 10 \pm 2$ keV	γ, n	11
6.905 ± 8				19

Table 20.2 (continued)
Energy Levels of ^{20}F [a])

E_x (MeV ± keV)	J^π; T	τ [b]) or Γ	Decay	Reactions [c])
6.936 ± 4				6
6.9678 ± 1.0	1^-	$\Gamma_{cm} = 5 \pm 1$ keV	γ, n	6, 11, 12
(7.0670 ± 1.2)	0^-	$(\Gamma_{cm} = 2.4 \pm 0.6$ keV)	γ, n	11, 12
7.08	(1^+)	$\Gamma_{cm} = 24$ keV	n	6, 12
7.166 ± 2	$2^{(+)}$	$\Gamma_{cm} = 8 \pm 1$ keV	γ, n	6, 11, 12, 13
7.232 ± 7				6
7.283 ± 4				6
7.319 ± 8	(1)	$\Gamma_{cm} = 33$ keV	γ, n	6, 11, 12
7.37 ± 20	(1)	$\Gamma_{cm} = 19$ keV	n	6, 12
7.42 ± 20	(2^+)	$\Gamma_{cm} = 10$ keV	γ, n	6, 11, 12
7.495 ± 5	(2)	$\Gamma_{cm} = 80$ keV	γ, n	6, 11, 12
7.655 ± 5	(2^+)	$\Gamma_{cm} = 65$ keV	γ, n	6, 11, 12
7.734 ± 6		$\Gamma_{cm} = 140$ keV	n	6, 12
7.843 ± 11	1^-	$(\Gamma_{cm} = 50 \pm 10$ keV)	γ, n	6, 11
7.985 ± 4	1	$\Gamma_{cm} = 14 \pm 2$ keV	γ, n	6, 11
8.05 ± 100	2^+; $T = 2$			18
8.062 ± 8				6
8.113 ± 4		$\Gamma_{cm} = 195$ keV	γ, n	6, 11, 12
8.147 ± 6		$\Gamma_{cm} = 15$ keV	n	6, 12
8.268 ± 12				6
8.349 ± 4				6
8.421		$\Gamma_{cm} = 27$ keV	n	12
8.50		$\Gamma_{cm} = 140$ keV	n	12
8.72		$\Gamma_{cm} \leq 30$ keV	n	6, 12
8.77		$\Gamma_{cm} = 76$ keV	n	6, 12
8.94		$\Gamma_{cm} = 73$ keV	n	6, 12
9.01				6
9.2			n	10, 12
9.52		$\Gamma_{cm} = 110$ keV	n	12
9.65		$\Gamma_{cm} = 100$ keV	n	12
9.83		$\Gamma_{cm} = 33$ keV	n	12
9.85		$\Gamma_{cm} = 120$ keV	n	12
(9.886 ± 10)			n	12
9.90		$\Gamma_{cm} \leq 30$ keV	n	12

Table 20.2 (continued)
Energy Levels of ^{20}F [a])

E_x (MeV ± keV)	J^π; T	τ [b]) or Γ	Decay	Reactions [c])
(9.929 ± 10)			n	12
(9.981 ± 10)			n	12
10.024 ± 10		$\Gamma_{cm} = 150$ keV	n, α	12, 13
10.10 ± 50			n, α	13
10.228 ± 10	0^-, 1	$\Gamma_{cm} \sim 200$ keV	n, α	12, 13
10.480 ± 10		$\Gamma_{cm} \sim 10$ keV	n, α	12, 13
10.641 ± 10	1, 2	$\Gamma_{cm} = 70$ keV	n	12
10.807 ± 10	0^-, 1	$\Gamma_{cm} \sim 310$ keV	n, α	12, 13
10.99		$\Gamma_{cm} = 190$ keV	n	12
(11.045 ± 10)		$\Gamma_{cm} \sim 30$ keV	n	12
(11.130 ± 10)		$\Gamma_{cm} < 25$ keV	n	12
(11.244 ± 10)		$\Gamma_{cm} < 25$ keV	n	12
(11.287 ± 10)			n	12
11.49 ± 50			n, α	13
12.0			n, α	13
12.2 ± 100			n, α	13
12.4			n, α	13
12.7			n, α	10, 13
13.2			n, α	13
13.7			n, α	12, 13
14.0				13

[a]) See also Tables 20.3–20.12.
[b]) Lifetimes quoted here are those adopted by (96RA04); see Table VII of that work.
[c]) Reaction numbers are underlined in cases where the resolution of the experiment was inadequate for unequivocal identification of the level observed.

Table 20.3
Radiative transitions in ^{20}F [a])

E_i (MeV ± keV)	J_i^π	E_f (MeV ± keV)	Branching (%)	δ
0.65602 ± 0.03	3^+	0	100 ± 5	0.10 ± 0.05
0.82273 ± 0.03	4^+	0	33.2 ± 1.8	
		0.65602 ± 0.03	66.8 ± 6.1	
0.98359 ± 0.03	1^-	0	100 ± 5	[b])
1.05682 ± 0.03	1^+	0	100 ± 4	
1.30919 ± 0.03	2^-	0	91.7 ± 3.6	[b])
		0.65602 ± 0.03	2.4 ± 0.4	
		0.98359 ± 0.03	4.9 ± 0.4	
		1.05682 ± 0.03	1.0 ± 0.2	
1.8238 ± 1.6	5^+	0.82273 ± 0.03	100 ± 5	-0.03 ± 0.07
1.84380 ± 0.03	2^-	0	91.3 ± 4.5	
		0.65602 ± 0.03	6.7 ± 0.4	
		1.30919 ± 0.03	1.9 ± 0.3	
1.97083 ± 0.04	(3^-)	0	17.7 ± 1.8	-0.06 ± 0.14
		0.82273 ± 0.03	51.9 ± 2.9	$+0.27 \pm 0.30$
		0.98659 ± 0.03	0.8 ± 0.4	
		1.30919 ± 0.03	29.7 ± 3.9	
2.04398 ± 0.03	2^+	0	7.5 ± 0.6	
		0.65602 ± 0.03	91.8 ± 3.3	$0.08^{+0.06}_{-0.1}$
		1.30919 ± 0.03	0.7 ± 0.2	
2.19430 ± 0.03	3^+	0	47.0 ± 2.1	0 ± 0.09
		0.82273 ± 0.03	51.2 ± 3.2	$+0.07 \pm 0.10$
		1.30919 ± 0.03	1.8 ± 0.4	
2.86486 ± 0.10	(3^-)	0	38.1 ± 9.5	
		0.65602 ± 0.03	4.8 ± 2.4	
		0.82273 ± 0.03	11.9 ± 4.8	
		1.30919 ± 0.03	11.9 ± 2.4	
		1.84380 ± 0.03	7.1 ± 2.4	
		1.97083 ± 0.04	7.1 ± 2.4	
		2.04398 ± 0.03	11.9 ± 4.8	
		2.19430 ± 0.03	7.1 ± 2.4	
2.96611 ± 0.03	3^+	0	27.1 ± 1.5	
		0.65602 ± 0.03	12.2 ± 1.2	
		0.82273 ± 0.03	58.3 ± 2.7	
		2.19430 ± 0.03	2.4 ± 0.6	
2.96800 ± 1.50	(4^-)	0.82273 ± 0.03	39 ± 4	
		1.97083 ± 0.04	61 ± 4	

Table 20.3 (continued)
Radiative transitions in ^{20}F [a])

E_i (MeV ± keV)	J_i^π	E_f (MeV ± keV)	Branching (%)	δ
3.17169 ± 0.14	$(0^-,\ 1^+)$	0.98359 ± 0.03	100 ± 15	
3.48841 ± 0.03	1^+	0	72.6 ± 3.0	
		0.98359 ± 0.03	3.8 ± 0.4	
		1.05682 ± 0.03	7.1 ± 3.0	
		1.30919 ± 0.03	9.2 ± 0.6	
		1.84380 ± 0.03	7.4 ± 0.6	
3.52631 ± 0.04	(0^+)	1.05682 ± 0.03	100 ± 4	
3.58654 ± 0.03	(2)	0	32.9 ± 1.4	
		0.65602 ± 0.03	9.8 ± 0.6	
		0.98359 ± 0.03	4.0 ± 0.3	
		1.05682 ± 0.03	10.2 ± 3.4	
		1.84380 ± 0.03	0.7 ± 0.2	
		2.04398 ± 0.03	31.1 ± 1.4	
		2.19430 ± 0.03	8.8 ± 0.7	
		2.96611 ± 0.03	2.6 ± 0.2	
3.58980 ± 0.04	(3)	0	83.2 ± 3.3	
		0.65602 ± 0.03	10.7 ± 1.4	
		2.04398 ± 0.03	6.1 ± 0.9	
3.669 ± 3		0	100 ± 24	
3.68017 ± 0.04	(2)	0	46.5 ± 3.2	
		0.65602 ± 0.03	17.1 ± 2.1	
		1.05682 ± 0.03	23.5 ± 1.6	
		1.30919 ± 0.03	4.3 ± 1.1	
		1.84380 ± 0.03	8.6 ± 1.1	
3.96507 ± 0.04	(1^+)	0.98359 ± 0.03	26.1 ± 3.0	
		1.30919 ± 0.03	58.2 ± 4.5	
		1.84380 ± 0.03	10.4 ± 1.5	
		3.17169 ± 0.14	5.2 ± 1.5	
4.08217 ± 0.04	(1^+)	0	35.5 ± 2.6	
		0.98359 ± 0.03	4.6 ± 1.3	
		1.05682 ± 0.03	50.0 ± 3.3	
		2.04398 ± 0.03	9.9 ± 1.3	
4.27709 ± 0.04	$(1^+,\ 2^+)$	0.98359 ± 0.03	24.1 ± 2.8	
		1.05682 ± 0.03	56.5 ± 3.7	
		2.04398 ± 0.03	19.4 ± 2.8	
4.37147 ± 0.11		0.98359 ± 0.03	93.8 ± 7.7	
		3.68017 ± 0.04	6.2 ± 3.1	

Table 20.3 (continued)
Radiative transitions in ^{20}F [a])

E_i (MeV ± keV)	J_i^π	E_f (MeV ± keV)	Branching (%)	δ
4.509 ± 3		0.65602 ± 0.03	100	
4.59172 ± 0.07		0.98359 ± 0.03	60.0 ± 8.6	
		1.05682 ± 0.03	40.0 ± 8.6	
4.89276 ± 0.17		0.82273 ± 0.03	35 ± 10	
		2.19430 ± 0.03	20 ± 5	
		3.58654 ± 0.03	45 ± 10	
5.28279 ± 0.17		0	57 ± 21	
		1.05682 ± 0.03	43 ± 7	
5.31917 ± 0.04		0	22.6 ± 3.6	
		0.98359 ± 0.03	56.0 ± 4.8	
		1.05682 ± 0.03	3.6 ± 1.2	
		1.30919 ± 0.03	11.9 ± 3.6	
		1.84380 ± 0.03	6.0 ± 1.2	
5.46589 ± 0.17		2.86486 ± 0.10	100 ± 50	
5.55534 ± 0.04		0	30.6 ± 2.4	
		0.65602 ± 0.03	4.1 ± 1.2	
		1.30919 ± 0.03	54.7 ± 2.9	
		1.84380 ± 0.03	7.1 ± 1.8	
		2.86486 ± 0.10	3.5 ± 0.6	
5.62313 ± 0.06		0	13.8 ± 3.4	
		0.98359 ± 0.03	39.7 ± 6.9	
		1.30919 ± 0.03	31.0 ± 5.2	
		2.04398 ± 0.03	15.5 ± 3.4	
5.93613 ± 0.03	2^-	0	6.6 ± 0.7	
		0.65602 ± 0.03	28.7 ± 1.4	
		0.98359 ± 0.03	4.0 ± 0.4	
		1.05682 ± 0.03	0.6 ± 0.1	
		1.30919 ± 0.03	0.5 ± 0.1	
		1.84380 ± 0.03	1.2 ± 0.2	
		1.97083 ± 0.04	30.0 ± 1.1	
		2.04398 ± 0.03	1.2 ± 0.2	
		2.19430 ± 0.03	4.0 ± 0.3	
		2.86486 ± 0.10	1.4 ± 0.2	
		2.96611 ± 0.03	1.1 ± 0.2	
		3.48841 ± 0.03	9.6 ± 0.5	
		3.58654 ± 0.03	2.1 ± 0.2	
		3.58980 ± 0.04	1.4 ± 0.3	

Table 20.3 (continued)
Radiative transitions in ^{20}F [a])

E_i (MeV ± keV)	J_i^π	E_f (MeV ± keV)	Branching (%)	δ
		3.68017 ± 0.04	5.9 ± 0.3	
		3.96507 ± 0.04	0.7 ± 0.2	
		4.08217 ± 0.04	0.9 ± 0.1	
5.93910 ± 0.10		0	12.4 ± 3.4	
		0.98359 ± 0.03	23.6 ± 3.4	
		1.84380 ± 0.03	31.5 ± 3.4	
		2.04398 ± 0.03	13.5 ± 3.4	
		3.58654 ± 0.03	19.1 ± 3.4	
6.01778 ± 0.03	2^-	0	26.0 ± 1.1	
		0.65602 ± 0.03	3.3 ± 0.1	
		0.98359 ± 0.03	17.2 ± 0.7	
		1.05682 ± 0.03	0.7 ± 0.1	
		1.30919 ± 0.03	1.4 ± 0.1	
		1.84380 ± 0.03	4.6 ± 0.2	
		1.97083 ± 0.04	1.0 ± 0.1	
		2.04398 ± 0.03	0.7 ± 0.1	
		2.19430 ± 0.03	2.9 ± 0.2	
		2.86486 ± 0.10	0.4 ± 0.1	
		2.96611 ± 0.03	8.2 ± 0.3	
		3.48841 ± 0.03	16.0 ± 0.8	
		3.58654 ± 0.03	9.7 ± 0.8	
		3.58980 ± 0.04	5.3 ± 0.2	
		3.68017 ± 0.04	0.4 ± 0.1	
		3.96507 ± 0.04	0.14 ± 0.03	
		4.08217 ± 0.04	2.0 ± 0.1	
6.04498 ± 0.08		1.30919 ± 0.03	27.7 ± 2.1	
		1.84380 ± 0.03	55.4 ± 3.1	
		3.48841 ± 0.03	8.2 ± 1.5	
		3.58654 ± 0.03	3.1 ± 0.5	
		3.96507 ± 0.04	5.6 ± 1.0	
6.60135 ± 0.17 [c])		0	9.85 ± 0.42	
		0.98359 ± 0.03	1.45 ± 0.06	
		1.05682 ± 0.03	4.30 ± 0.17	
		1.30919 ± 0.03	2.47 ± 0.10	
		1.84380 ± 0.03	1.98 ± 0.08	
		1.97083 ± 0.04	0.06 ± 0.01	
		2.04398 ± 0.03	5.47 ± 0.21	

Table 20.3 (continued)
Radiative transitions in ^{20}F [a])

E_i (MeV ± keV)	J_i^π	E_f (MeV ± keV)	Branching (%)	δ
		3.48841 ± 0.03	2.52 ± 0.09	
		3.52631 ± 0.04	1.98 ± 0.08	
		3.58654 ± 0.03	4.24 ± 0.17	
		3.68017 ± 0.04	0.99 ± 0.05	
		3.96507 ± 0.04	1.02 ± 0.05	
		4.08217 ± 0.04	0.73 ± 0.05	
		4.27709 ± 0.04	1.23 ± 0.05	
		4.37147 ± 0.11	0.54 ± 0.03	
		4.59172 ± 0.07	0.49 ± 0.04	
		4.89276 ± 0.17	0.27 ± 0.03	
		5.22610 ± 0.40	0.05 ± 0.02	
		5.28279 ± 0.17	0.24 ± 0.02	
		5.31917 ± 0.04	0.90 ± 0.05	
		5.46589 ± 0.17	0.09 ± 0.02	
		5.55534 ± 0.04	1.85 ± 0.09	
		5.62313 ± 0.06	0.64 ± 0.10	
		5.81010 ± 0.40	0.04 ± 0.01	
		5.93613 ± 0.03	15.62 ± 0.84	
		5.93910 ± 0.10	1.07 ± 0.16	
		6.01778 ± 0.03	37.70 ± 0.16	
		6.04498 ± 0.08	2.17 ± 0.14	
		6.29910 ± 0.03	0.05 ± 0.02	
[d])				

[a]) Branching ratios from (96RA04) renormalized to add to 100%.
[b]) Pure E1.
[c]) Capturing state. See Table 20.8 and (96RA04).
[d]) For higher states see Tables 20.6. See also Table 20.7 in (87AJ02).

1. ^{20}F(β^-)^{20}Ne $Q_m = 7.025$

The half-life of ^{20}F is 11.163 ± 0.008 s (92WA04). ^{20}F decays principally to ^{20}Ne* (1.63): see ^{20}Ne, reaction 33.

1.3 (a) ^{6}Li(^{15}N, p)^{20}F $Q_m = 6.915$
(b) ^{7}Li(^{15}N, d)^{20}F $Q_m = 1.068$

Excitation functions were measured for incident energies E_i = 10–30 MeV (89CO22).

1.5 ^{6}Li(^{18}O, α)^{20}F $Q_m = 10.896$

Activation cross sections were measured for E_i = 10–40 MeV by (87DI07).

1.8 (a) ^{10}B(^{11}B, p)^{20}F $Q_m = 13.447$
(b) ^{11}B(^{11}B, d)^{20}F $Q_m = 4.217$

Excitation functions have been measured at E_i = 6–32 MeV (88CO12).

2. ^{12}C(^{9}Be, p)^{20}F $Q_m = 4.076$

For excitation curves involving ^{20}F* (0, 1.82 + 1.84 + 1.97 + 2.04 + 2.19) see (82HU06, 83JA09). At $E(^{9}\text{Be})$ = 12 to 27 MeV angular distributions are reported for p_0 and $p_{1+2+3+4}$: see (83AJ01).

3. ^{13}C(^{7}Li, ^{7}Li)^{13}C $E_b = 18.050$

For fusion cross sections see (82DE30). See also ^{13}C in (91AJ01).

4. ^{13}C(^{9}Be, d)^{20}F $Q_m = 1.354$

See (83AJ01).

5. ^{13}C(^{11}B, α)^{20}F $\quad Q_{\rm m} = 9.385$

The upper of the two states at 2.97 MeV has an excitation energy of 2968 ± 1.5 keV and γ branching ratios of (61 ± 4) and (39 ± 4)%, respectively, to ^{20}F* (1.97, 0.82) [$J^\pi = (3^-),\ 4^+$]: this is consistent with $J^\pi = (4^-)$ for ^{20}F* (2.968) (78LE19).

The reactions ^{13}C(^{11}B, α)^{20}F and ^{11}B(^{13}C, α)^{20}F were used to populate ^{20}F states up to $E_{\rm x} = 10.1$ MeV by (88LI28). Comparisons with ^{14}N(^{7}Li, p)^{20}F were discussed.

6. ^{14}N(^{7}Li, p)^{20}F $\quad Q_{\rm m} = 10.499$

Tables 20.5 here and in (83AJ01) display ^{20}F states reported in this reaction.

7. ^{16}O(^{7}Li, ^{3}He)^{20}F $\quad Q_{\rm m} = -4.743$

For reported states see Table 20.6 in (83AJ01).

8. (a) ^{18}O(d, n)^{19}F $\quad Q_{\rm m} = 5.770$ $\quad E_{\rm b} = 12.371$
   (b) ^{18}O(d, p)^{19}O $\quad Q_{\rm m} = 1.731$
   (c) ^{18}O(d, d)^{18}O
   (d) ^{18}O(d, ^{3}He)^{17}N $\quad Q_{\rm m} = -10.448$
   (e) ^{18}O(d, α)^{16}N $\quad Q_{\rm m} = 4.246$

See (83AJ01) for a listing of the polarization measurements. For VAP measurements at $E_{\rm d} = 52$ MeV (reaction (e)), see (82MA25). See also ^{19}O and ^{19}F in (95TI1C), and ^{16}N and ^{17}N in (93TI07). See also (86SE1B).

9. ^{18}O(^{3}He, p)^{20}F $\quad Q_{\rm m} = 6.877$

Table 20.5
Some states of ^{20}F reported in ^{14}N(^{7}Li, p) [a])

E_x (keV)	J^π	E_x (keV)	J^π	E_x (keV)	J^π
0	2^+	5128 ± 5	$(2^-, 3, 4^+)$	6936 ± 4	
657 ± 6	3^+	5222 ± 4	$(1, 2)^-$	6968 ± 4	
820 ± 5	4^+	5282 ± 11	[c])	6991 ± 7	
984 ± 5	1^-	5316 ± 7	[c])	7034 ± 9 [d])	
1049 ± 5	1^+	5350 ± 5	3^+	7080 ± 7	
1310 ± 6	2^-	5405 ± 4	[c])	7154 ± 5	
1826 ± 4 [b])	5^+	5448 ± 6 [b])		7232 ± 7	
1969 ± 5	(3^-)	5560 ± 6 [b])		7283 ± 4	
2040 ± 3	2^+	5612 ± 5 [b])	[c])	7319 ± 8	
2194 ± 6	3^+	5725 ± 10	$(2 \rightarrow 5)$	7370 ± 20	
2863 ± 5	(3^-)	5765 ± 8	3^+	7419 ± 20	
2962 ± 3 [b])		5803 ± 7	1^+	7495 ± 5	
3171 ± 4	1^+	5940 ± 5	[c])	7655 ± 5	
3491 ± 3 [b])	0^+	6021 ± 4 [b])		7734 ± 6	
3578 ± 5 [e])		6090 ± 7	(0^-)	7865 ± 16	
3674.2 ± 2.8 [e])		6160 ± 5	$((1^-), 2, 3^+)$	7975 ± 5	
3756.5 ± 2.3	$(2^-, 3^+)$ [f])	6193 ± 6	$(2^-, 3, 4^+)$	8062 ± 8	
3967 ± 5	1^+	6297 ± 5 [b])	[c])	8113 ± 4	
4080 ± 4 [e])		6344 ± 9 [b])	[c])	8147 ± 6	
4198 ± 3 [b])		6379 ± 5 [b])	[c])	8268 ± 12	
4274 ± 3 [b])		6417 ± 4	$(3^-, 4, 5, (6^+))$	8349 ± 4	
4366 ± 8	$0^{(-)}$	6470 ± 4	[c])	8573	
4512 ± 4	$(3^-, 4^-, 5^+, 6^+)$	6565 ± 6 [b])	[c])	8697	
4579 ± 4 [b])		6600 ± 8 [b])	[c])	8754	
4728 ± 5	$(3^-, 4^-, 4^+, 5^+)$	6633 ± 3 [b])		8792	
4760 ± 5	$(4 \rightarrow 6^-, 6 \rightarrow 8^+)$	6695 ± 3	[c])	8907	
4889 ± 4 [b])	[c])	6756 ± 3	$(2^-, 3, 4^+)$	8946	
5032 ± 4	2^-	6823 ± 3		9022	
5064 ± 5	$(1^-, 2, 3^+)$				

[a]) $E(^7\text{Li}) = 16$ MeV. Levels for $E_x = 0$–4366 keV are from (77FO11). Levels for 4512–9022 are from (85FO01). Please note that the density of states is very high and that when J^π assignments are made [based on cross sections and the $2J_f + 1$ relationship, with slopes which are different for even- and odd-parity states], these depend on the states having been resolved.
[b]) Unresolved.
[c]) See (85FO07).
[d]) All the observed groups for $E_x \geq 7.0$ MeV appear to be due to unresolved states. See (85FO07) for $\sigma_{\text{tot}}(0^\circ - 90^\circ)$ and J^π.
[e]) Possible doublet.
[f]) If single state.

Table 20.5.5
Some states in ^{20}F from ^{18}O(^{3}He, p)^{20}F [a])

E_x (keV)	L transfer	J^π	E_x (keV)	L transfer	J^π
0	2		5404 ± 10		$(3,4,5)^+$
656 ± 10	2		5445 ± 14	2	$(1,2,3)^+$
823 ± 10	4		5543 ± 12	1	$(0,1,2)^-$
997 ± 10			5562 ± 12	1	$(0,1,2)^-$
1058 ± 11	$0+2$		5627 ± 12	1	$(0,1,2)^-$
1317 ± 10	1		5645 ± 12	3	$(2,3,4)^-$
1824 ± 10	4		5661 ± 12		
1974 ± 11	3		5708 ± 12		
2047 ± 11	2		5761 ± 14	2	
2201 ± 11	$2+4$	3^+	5795 ± 14	0	
2860 ± 11	(2)	$(1,2,3)^+$	5930 ± 14	1	
2968 ± 10	$2+4$		6006 ± 14		
3176 ± 11	2		6049 ± 14		
3486 ± 10	$0+2$		6065 ± 14		
3587 ± 10	2		6079 ± 14		
3680 ± 11	4	$(3,4,5)^+$	6095 ± 14		
3762 ± 11	3	2^-	6111 ± 14		
3961 ± 12	$0+2$		6136 ± 14		
4082 ± 10	0	1^+	6154 ± 14	4	3^+
4210 ± 14	4	$(3,4,5)^+$	6189 ± 14		
4282 ± 10	4	$(3,4,5)^+$	6213 ± 14	1	2^-
4516 ± 10	3	2^-	6251 ± 14		
4590 ± 12			6287 ± 14		
4722 ± 12	4	$(3,4,5)^+$	6335 ± 14		
4744 ± 12	4	$(3,4,5)^+$	6355 ± 14		
4768 ± 11			6391 ± 14		
4904 ± 12			6413 ± 14		
5041 ± 10	1		6444 ± 14		
5126 ± 12			6458 ± 14		
5223 ± 10	1		6481 ± 14		
5278 ± 10	0	$(1)^+$	6509 ± 14	0	
5319 ± 10	1		6578 ± 14		
5340 ± 12	2				

[a]) (92CH39). For earlier work see table 20.8 in (78AJ03).
[b]) Uncertainties in E_x were supplied by M.S. Chowdhury in a private communication to S. Raman, 22 March 1994.

In earlier work, proton groups have been observed to states of ^{20}F with $E_x < 4.1$ MeV: see Table 20.8 in (78AJ03). Angular distributions, γ-ray polarization data and branching ratios lead to the J^π values shown in that table. A state at $E_x = 6519 \pm 3$ keV is also populated. It decays primarily ($> 90\%$) to ^{20}F* (1.06) [$J^\pi = 1^+$]: the γ-rays are isotropic. ^{20}F* (6.52) is the 0^+; $T = 2$ analog of the ground state of ^{20}O: see (78AJ03).

More recently, the reaction was studied at $E(^{18}\text{O}) = 18$ MeV (92CH39). Energy levels were measured up to $E_x \approx 8$ MeV. See Table 20.5.5. See also (87SE17).

10. ^{18}O(α, d)^{20}F $\qquad Q_m = -11.476$

At $E_\alpha = 64.4$ MeV angular distributions have been reported to ^{20}F* (0, 0.66, 0.82, 1.06, 1.82, 2.20, 2.97, 4.24, 5.07, 5.44, 5.80, 6.67, 7.29, 7.75, 8.34, 8.75, 9.00, 9.24, 9.78, 10.01, 10.51, 10.85, 11.56, 12.32, 12.72): L assignments are made [the groups above $E_x \approx 2.9$ MeV are probably unresolved] (86KA36).

11. ^{19}F(n, γ)^{20}F $\qquad Q_m = 6.601$

$Q_0 = 6601.35 \pm 0.04$ keV (96RA04)

The thermal capture cross section is 9.51 ± 0.09 mb. A number of resonances have been observed: see Table 20.6. The primary γ-rays resulting from capture at thermal energies (^{20}F* (6.60); $J^\pi = 1^+$) and at $E_n = 27$, 44, and 49 keV (^{20}F* (6.63, 6.643, 6.647); $J^\pi = 2^-$, (3, 4) and 1^-) have been studied by several groups: see (72AJ02) and Table 20.7 in (87AJ02). For more recent high precision work see (87KE09) and the very comprehensive study of (96RA04), which included measurements of excitation energies and lifetimes and comparison of level properties with a large-basis shell-model calculation. It appears that the thermal capture [^{20}F* (6.60)] is dominated by two intense transitions (E1) to ^{20}F* (5.94, 6.02) [both $J^\pi = 2^-$]. If the ground-state transition is mainly M1, these two E1 transitions are about 150 times stronger (in terms of W.u.) than the M1 transition (68SP01). See also (83HU12). It appears also that at ^{20}F* (6.63, 6.64, 6.65) [$J^\pi = 2^-$, (3, 4) and 1^-] the E1 transitions to the ground state are very weak, even though other E1 transitions in the decay of these three states have approximately normal strengths. The strongest transitions from the 27 keV resonance appear to be M1. On the basis of the J^π values of the final states involved in the decay of the 44 keV resonance, it appears that $J = 3$ or 4 for this resonance, assuming dipole transitions. Branching ratios for other ^{20}F states involved in this reaction are shown in Table 20.3.

Table 20.8 displays excitation energies for ^{20}F states involved in cascade and in primary γ-transitions from the recent work of (96RA04). For earlier references see (78AJ03). See also (91IG1A, 91HI23).

Table 20.6
Resonances in ^{19}F(n, γ)^{20}F [a])

E_n (keV)	J^π [b])	Γ_γ (eV)	$\Gamma_{c.m.}$ (keV)	E_x in ^{20}F (MeV)
27.07 ± 0.05	2^-	1.4 ± 0.3	0.355 ± 0.03	6.6270
43.5 ± 0.1	(3, 4)	[c])	< 0.08	6.6426
48.7 ± 0.3	1^-	1.6 ± 0.3	1.96 ± 0.3	6.6475
97.0 ± 0.5	1^-	6.0 ± 1.8 [d])	13.5 ± 1.5	6.6934
173.5 ± 0.9		[e])	≤ 0.6	6.7661
269 ± 1	2	3.5 ± 0.8	10 ± 2	6.8567
(270 ± 8)	1	≤ 4.4		(6.859)
386 ± 1	1^-	2.4 ± 0.8	5 ± 1	6.9678
(490.5 ± 1)	0^-	$(\geq 10 \pm 3)$	(2.4 ± 0.6)	(7.0671)
595 ± 2	2	6.3 ± 1.2	8 ± 1	7.166
760		2.9	60	7.32
865			60	7.42
950		2.8	95	7.50
1125		3.9	80	7.67
(1295 ± 12)	1^-	8.6	(50 ± 10)	(7.831)
1460 ± 3	1	$\geq 11 \pm 3$	14 ± 2	7.988
1635		11 ± 3	180	8.15

[a]) For complete references see Table 20.9 in (78AJ03).
[b]) Assumed.
[c]) $g\Gamma_n = 0.086 \pm 0.02$ eV.
[d]) May be two resonances.
[e]) $g\Gamma_n = 0.35 \pm 0.1$ eV.

Table 20.8
States of ^{20}F involved in ^{19}F(n, γ)^{20}F [a])

E_x (keV)	E_x (keV)	E_x (keV)	E_x (keV)
0	2864.86 ± 0.10	4082.17 ± 0.04	5555.34 ± 0.04
656.02 ± 0.03	2966.11 ± 0.03	4277.09 ± 0.04	5623.13 ± 0.06
822.73 ± 0.03	3171.69 ± 0.14	4371.47 ± 0.11	5810.1 ± 0.4
983.59 ± 0.03	3488.41 ± 0.03	4591.72 ± 0.07	5936.13 ± 0.03
1056.82 ± 0.03	3526.31 ± 0.04	4892.76 ± 0.17	5939.10 ± 0.10
1309.19 ± 0.03	3586.54 ± 0.03	5226.1 ± 0.4	6017.78 ± 0.03
1843.80 ± 0.03	3589.80 ± 0.04	5282.79 ± 0.10	6044.92 ± 0.03
1970.83 ± 0.04	3680.17 ± 0.04	5319.17 ± 0.04	6299.1 ± 0.3
2043.98 ± 0.03	3965.07 ± 0.04	5465.89 ± 0.17	6601.35 ± 0.03
2194.30 ± 0.03			

[a]) (96RA04). For the earlier work see Tables 20.11 in (78AJ03) and 20.8 in (87AJ02).

Table 20.9
Resonances in ^{19}F(n, n)^{19}F [a])

E_n (keV)	Γ_{lab} (keV)	J^π	^{20}F* (MeV)
26.99	0.325 ± 0.020	2^-	6.6269
48.78	1.67 ± 0.10	1^-	6.6476
97.50	14.5 ± 0.8	1^-	6.6939
500	25 [b])	(1^+)	7.076
600	15 [b])	(2^+)	7.171
747	35 [b])	(1)	7.311
794	20	(1)	(7.355)
852	11 [b])	(2^+)	7.410
935	60	(2)	7.489
1100	50	(2^+)	7.65
1250	150		7.79
1620	220		8.14
2000	150		8.50
2250	≤ 30		8.74
2280	80		8.77
2520	150		8.99
3250	150		9.69
3420	130		9.85
3460 ± 10			(9.886)
3505 ± 10			(9.929)
3560 ± 10			(9.981)
3605 ± 10	200		10.024
3820 ± 10	≈ 200	0^-, 1	10.228
4085 ± 10	≈ 10		10.480
4255 ± 10	≈ 60	1, 2	10.641
4430 ± 10	≈ 330	0^-, 1	10.807
4680 ± 10	≈ 30		11.045
4770 ± 10	< 25		11.130
4890 ± 10	< 25		11.244
(4935)			(11.287)

[a]) For references see Table 20.12 in (78AJ03).
[b]) $\Gamma_\gamma = 3.3 \pm 1.0$, 6.3 ± 1.2, 2.4 ± 0.8 and 1.5 ± 0.5 eV for ^{20}F* (7.08, 7.17, 7.31, 7.41).

12. (a) ^{19}F(n, n)^{19}F $E_{\rm b} = 6.601$
(b) ^{19}F(n, n′)^{19}F*
(c) ^{19}F(n, 2n)^{18}F $Q_{\rm m} = -10.431$

The scattering length (bound) $b = 5.654 \pm 0.010$ fm, $\sigma_{\rm free} = 3.641 \pm 0.010$ b (79KO26). The difference in the spin-dependent bound scattering lengths, $b^+ - b^- = -0.19 \pm 0.02$ fm (79GL12). The total cross section has been measured for $E_{\rm n} = 0.5$ to 29.1 MeV: see (78AJ03). Observed resonances are displayed in Table 20.9.

Average cross sections for the region $E_{\rm n} = 0.55$–5.5 MeV were measured by (88KO18). See also the neutron cross section tables and curves of (88MCZT, 90NA1E).

Observed resonances in the excitation functions involving ^{19}F*(0.11, 1.5(u)) are displayed in Table 20.10. For reaction (c) see (83CS1A). See also (86BA1M, 86SA1F).

13. ^{19}F(n, α)^{16}N $Q_{\rm m} = -1.524$ $E_{\rm b} = 6.601$

Reported resonances are shown in Table 20.11. See also the neutron cross section curves and tables of (90NA1E).

14. ^{19}F(d, p)^{20}F $Q_{\rm m} = 4.377$

States of ^{20}F observed in this reaction are displayed in Table 20.12. See (78AJ03) for a discussion of the earlier work. See also (83JI04, 88RO10, 92WA04, 94GO16).

15. ^{20}O(β^-)^{20}F $Q_{\rm m} = 3.814$

The decay is to ^{20}F*(1.06, 3.49), $J^\pi = 1^+$: see ^{20}O. For ^{20}F*(1.06) $E_{\rm x} = 1056.848 \pm 0.004$ keV. The β branch to ^{20}F* (3.17) (1^+) is $< 0.012\%$, $\log f_0 t > 5.1$ (87AL06).

16. ^{20}Ne(π^-, γ)^{20}F $Q_{\rm m} = 132.543$

Table 20.10
States of ^{20}F from resonances in ^{19}F(n, n$'\gamma$)^{19}F

E_n (keV)	Γ_{lab} (keV)	Resonance in		E_x in ^{20}F (MeV)
		$\gamma_{0.11}$ [a])	$\gamma_{1.5}$ [b])	
240		r		6.829
270		r		6.858
386		r		6.968
420		r		7.000
490		r		7.066
620		r		7.190
800		r		7.361
860		r		7.418
1150 [c])		r		7.693
1250		r		7.788
1580		r		8.101
1645	15	r	r	8.163
1916	28		r	8.421
2240	45		r	8.728
2465	75	r	r	8.942
2700		r		9.165
3075	120		r	9.521
3215	80		r	9.654
3400	35		r	9.830
3475	≤ 30		r	9.901
3620	120	r	r	10.038
4240	90	r	r	10.627
4620	200		r	10.988
4900	≤ 50		r	11.254
7300		r		13.532

r = resonant
[a]) Resonances in yield of 0.11 MeV γ-rays at $\theta = 92°$: values for E_n read by reviewer from differential cross section tables. See Table 20.13 in (78AJ03) for references.
[b]) Resonances in (n, n$'\gamma$) yields with $E_x(^{19}F) \approx 1.5$ MeV: see (73MA14).
[c]) Appears to be unresolved.

Table 20.11
Resonances in ^{19}F(n, α)^{16}N [a])

E_n (MeV $\pm$ keV)	E_x (MeV)
3.4	9.8
3.61 ± 50	10.03
3.69 ± 50	10.10
3.76 ± 40	10.17
4.09 ± 40	10.48
4.39 ± 40	10.77
4.52 [b])	10.89
4.82 ± 40	11.18
5.15 ± 50	11.49
5.40 [b])	11.73
5.7	12.0
5.9 ± 100 [b])	12.2
6.10	12.39
6.55	12.82
6.9	13.2
7.44	13.66
7.8	14.0

[a]) For references see Table 20.14 in (78AJ03). See also graph in (76GA1A).
[b]) Not resolved.

The branching ratio to ^{20}F* (1.06) [$J^\pi = 1^+$] is compared to the analogous M1 decay width ^{20}Ne* (11.24) [$J^\pi = 1^+$] $\rightarrow$ ^{20}Ne$_{gs}$. The M1 amplitude contains (47 ± 16)% spin-flip, in agreement with shell-model calculations. The population of ^{20}F* (0, 1.31, 1.84) [$J^\pi = 2^+, 2^-, 2^-$] is also reported (81MA04). See also (86BA1P) and (83KN05).

16.2 ^{20}Ne(n, p)^{20}F $\qquad\qquad$ $Q_m = -6.243$

Differential cross sections were measured at $E_n = 198$ MeV to study Gamow-Teller strength up to $E_x \approx 10$ MeV in ^{20}F (90HE1G, 91PO14). See also the measurement of ground-state correlations described in (88MA53). Cross sections for 14 MeV neutrons are presented for use in activation analysis by (89PE04).

16.4 ^{20}Ne(d, pp)^{20}F $\qquad\qquad$ $Q_m = -8.467$

Angular distribution measurements with polarized deuterons ($E \approx 2$ GeV) were made in a study of spin-isospin excitations by (88HE1I).

16.6 ^{20}Ne(t, ^{3}He)^{20}F $\qquad Q_{\rm m} = -7.006$

Measurements at $E_{\rm t} = 33.4$ MeV (90CL06) reveal a strongly excited state in ^{20}F at $E_{\rm x} = 6.75 \pm 0.04$ MeV with an angular distribution suggesting $(3 < J < 6)$. In more recent work by the same authors (93CL1B), the reactions ^{20}Ne(t, ^{3}He)^{20}F and ^{20}Ne(^{3}He, t) were studied at $E_{\rm t} = 33.4$ MeV. Evidence was obtained that the $J^{\pi} = (3^{+})$, $E_{\rm x} = 2.966$ MeV state in ^{20}F should be identified as the analog of the $E_{\rm x} = 2.646$ MeV state in ^{20}Na.

16.8 ^{20}Ne(^{12}C, ^{20}F)^{12}N $\qquad Q_{\rm m} = -13.870$

Measurements at 900 MeV/nucleon for studies of spin-isospin excitations were reported by (88RO1H).

17. ^{21}Ne(d, ^{3}He)^{20}F $\qquad Q_{\rm m} = -7.510$

The ^{20}F states observed at $E_{\rm d} = 26$ MeV in this reaction and analog [$T = 1$] states observed in ^{20}Ne in the (d, t) reaction are displayed in Table 20.16 of (78AJ03). The spectroscopic factors of analog states are consistent to within 20% for states excited by a single l-transfer.

17.5 ^{21}Ne(t, α)^{20}F $\qquad Q_{\rm m} = 6.810$

Angular distributions were measured at $E_{\rm t} = 15.0$ MeV by (88LI10). States in ^{20}F up to $E_{\rm x} = 4.0$ MeV were observed and analyzed with DWBA calculations. Spectroscopic factors were deduced.

18. ^{22}Ne(p, ^{3}He)^{20}F $\qquad Q_{\rm m} = -15.649$

At $E_{\rm p} = 43.7$ to 45.0 MeV analog states have been studied in ^{20}F and ^{20}Ne [the latter via ^{22}Ne(p, t)^{20}Ne]. Angular distributions for the ^{3}He ions and the tritons corresponding to the first $T = 2$ states ($J^{\pi} = 0^{+}$) [^{20}Ne*(16.722 $\pm$ 0.025) and

^{20}F*(6.513 ± 0.033)] have been compared. There is indication also for the excitation of the 2^+; $T = 2$ states [at $E_x = 8.05$ MeV in ^{20}F and at 18.5 MeV in ^{20}Ne (estimated ± 0.1 MeV)]: see (78AJ03).

19. ^{22}Ne(d, α)^{20}F $\quad Q_m = 2.704$

Angular distributions have been obtained at $E_d = 10$ MeV to ^{20}F states with $E_x < 4.4$ MeV: they are generally featureless. Observed states are displayed in Table 20.17 of (78AJ03).

An experiment which would use this reaction to investigate the weak parity-nonconserving coupling in ^{20}F by observing the asymmetry in the gamma rays from the ^{20}F $E_x = 0.983$ MeV 1^- state has been proposed (93HO14, 93HO1N).

19.3 ^{23}Na(n, α)^{20}F $\quad Q_m = -3.866$

Reaction-model calculations for cross sections are described in (93ST10). The use of this reaction in connection with neutron detection is discussed in (87LE1G).

19.7 ^{24}Mg(n, pα)^{20}F $\quad Q_m = -15.559$

Cross sections calculated with pre-equilibrium emission, constant temperature evaporation models were reported in (93KH09).

20. ^{27}Al(^{20}Ne, ^{27}Si)^{20}F $\quad Q_m = -11.838$

The Δ resonance is very strongly excited in this reaction at $E(^{20}\text{Ne}) = 950$ MeV/A (86BA1P).

^{20}Ne

(Figs. 20.3 and 20.5)

GENERAL: See table 20.12.5.

Static quadrupole moment: $Q_{1.63} = -0.27 \pm 0.03$ $e \cdot$ b (78GR06)
$g_{1.63} = +0.54 \pm 0.04$ (75HO15)
$B(\text{E2})\uparrow\ [0 \rightarrow 1.63] = 0.0330 \pm 0.0015$ $e^2 \cdot \text{b}^2$ (78GR06). See also (87RA01).
Intrinsic haexadecapole moment: $Q_{4.25} = 0.022 \pm 0.003$ $e^2 \cdot \text{b}^2$ (78GR06)
$g_{4.25} = +0.13 \pm 0.15$ (86TR08). See also (84BR15).
Isotopic abundance: (90.51 ± 0.09)% (84DE1A).

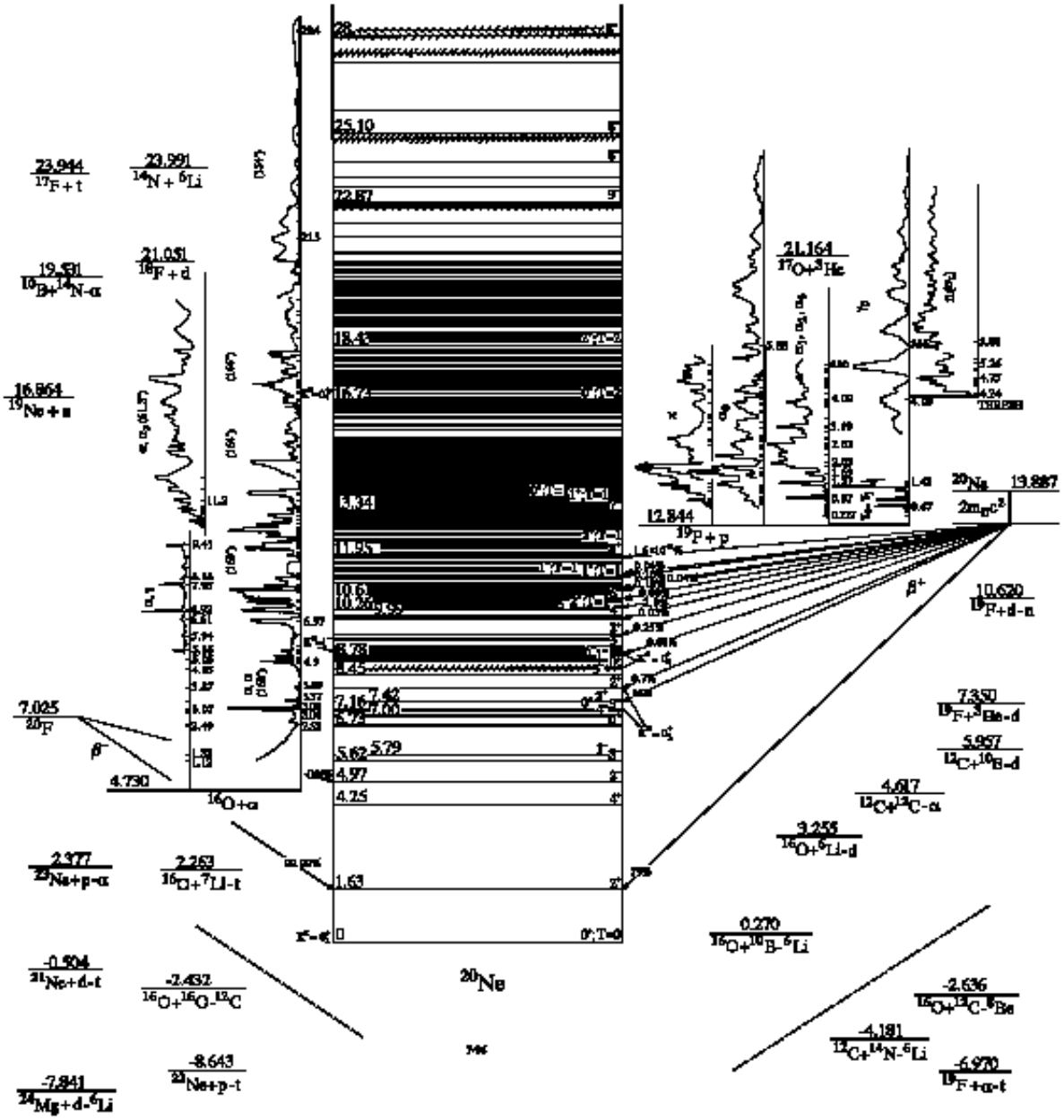

Figure 3: Energy levels of ^{20}Ne. For notation see fig. 1.

Table 20.12.5
^{20}Ne – General

Reference	Description
	Shell Model
Review:	
87SC1J	Microscopic nuclear structure theory in large single particle basis systems
88BR1P	Status of the nuclear shell model
88RA1G	Clustering phenomena & shell effects in nuclear structure and reactions
93PI1E	Unified shell-model picture of nuclear deformation
Other articles:	
87HA16	Test of the fermion dynamical symmetry model microscopy in the sd shell
87HA41	SU(3) × SU(4) limit of an isospin invariant fermion dynamical symmetry model
87HI08	Systematics of total strength & contribution of orbital current for M1 excitations
87KR08	Discontinuity in ground state band plot of even-even nuclei is traced to p-n interaction
87LI26	Rotational model and shell model pictures of magnetic dipole excitations
87MU16	Relativistic effects in the low-energy spectra of 1s0d-shell nuclei
87SU13	Symplectic model for isoscalar giant resonances & its coupling with cluster basis in ^{20}Ne
88BR11	Semi-empirical effective interactions for the 1s-0d shell
88CA09	Rotational collectivity in shell model wave functions for $A = 20$–28 nuclei
88FI01	Effective interactions from sd-shell-model calculations
88HI05	Effect on Gamow-Teller strength of config. mixing & p-n correlation in e-e sd-shell nucl.
88MU10	The BAGEL approach in the nuclear shell model
89CA05	Contracted symplectic model with sd-shell applications
89ET01	n-p weak coupling: reducing shell-model dimensions by truncations in n & p subspaces
89OR02	Empirical isospin-nonconserving Hamiltonians for shell-model calculations
89PO04	Shell-model realization of scissors mode; collective features described in Elliott's SU(3) limit
89SA26	Gamow-Teller & M1 strength sums for sd shell nuclei by spectral distribution methods
89SC14	Variational proced. for struct. calcs., beyond symmetry-projected quasi-particle mean fields
89ZH05	Evidence for unnatural parity-pairing correlations in some light nuclei
90BR26	Isospin-forbidden β-delayed proton emission
90DI12	Hybrid treatment of rotational symmetry; calc. low-lying states of ^{20}Ne, ^{21}Ne, ^{28}Si
90GU35	Calc. charge density distrib. using Hartree-Fock method & harmonic oscillator model
90HA07	Neutrino nucleosynthesis in supernovae: shell model predictions
90HA38	Resonating group model study of the ^{16}O + nucleon problem
90RE06	1^+ excitations in light nuclei: SU(3) versus realistic shell model results
90SK04	$A = 18$ nuclei, effective interaction in the sd shell (also calc. $A = 20$ energy spectra)
90ZH01	Nuclear structure studies of double Gamow-Teller and double beta decay strength
91BO45	Democratic mapping used to calc. low-lying states of sd- and fp-shell nuclei
91DU05	SU(3) Elliott model used to study the thermal description of ^{20}Ne; e.g. phase transitions
91MA41	Calculations of sd-shell nuclei with realistic potential models (Bonn, Paris, Argonne)
92GU02	Effective sd-shell interaction from nuclear multishell configurations
92HA1N	Cluster-orbital shell model applied to α-cluster formation in ^{20}Ne
92JI04	Bonn potential used to evaluate energy spectra of some light sd-shell nuclei using G-matrix
92JO07	Monte Carlo methods used to calc. the shell model Hamiltonian
92QU02	Effect of model space size on finite-temperature Hartree-Fock calculations
92RO08	Electron scattering multipoles for symplectic shell model applications
92WA22	Effective interactions for the 0p1s0d nuclear shell-model space
93AU01	Correlation between the quenching of total GT_+ strength and the increase of E2 strength

Table 20.12.5 (continued)
^{20}Ne – General

Reference	Description
	Shell Model (continued)
93KU1F	Criteria for distinguishing spherical nuclei; advantages of deformed-shell model
93LA24	Monte Carlo evaluation of path integrals for the nuclear shell model
93VO01	Spin-isospin SU(4) symmetry in sd- and fp-shell nuclei
94CI02	Specific heat and shape transitions in light sd nuclei: finite size vs. phase transition
94OR02	Application of auxilliary-field Monte Carlo techniques to GDR in hot nuclei
94VE04	Spectroscopic factors from one-proton stripping reactions on sd-shell nuclei
94ZH03	Systematic relativistic Hartree-Fock calculation of deformed nuclei in s-d shell
	Collective, Deformed & Rotational Models
Review:	
87TA1C	Microscopic cluster theory review from conf. on few-body syst. & multiparticle dynamics
Other articles:	
87HA41	SU(3) × SU(4) limit of an isospin invariant fermion dynamical symmetry model
87KR08	Discontinuity in ground state band plot of even-even nuclei is traced to p-n interaction
87LI26	Rotational model and shell model pictures of magnetic dipole excitations
87PA29	Relativistic mean-field theory used to describe ground-state deformation of nuclei
87PR03	Self-consistent Hartree description of deformed nuclei in a relativistic quantum field theory
87RE04	The generator coordinate method and quantised collective motion in nuclear systems
87SU13	Symplectic model for isoscalar giant resonances & its coupling with cluster basis in ^{20}Ne
88CA09	Rotational collectivity in shell model wave functions for $A = 20$–28 nuclei
88JO02	Relativistic DWBA calculations for proton inelastic scattering
89CA05	Contracted symplectic model with sd-shell applications
89KO13	A relativistic description of rotating nuclei: the yrast line of ^{20}Ne
89MI18	Evidence for phase transitions in finite systems
89MI1M	The phase structure of nuclei at low temperatures
89PO04	Shell-model realization of scissors mode; collective features described in Elliott's SU(3) limit
89RI1D	Relativistic mean field theory of nuclear structure
89RO1G	Broken symplectic dynamical symmetry in the microscopic collective model (A)
89TO05	α-decay widths of ground band of ^{20}Ne studied with cluster & deformed models
90CA07	Momentum distributions in axially symmetric deformed nuclei: the Nilsson model
90CO04	Effect of the continuum on thermally induced phase transitions in nuclei
90DI12	Hybrid treatment of rotational symmetry; calc. low-lying states of ^{20}Ne, ^{21}Ne, ^{28}Si
90GA09	Studies of (e, e$'\gamma$) reactions and electromagnetic currents in rotational nuclei
90PH01	Inelastic ^{20}Ne-$\vec{\text{p}}$ scattering data analyzed for evidence of a real tensor potential
90YA08	Competition between α clustering and the spin-orbit force in the ground bands of ^{20}Ne
91AM1A	Analysis of inelastic ^{20}Ne-p scattering (exciting gs rot. band) using several models
92HJ01	Folded-diagram effective interactions with the Bonn meson-exchange potential model
92RO16	Self-consistent anisotropic oscillator with cranked angular and vortex velocities
93BY03	Study of the quadrupole resonances in α-^{16}O scattering
93SA31	Dynamic microscopic basis for IBM-2; compared with shell model calcs. & exp. data
94CI02	Specific heat and shape transitions in light sd nuclei: finite size vs. phase transition
94MI05	Correlated finite temperature mean field approximations

Table 20.12.5 (continued)
^{20}Ne – General

Reference	Description
	Cluster Models
Reviews:	
87TA1C	Microscopic cluster theory review from conf. on few-body syst. & multiparticle dynamics
88RA1G	Clustering phenomena & shell effects in nuclear structure and reactions
Other articles:	
87DE40	The α+^{20}Ne cluster structure of ^{24}Mg in a microscopic three-cluster model
87KA24	Structure of yrast states in ^{20}Ne investigated in the framework of a cluster model
87SA55	The orthogonality condition model applied to (α, α) scattering on ^{12}C and ^{16}O
87SU13	Symplectic model for isoscalar giant resonances & its coupling with cluster basis in ^{20}Ne
88CS01	Core-plus-alpha-particle states of ^{20}Ne and ^{16}O in terms of vibron models
88KA1Z	Systematic construction method of multi-cluster Pauli-allowed states
88LE05	Distribution of alpha-particle strength in light nuclei
88LE06	Influence of target clustering on exchange effects in internuclear interaction
89DE32	Distortion effects in a microscopic ^{16}O + 2α and ^{20}Ne + α description of ^{24}Mg
89GA05	Parity-dependent potential for ^{16}O + ^{20}Ne (linear combination of nuclear orbitals model)
89RU08	Binding energies & gs band levels of light nuclei in the strictly restricted dynamics model
89TO05	α-decay widths of ground band of ^{20}Ne studied with cluster & deformed models
90BA01	α-like part of four-nucleons moving in a single-particle potential of arbitrary shape
90VA14	Features of α-cluster type nuclei in the framework of the restricted dynamics model
90YA08	Competition between α clustering and the spin-orbit force in the ground bands of ^{20}Ne
91CS01	Cluster spectroscopic factor in the vibron model
91OM03	The role of the Pauli principle in the elastic scattering of α + ^{16}O clusters
91SZ02	Alpha particles from the reaction ^{12}C + ^{12}C at 28.7 MeV/nucleon
91WA11	Composite Particle Representation Theory calcs. for $A = 20$ nuclei compared to shell model
92AN1F	α-particle momentum distributions in nuclei in the coherent density fluctuations model
92AR11	α-cluster structure of excited states in light nuclei
92CS03	The relation between cluster and superdeformed states of light nuclei
92HA1N	Cluster-orbital shell model applied to α-cluster formation in ^{20}Ne
92KR12	Elimination of Pauli resonances in the generator-coordinate description of scattering
92ME09	Alpha-chain states in 4N-nuclei from ^{20}Ne to ^{32}S
92ME11	Systematics of alpha-chain states in 4N-nuclei
93AB02	α-^{16}O & α-^{15}N optical potentials in the range between 0 and 150 MeV
93BY03	Study of the quadrupole resonances in α-^{16}O scattering
93CS03	^{16}O+α cluster states in terms of a $U_q(3)$ anharmonic oscillator model
93LI25	Alpha-particle elastic scattering on ^{16}O in the four α-particle model
93RA1G	Shape eigenstates & other one- and two-dimensional α-cluster structures in light nuclei
93SZ02	Treatment of hot composite systems (^{19}F & ^{20}Ne) as liquid droplets
93VA07	Relation between phenomenological algebraic cluster model & effective nn forces
93YA08	Description of α + ^{16}O elastic scattering by a single-folding potential
93ZH22	Systematics of 2-dimensional α-cluster configurations in 4N nuclei from ^{12}C to ^{44}Ti
94ME18	Alpha chain states in 4N-nuclei
94RA03	Geometry and collectivity in the Bloch-Brink α-cluster model
94TO04	New effective internucleon forces in microscopic α-cluster model

Table 20.12.5 (continued)
^{20}Ne – General

Reference	Description
	Special states
Reviews:	
87SC1J	Large-scale nuclear structure studies
88RA1G	Clustering phenomena & shell effects in nuclear structure and reactions
92MA29	High spin spectra in light nuclei in terms of the rotating harmonic oscillator
93EN03	Strengths of γ-ray transitions in $A = 5$–44 nuclei
Other articles:	
87BL18	Gogny's effective inter. used to calc. ground & excited states of specific spin-isospin order
87CO31	Simple parametrization for low energy octupole modes of sd-shell nuclei
87DE40	The $\alpha + {}^{20}$Ne cluster structure of ^{24}Mg in a microscopic three-cluster model
87KA24	Structure of yrast states in ^{20}Ne investigated in the framework of a cluster model
87MU16	Relativistic effects in the low-energy spectra of 1s0d-shell nuclei
87PR03	Self-consistent Hartree description of deformed nuclei in a relativistic quantum field theory
87SU13	Symplectic model for isoscalar giant resonances & its coupling with cluster basis in ^{20}Ne
88BA16	Dynamics of nuclear integral characteristics
88CA09	Rotational collectivity in shell model wave functions for $A = 20$–28 nuclei
88GU12	Electron scattering from ^{20}Ne (and other light nuclei) and transition charge densities
88KU07	Electron scattering from ^{20}Ne and ^{24}Mg in a microscopic boson model
88KU17	Microscopic boson descrip. of p-n systems applied to electron scatt. from ^{18}O and ^{20}Ne
88KU22	Microscopic foundation of the interacting boson model in sd-shell nuclei
88MU10	The BAGEL approach in the nuclear shell model
88ST04	Spectral distribution calculations of the level density of ^{20}Ne
89DE12	Spectroscopy of ^{20}Ne & ^{24}Mg nuclei in the interacting boson model including g bosons
89ET01	n-p weak coupling: reducing shell-model dimensions by truncations in the n & p subspaces
89KO13	A relativistic description of rotating nuclei: the yrast line of ^{20}Ne
89PO04	Shell-model realization of scissors mode; collective features described in Elliott's SU(3) limit
89PO05	Isobaric multiplets reconstructed from the equidistance rule for separation & decay energies
89RO1G	Broken symplectic dynamical symmetry in the microscopic collective model (A)
89SC14	Extension of the variational mean field procedure for structure calcs.
89TO05	α-decay widths of ground state band of ^{20}Ne studied with cluster & deformed models
89ZH05	Evidence for unnatural parity-pairing correlations in some light nuclei
90AM01	Large basis space effects in electron scattering form factors of ^{12}C, ^{20}Ne, ^{24}Mg
90RE06	1^+ excitations in light nuclei: SU(3) versus realistic two-rotor and shell model results
90SK04	$A = 18$ nuclei, effective interaction in the sd shell (also calc. $A = 20$ energy spectra)
90YA08	Competition between α clustering and the spin-orbit force in the ground bands of ^{20}Ne
91BA25	Collective 3^- and 2^- excitations with Skyrme forces
92CA05	Fragmentation of stretched spin strength in $N{=}Z$ sd-shell nuclei
92DE31	Higher order deformations in sd-shell nucl. from CC analysis of inelastic $\vec{p}$ scattering
92HA18	Coupled-channel description of rotational and vibrational states in ^{20}Ne and ^{22}Ne
93PA25	Shapes of $N{=}Z$ nucl. studied with axially symmetric deformed relativistic mean-field theory
93PE18	Nucleon pair structure of realistic many body wave functions
94HE1A	Systematics of rotational isomers & band terminations in the $A = 20$–26 region

Table 20.12.5 (continued)
^{20}Ne – General

Reference	Description
	Electromagnetic
Reviews:	
89RA16	Predictions of B(E2; $0_1^+ \rightarrow 2_1^+$) values for even-even nuclei
89SP01	Reduced electric-octupole transition probabilities, B(E3; 0_1^+–3_1^-), for even-even nucl.
93EN03	Strengths of γ-ray transitions in $A = 5$–44 nuclei
Other articles:	
86SC1E	Large scale calculations of the nuclear spectrum (calc. isoscalar E2 resonance in ^{20}Ne)
87HI08	Systematics of total strength & contribution of orbital vs. spin current for M1 excitations
87SU13	Symplectic model for isoscalar giant resonances & its coupling with cluster basis in ^{20}Ne
88BA80	Dynamics of integral characteristics of atomic nuclei (M2 resonance calc. for ^{20}Ne)
89CA05	Contracted symplectic model with ds-shell applications (calc. excit. spectra & E2 strengths)
89DE12	Spectroscopy of ^{20}Ne & ^{24}Mg nuclei in the interacting boson model including g bosons
89ET01	n-p weak coupling: reducing shell-model dimensions by truncations in n & p subspaces
89PO04	Shell-model realization of scissors mode; collective features described in Elliott's SU(3) limit
89RO1G	Broken symplectic dynamical symmetry in the microscopic collective model (A)
89SA26	Gamow-Teller and M1 strength sums for sd-shell nuclei by spectral distribution methods
89VAZN	E2 transition probabilities in strongly restricted dynamics model
90GUZV	Calc. charge density distrib., rms radii, moments by Hartree-Fock meth& harm. osc. model
90RE06	1^+ excitations in light nuclei: SU(3) versus realistic two-rotor and shell model results
92HE17	Manifestation of quadrupole collectivity in the magnetic dipole strength
92ZA10	Relation between E2 and orbital M1 transition strengths using a $Q \cdot Q$ interaction
93AU01	Correlation between the quenching of total GT_+ strength and the increase of E2 strength
93RUZX	Electromagnetic properties of light nuclei in the strictly restricted dynamics model
	Astrophysics
Reviews:	
86WO1A	Physics of supernova explosions
87RA1D	Nuclear processes and accelerated particles in solar flares
88BA1H	Solar models, neutrino experiments, and helioseismology
89AR1R	Supernova 1987A: observations, analysis, implications
90AR10	Nuclear reactions in astrophysics
90SC1N	New physics from supernova 1987A
90SI1D	Spallation processes and nuclear interaction products of cosmic rays
93HA1D	Core-collapse supernovae & other topics that combine nuclear, particle, and astrophysics
93LE1J	Solar-neutrino problem (A)
Other articles:	
87DW1A	Cosmic-ray elemental abundances from 1 to 10 GeV per amu for boron through nickel
88AP1B	Primordial nucleosynthesis as a probe of cosmological QCD
88BU01	Stellar reaction rates of α capture on light ($N \neq Z$) nuclei; astrophysical implications
88CA1N	Reaction rates of astrophysically important thermonuclear reactions involving light nucl.
88CU1A	Compos. of anomalous cosmic-ray component; implications for local interstellar medium (A)
88FO1E	Observ. & analysis of 27 April 1981 flare yield info on solar atmosphere elem. abundances
88MA1U	Late-time neutron diffus. & nucleosynthesis in a post-QCD inhomogeneous $\Omega_b = 1$ universe

Table 20.12.5 (continued)
^{20}Ne – General

Reference	Description
	Astrophysics (continued)
88RE1F	Solar neon abundances from gamma-ray spectroscopy and ^{3}He-rich particle events
88WO1C	Supernova neutrinos, neutral currents and the origin of fluorine
89BE2H	The effect of enhanced α-elements in helium-burning population II stars
89GO1N	Hydrogen burning in the NeNa cycle: ^{23}Na(p, α)^{20}Ne and ^{23}Na(p, γ)^{24}Mg
89GU1I	Thermonuclear breakup reactions of light nuclei, part 1: Processes and effects
89GU1J	Thermonuclear ... " , part 2: Gamma-ray line production and other applications
89GU1Q	Abundance of ^{14}N at the cosmic-ray source obtained using new fragmentation cross sections
89HE1N	O & Ne abundance in planetary nebulae: implications for stellar nucleosynthesis
89JI1A	Nucleosynthesis inside thick accretion disks around massive black holes
89ME1C	Isotope abundances of solar coronal material derived from solar energetic particle meas.
89SA26	Gamow-Teller & M1 strength sums for sd-shell nuclei by spectral distribution methods
89TA26	Microscopic calc. of rates of electron captures which induce O + Ne + Mg core collapse
90BL1K	Slowly accreting neutron stars and the origin of gamma-ray bursts
90CO1N	Space-based meas. of elemental abundances and their relation to solar abundances
90HA07	Neutrino nucleosynthesis in supernovae: shell model predictions
90MU1H	Nuclear line spectroscopy of the 27 April 1981 solar flare
90SI1A	An explanation for cosmic-ray source abundances including nitrogen
90TH1C	Explosive nucleosynthesis in SN 1978A: composition, radioactivities & neutron star mass
90WE1A	Total charge and mass changing cross sections of relativistic nuclei in H, He, C targets
90WE1I	Cosmic-ray source charge & isotopic abund. obtained using new fragmentation X-sects.
91RA1C	Carbon burning and galactic enrichment in massive stars
92CA1J	Quasi-static evolution of ONeMg cores, explosive ignition densities & the collapse explosion
93DE32	Microscopic three-cluster study of 21-nucleon systems
94PA42	Exp. limit on ^{19}Ne(p, γ)^{20}Na resonance strength; implications for stellar H burning
	Complex reactions
86MA13	Experimental search for nonfusion yield in the heavy residues emitted in ^{11}B + ^{12}C
87BA1T	Spin-isospin excitations in nuclei with relativistic heavy ions
87BE1F	Target fragmentation at ultrarelativistic energies
87BO23	Intermediate-mass fragments from nonbinary processes in ^{14}N + ^{nat}Ag at $E/A = 35$ MeV
87BU07	Projectile-like fragments from ^{20}Ne + ^{197}Au – counting simultaneously emitted neutrons
87KA2B	Measurement of the decay time of excited products of inelastic Ne + Ge interactions
87LY04	Fragmentation and the emission of particle stable and unstable complex nuclei
87MU03	Study of the emission of clusters by excited compound nuclei
87SH23	Dissipative phenomena and α-particle emission in ^{16}O + ^{27}Al between 46 and 85 MeV
87SO1D	Angular momentum dependence of complex fragment emission
87SU07	Correlated fluctuations in the ^{89}Y(^{19}F, x)y excitation functions
87VI1B	Mechanisms of momentum and energy transfer in intermediate-energy collisions
87WA1P	Radioactive decay of ^{234}U via Ne and Mg emission
87YI1A	Research for the deep inelastic collision induced by 93 MeV ^{14}N on ^{nat}Ca (A)
88AI1A	Quantum molecular dynamics approach to HI collisions compared to fragmentation data
88CA1G	Experimental indications of selective excitations in disspative heavy ion collisions

Table 20.12.5 (continued)
^{20}Ne – General

Reference	Description
	Complex Reactions (continued)
88CE01	Multifragmentation & incomplete fusion in heavy ion collisions; schematic model
88CH28	Nucleon transfer contribution to absorptive heavy ion potential by Monte Carlo simulation
88GA1K	Formation and decay of hot nuclei
88MI1I	Multifragmentation as a possible signature of liquid-gas phase transitions
88SM1B	Cross section for the ^{12}C(^{139}La, X)^{11}C reaction at relativistic energies
88UT02	Quasi-free stripping reactions studied using extended Serber model
89BA2N	Strangeness production by heavy ions
89BE17	Fusion of ^{16}O + ^{40}Ca at $E_{\rm lab}(^{16}{\rm O}) = 13.4$ MeV/nucleon
89BR1G	Fragmentation cross sections of ^{28}Si at 14.5 GeV/nucleon
89CA15	Fusion and binary reactions in the collision of 32S on 26Mg at Elab=163.5 MeV
89FI05	Non-eq. vs. equilibrium emission of complex frag. emiss; ^{14}N + Ag,Au at $E/A = 20$–50 MeV
89GH01	Subthreshold π^0 production in heavy-ion collisions induced by nuclear cooperation
89HO16	Radioactivities by light fragment (C, Ne, Mg) emission
89KI13	Fragment production in ^{14}N + C, Ni, Ho reactions at 35 MeV/nucleon
89MA45	Target excitation & ang. mom. transfer in ^{28}Si + ^{181}Ta from multiplicity meas.
89PA06	Complete & incomplete fusion of 6 MeV/nucleon light heavy ions on ^{51}V
89SA10	Total cross sections of reactions induced by neutron-rich light nuclei
89YO09	Energy damping feature in light heavy-ion reactions
89ZHZV	Mass measurement of $Z = 7$–19 neutron-rich nuclei using the TOFI spectrometer (A)
90BEYY	Production of neutron-rich He isotopes in the ^{9}Be + ^{18}O reaction
90BL09	Elastic magnetic electron scattering and vacuum polarization
90BO01	Critical excitation energy in fusion-evaporation reactions
90BO04	Three paths for intermediate-mass fragment formation from 640 MeV ^{86}Kr + ^{63}Cu
90BO16	Revising the chart of the nuclides by exotic decay
90CH09	Coulomb-modified Glauber model description of heavy-ion reaction cross sections
90FO04	One-nucleon-transfer reactions induced by ^{20}Ne at 500 and 600 MeV
90GU08	Deviations from pure target fragmentation in ^{16}O induced heavy ion reactions
90WE1A	Total charge & mass changing cross sections of relativistic nuclei in H, He & C targets
90YE02	Intermediate mass fragment emission in the 161-MeV p + Ag reaction
91LI33	Subthreshold pion production in nucleus-nucleus collisions; quantum molecular dynamics
	Muons & Neutrinos
87HE1D	Nuclear charge radii of stable neon isotopes from muonic atoms
89AD1C	Coherent pion prod. by charged-current interactions of neutrinos & antineutrinos on Ne
89MA1U	Coherent production of π^+ mesons in ν-neon interactions
89SO1C	Radiative muon capture in light atoms
90CH13	Muon capture rates in nuclei calculated & compared to experimental values
90DE1I	Neutral strange particle production in ν_μ-Ne interactions (A)
90HA07	Neutrino nucleosynthesis in supernovae: shell model predictions
90LA1M	Proton production in charged-current ν_μNe interactions (A)
92FR01	Nuclear charge radii systematics in the sd shell from muonic atom measurements
92RO09	Hyperfine interaction of μ^- & an e^- shell in forming P-odd correlations in μ^{20}Ne

Table 20.12.5 (continued)
^{20}Ne – General

Reference	Description
	Pions & Kaons
Reviews:	
88BA82	Production and decay of hypernuclei
88HA12	Charge exchange reactions and the study of giant resonances
Other articles:	
87SU1I	Neutral pion production cross sections in Ne + NaF collisions from 80 to 219 MeV/nucleon
88EL06	On the s-wave repulsion of the pion-nuclear interaction
88FR02	Strong-interaction finite-range effects in light pionic atoms
88RO19	Photoproduction of ^{20}F(Λ); analogy to ^{20}Ne(Λ) also discussed
89AD1C	Coherent pion prod. by charged-current interactions of neutrinos & antineutrinos on Ne
89GA09	Pionic distortion factors for radiative pion capture studies
89GE10	Threshold pion-nucleus amplitudes as predicted by current algebra
89GH01	Subthreshold π^0 prod. via ^{16}O and ^{27}Al beams at E = 38–200 MeV/A by nucl. cooperation
89KA37	Finite-range effects in pionic atoms
89MA1U	Coherent production of π^+ mesons in ν-neon interactions
89SH1N	Subthreshold $\bar{p}$, K^-, K^+, and energetic-pion production in relativistic nuclear collisions
89WA14	Mesonic atom production in high-energy nuclear collisions
89ZU02	Statistical description of multiple production of π-mesons in nuclear collisions
91AM1B	Scaling properties of π^- spectra in π^- Ne interactions at initial momentum 6.2 GeV/c
91CI08	Momentum-space method for pionic atoms
91CI11	Nuclear structure effects in light π-mesoatoms
91GO21	Pionic atoms, the relativistic mean-field theory and the pion-nucleon scattering lengths
91LI33	Subthreshold pion production in nuclear collisions; quantum molecular dynamics approach
92KI1C	Multiplicities of secondary particles in inelastic π^- + Ne at initial momentum 6.2 GeV/c
93PE09	Isospin symmetry in nuclear transitions from pion scattering
	Antiproton
Review:	
89CU06	Summary of experimental work on antiproton-nucleus interactions
Other articles:	
87BA2G	Neutral strange-particle production in $\bar{p}$ ^{20}Ne reactions at 607 MeV/c
87DA12	$\bar{p}$-nucleus scattering at E = 20–200 MeV; Glauber approx. compared to data
87DA1D	Interaction of low-energy antiprotons with nuclei
88CU03	Charge distribution and charge correlation in the annihilation of antiprotons on nuclei
88CU1D	Dynamical model of antiproton annihilation on nuclei
88SI1E	Recent results on antiprotonic atoms using a cyclotron trap at LEAR
89BA10	Antiproton-neon annihilation at rest and at 607 MeV/c
89BA1S	An observation of a leading meson in $\bar{p}$ + Ne reaction at 607 MeV/c incident momentum
89TO1D	Strangeness production by antiprotons
90CU01	Strangeness production in antiproton annihilation on nuclei
90CU04	Antiproton annihilation at rest on light nuclei
91BA18	Strangeness production in antiproton annihilation at rest on ^{3}He, ^{4}He and ^{20}Ne
91BA49	Glueball candidates seen in the reactions $\bar{p}$ ^{20}Ne and $\bar{p}$ ^{4}He at 607 MeV/c

Table 20.12.5 (continued)
^{20}Ne – General

Reference	Description
	Antiproton (continued)
91KH09	Strange-particle production in antiproton annihilation on nuclei at low energies
91MA1D	Coherent production of a_1^- mesons and $(\rho\pi)^-$ systems by antineutrinos on neon
93DA1N	Observation of parton fragmentation in $\bar{p}$ ^{20}Ne reactions at 607 MeV/c
93ZA01	$\bar{p}$ annihilation on nuclei at $E = 50$–2000 MeV as a result of one or more collisions
	Hypernuclei
87SA1Q	Structure of ^{20}Ne(Λ) hypernucleus: prediction of the negative parity ground state
88BA82	Production and decay of hypernuclei using the (π, K^+) reaction
88IW1A	Isotropic features of Λ-particle production in central collisions of light nuclei; cascade model
88MA1Q	Identification of one glue-like mechanism of the Λ-hyperon in hypernuclei
88RO19	Photoproduction of ^{20}F(Λ) via ^{20}Ne(γ, K^+)^{20}F(Λ); analogy to ^{20}Ne(Λ) also discussed
88WA1H	Hypernucleus formation in high-energy nuclear collisions
89TO1D	Strangeness production by antiprotons
	Other topics
87HA16	Test of the fermion dynamical symmetry model microscopy in the sd shell
87LI34	Probability of forming six-quark clusters and the increase of nucleon radius in nuclei
87SA1P	Spectral distribution calculations using Wildenthal's universal sd interaction
88BO27	Quasiparticle model for nuclear dynamics studies used to calc. ground state properties
88HI05	Effect on Gamow-Teller strength of config. mixing & p-n correlation in e-e sd-shell nucl.
88ME09	Three-dimensional, spherically symmetric, saturating model of an N-boson condensate
88ST04	Spectral distribution calculations of the level density of ^{20}Ne; Lanczos method
89FI04	Systematic study of potential energy surfaces of light nuclei in relativistic Hartree calcs.
89MI1M	The phase structure of nuclei at low temperatures studied in the canonical ensemble
89OR02	Empirical isospin-nonconserving Hamiltonians for shell-model calculations
89PO05	Isobaric multiplets reconstructed from the equidistance rule for separation & decay energies
89QU01	Comparison of finite temperature Hartree-Fock approximation & canonical ensemble calcs.
89QU1A	Strategy for finding low-lying solutions of the restricted nuclear Hartree-Fock equations
89RO01	Fission barrier of projectiles in heavy-ion reactions
90CO04	Effect of the continuum on thermally induced phase transitions in nuclei
90PR1B	Electron capture by protons from K-shell of C, N, O, Ne and Ar; binary encounter approx.
91RE10	Fast-neutron-induced cross sections on ^{20}Ne, theory vs. experiment, $E = 1$–30 MeV
92CA19	Dynamical dependence of thermal phase transformations in finite systems
92GR11	Parameterization of the nuclear level density at energies above 100 MeV
92MU01	Nuclear level densities at high excitations
93SZ02	Treatment of hot composite systems (^{19}F & ^{20}Ne) as liquid droplets
93ZH18	Effects of the Dirac sea on deformed nuclei (^{20}Ne & ^{24}Mg)

Table 20.12.5 (continued)
^{20}Ne – General

Reference	Description
	Ground state properties
Reviews:	
89RA17	Compilation of exp. data on nuclear moments for ground & excited states of nuclei
92PY1A	Nuclear quad. moments for $Z = 1$–20 rev., related to numerical methods in quant. chem.
Other articles:	
87BL18	Gogny's effective inter. used to calc. ground & excited states of specific spin-isospin order
87FU12	Systematics of even-even sd-shell nuclei in relativistic mean-field models
87HE1D	Nuclear charge radii of stable neon isotopes from muonic atoms
87PA29	Relativistic mean-field theory used to describe ground-state deformation of nuclei
87PR03	Self-consistent Hartree description of deformed nuclei in a relativistic quantum field theory
87SA1P	Spectral distribution calcs. using Wildenthal's universal sd interaction
88AI1A	Quantum molecular dynamics approach to HI collisions compared to fragmentation data
88BO27	Quasiparticle model for nuclear dynamics studies used to calc. ground state properties
88DO17	Classical simulation of nuclear systems; calc. sizes and binding energies of finite nuclei
88ME09	Three-dimensional, spherically symmetric, saturating model of an N-boson condensate
88RA1G	Clustering phenomena & shell effects in nuclear structure and reactions
88ZH09	Relativistic Hartree calculation of deformed $A = 16$–40 nucl.; underpredict deformations
89AN12	A-dependence of the difference $(r_{el} - r_{mu})$, a dispersion effect in electron scattering
89FI04	Systematic study of potential energy surfaces of light nuclei in relativistic Hartree calcs.
89GA05	Parity-dependent potential for $^{16}O + ^{20}Ne$ (linear combination of nuclear orbitals model)
89GA16	Relativistic mean-field description of ground-state nuclear properties
89KO13	A relativistic description of rotating nuclei: the yrast line of ^{20}Ne
89RU08	Binding energies & grnd. state band levels of light nucl.; strictly restricted dynamics model
89SA10	Total cross sections of reactions induced by neutron-rich light nuclei
89TO05	α-decay widths of ground band of ^{20}Ne studied with cluster & deformed models
90GA10	Relativistic mean field theory for finite nuclei
90GU10	Charge densities of sp- and sd-shell nuclei & occupation numbers of 2s states
90GUZV	Calc. charge density distrib., rms radii, moments by Hartree-Fock meth& harm. osc. model
90LO11	Self-consistent calcs. of light nuclei using density-functional method
90MA63	Correlated charge form factor and densities of the s-d shell nuclei
90VA14	Features of α-cluster type nuclei in the framework of the restricted dynamics model
91PO11	Single-nucleon transfer sum-rules in the 2s1d shell; compared to data
91ZH02	Relativistic Hartree-Fock calcs. of deformed nuclei in rel. quantum-field-theory framework
91ZH05	Vacuum polariztion in a relativistic description of open shell nuclei
91ZH06	Relativistic Hartree study of deformed nucl.; binding energies, moments, single part. spec.
92FR01	Behavior of nuclear charge radii systematics in the sd shell from muonic atom meas.
92KN06	Exchange correlation function and surface effects; uses density matrix formalism
92RO06	Correlated finite temperature mean field approximations comp. with canonical results
92ZA10	Relation between E2 and orbital M1 transition strengths using a $Q \cdot Q$ interaction
93GO38	^{20,22}Ne masses determined by Fourier transform ion cyclotron resonance mass spectrometry
93PA25	Shapes of light N=Z nucl. studied using axially symmetric deformed rel. mean-field theory

(A) denotes that only an abstract is available for this reference.

Table 20.13
Energy Levels of ^{20}Ne [a])

E_x (MeV ± keV)	J^π; T	K^π	τ [b]) or Γ	Decay	Reactions
0	0^+; 0	0_1^+		stable	2, 3, 7, 8, 12, 15, 16, 18, 20, 24, 25, 29, 30, 31, 32, 33, 34, 35, 36, 37, 38, 39, 40, 41, 42, 43, 45, 46, 47, 48, 49, 50, 51, 52, 53, 54, 56, 57, 58, 59, 60, 61, 62, 63, 64
1.633674 ± 0.015	2^+; 0	0_1^+	$\tau_m = 1.05 \pm 0.06$ ps $g = +0.54 \pm 0.04$	γ	2, 3, 7, 8, 9, 11, 12, 15, 16, 18, 19, 20, 23, 24, 25, 29, 30, 31, 32, 33, 35, 36, 40, 41, 42, 43, 46, 47, 49, 52, 53, 54, 55, 56, 57, 60, 61
4.2477 ± 1.1	4^+; 0	0_1^+	$\tau_m = 93 \pm 9$ fs $g = +0.13 \pm 0.15$	γ	2, 3, 7, 8, 9, 12, 15, 16, 18, 19, 20, 23, 24, 29, 30, 31, 32, 33, 36, 38, 41, 42, 47, 54, 57, 60, 61
4.96651 ± 0.20	2^-; 0	2^-	$\tau_m = 4.8 \pm 0.5$ ps	γ	2, 3, 7, 8, 9, 12, 15, 24, 25, 29, 30, 31, 32, 33, 54, 56, 57, 60, 61
5.6214 ± 1.7	3^-; 0	2^-	$\tau_m = 200 \pm 50$ fs	γ, α	2, 3, 7, 8, 12, 15, 29, 30, 32, 33, 55, 56, 57, 60, 61
5.7877 ± 2.6	1^-; 0	0^-	$\Gamma_{cm} = (2.8 \pm 0.3) \times 10^{-2}$ keV	γ, α	2, 3, 7, 8, 12, 14, 15, 16, 18, 30, 32, 33, 52, 55, 60
6.725 ± 5	0^+; 0	0_2^+	$\Gamma_{cm} = 19.0 \pm 0.9$ keV	γ, α	8, 12, 14, 15, 24, 29, 30, 32, 33, 36, 52, 60
7.004 ± 3.6	4^-; 0	2^-	$\tau_m = 440 \pm 90$ fs	γ	2, 7, 8, 15, 30, 33, 56, 60
7.1563 ± 0.5	3^-; 0	0^-	$\Gamma_{cm} = 8.2 \pm 0.3$ keV	γ, α	2, 4, 7, 8, 14, 15, 16, 18, 20, 23, 24, 29, 30, 52
7.191 ± 3	0^+; 0	0_3^+	$\Gamma_{cm} = 3.4 \pm 0.2$ keV	γ, α	5, 6, 7, 12, 14, 36, 60
7.4219 ± 1.2	2^+; 0	0_2^+	$\Gamma_{cm} = 15.1 \pm 0.7$ keV	γ, α	2, 5, 6, 7, 12, 14, 15, 29, 30, 32, 36, 53, 55, 60
7.829 ± 2.4	2^+; 0	0_3^+	$\Gamma_{cm} = 2$ keV	γ, α	2, 6, 7, 12, 14, 24, 30, 36, 53, 55, 60
8.453 ± 4	5^-; 0	2^-	$\Gamma_{cm} = 0.013 \pm 0.004$ keV	γ, α	2, 6 7, 12, 14, 15, 30, 60
≈ 8.7	0^+; 0	0_4^+	$\Gamma_{cm} > 800$ keV	α	14
8.708 ± 7	1^-; 0		$\Gamma_{cm} = 2.1 \pm 0.8$ keV	γ, α	7, 12, 14, 30, 60
8.7776 ± 2.2	6^+; 0	0_1^+	$\Gamma_{cm} = 0.11 \pm 0.02$ keV	γ, α	2, 4, 6, 7, 8.3, 12, 14, 15, 16, 18, 19, 20, 23, 24, 30, 52, 60

Table 20.13 (continued)
Energy Levels of ^{20}Ne [a])

E_x (MeV ± keV)	J^π; T	K^π	τ [b]) or Γ	Decay	Reactions
8.82	(5^-); 0		$\Gamma_{cm} < 1$ keV	α	14
8.854 ± 5	1^-; 0	1^-	$\Gamma_{cm} = 19$ keV	α	7, 14, 55
9.00 ± 180	2^+; 0	0_4^+	$\Gamma_{cm} \approx 800$ keV	α	14, 30, 39.3
9.031 ± 7	4^+; 0	0_3^+	$\Gamma_{cm} = 3$ keV	γ, α	2, 6, 7, 12, 14, 24, 30, 60
9.116 ± 3	3^-; 0		$\Gamma_{cm} = 3.2$ keV	γ, α	2, 7, 12, 14, 29, 30, 60
9.318 ± 2	(2^-); 0			γ	7, 12, 30, 60
9.487 ± 5	2^+; 0		$\Gamma_{cm} = 29 \pm 15$ keV	γ, α	12, 14, 53, 60
9.873 ± 4	3^+; 0			γ	7, 30, 53
9.935 ± 12	(1^+); 0		$\tau_m < 35$ fs	γ	7, 30, 60
9.990 ± 8	4^+; 0	0_2^+	$\Gamma_{cm} = 155 \pm 30$ keV	γ, α	2, 7, 12, 14, 29, 30, 60
10.262 ± 5	5^-; 0	0^-	$\Gamma_{cm} = 145 \pm 40$ keV	α	2, 4, 7, 14, 15, 16, 18, 20, 30, 52
10.274 ± 3	2^+; 1		$\Gamma_{cm} \leq 0.3$ keV	γ, α	12, 14, 53, 55
10.406 ± 5	3^-; 0	1^-	$\Gamma_{cm} = 80$ keV	α	7, 14, 30, 60
10.553 ± 5	4^+; 0		$\Gamma_{cm} = 16$ keV	α	7, 14, 30
10.584 ± 5	2^+; 0		$\Gamma_{cm} = 24$ keV	α	14, 30, 53, 60
10.609 ± 6	6^-; 0	2^-	$\tau_m = 23 \pm 7$ fs	γ	2, 6, 7
10.694 ± 6	4^-, 3^+; 0			γ	6, 7
10.80 ± 75	4^+; 0	0_4^+	$\Gamma_{cm} = 350$ keV	α	14, 15, 30
10.843 ± 4	2^+; 0		$\Gamma_{cm} = 13$ keV	α	14, 53, 60
10.840 ± 6	3^-; 0		$\Gamma_{cm} = 45$ keV	γ, α	7, 14
10.884 ± 3	3^+; 1		$\tau_m < 30$ fs	γ	53, 55
10.917 ± 6	3^+; 0			γ	7
10.97 ± 120	0^+; 0	0_5^+	$\Gamma_{cm} = 580$ keV	α	14
11.020 ± 8	4^+; 0		$\Gamma_{cm} = 24$ keV	α	6, 7, 14, 60
11.090 ± 3	4^+; 1		$\Gamma_{cm} \leq 0.5$ keV	γ, α	12, 14, 30, 55
11.24 ± 23	1^-; 0		$\Gamma_{cm} = 175$ keV	α	14, 30
11.2623 ± 1.9	1^+; 1			γ	12, 35, 36, 38, 53
11.270 ± 5	1^-; 1		$\Gamma_{cm} \leq 0.3$ keV	γ, α	12, 14
11.320 ± 9	2^+; 0		$\Gamma_{cm} = 40 \pm 10$ keV	α	14, 53
11.528 ± 6	3^+, 4^-; 0		$\tau_m \leq 30$ fs	γ	7, 30
11.555 ± 6	(3^+); 0			γ	7, 30
11.558 ± 4	0^+; 0	0_6^+	$\Gamma_{cm} = 1.1 \pm 0.4$ keV	γ, α	12, 14

Table 20.13 (continued)
Energy Levels of ^{20}Ne [a])

E_x (MeV ± keV)	J^π; T	K^π	τ [b]) or Γ	Decay	Reactions
11.601 ± 10	2^-; 1				55
11.653 ± 5	(3^+); 0			γ	6, 7, 36
11.885 ± 7	2^+; 0		$\Gamma_{cm} = 46$ keV	γ, α	7, 14, 30, 53, 60
11.928 ± 4	4^+; 0		$\Gamma_{cm} = 0.44 \pm 0.15$ keV	γ, α	12, 14, 60
11.951 ± 4	8^+; 0	0_1^+	$\Gamma_{cm} = (3.5 \pm 1.0) \times 10^{-2}$ keV	γ, α	4, 6, 7, 8, 12, 14, 15, 16, 18, 19, 23, 30, 52
11.985 ± 16	1^-; 0		$\Gamma_{cm} = 30 \pm 5$ keV	γ, α	7, 12, 14
12.098 ± 6	2^-; 1			γ	7, 30, 38, 55
12.137 ± 5	6^+; 0	0_3^+		α	5, 6, 7, 8, 14, 15
12.221 ± 4	2^+; 1		$\Gamma_{cm} < 1$ keV	γ, α	7, 12
12.253 ± 10	4^+; 0		$\Gamma_{cm} = 155 \pm 15$ keV	α	14
12.256 ± 3	3^-; 1		$\Gamma_{cm} < 1$ keV	γ, α	12, 14
12.327 ± 10	2^+; 0	0_5^+	$\Gamma_{cm} = 390 \pm 50$ keV	α	14
12.401 ± 5	3^-; (1)	0_7^+	$\Gamma_{cm} = 37.3 \pm 0.9$ keV	γ, α	6, 7, 12, 14, 29, 60
12.436 ± 4	0^+; 0		$\Gamma_{cm} = 24.4 \pm 0.5$ keV	γ, α	7, 12, 14
12.472 ± 10	(2^+); 0		$\Gamma_{cm} = 124 \pm 6$ keV	α	14
12.585 ± 5	6^+; 0	(0_2^+)	$\Gamma_{cm} = 72 \pm 9$ keV	α	6, 7, 14, 15, 16, 18, 19
12.592 ± 15	(2^+); 0		$\Gamma_{cm} = 145 \pm 25$ keV	α	14
12.713 ± 5	5^-; 0	1^-	$\Gamma_{cm} = 84 \pm 8$ keV	α	6, 7, 14
12.743 ± 10	(2^+); 0		$\Gamma_{cm} = 61 \pm 12$ keV	α	6, 7, 14
12.836 ± 5	1^-; 0		$\Gamma_{cm} = 30 \pm 5$ keV	α	7, 14
12.957 ± 5	2^+; 0	(0_7^+)	$\Gamma_{cm} = 38 \pm 4$ keV	α	7, 14, 60
13.048 ± 5	4^+; 0		$\Gamma_{cm} = 18 \pm 3$ keV	α	6, 7, 14
13.0607 ± 2.1	2^-		$\Gamma_{cm} = 1.0$ keV	p, α	28
13.095 ± 6	2^+; 0		$\Gamma_{cm} = 162 \pm 13$ keV	α	3.5, 14
13.105 ± 5	6^+; 0	(0_2^+)	$\Gamma_{cm} = 102 \pm 5$ keV	α	14
13.137 ± 5	3^-; 0		$\Gamma_{cm} = 48 \pm 4$ keV	α	14
13.1713 ± 2.1	1^+; (1)		$\Gamma_{cm} = 2.3 \pm 0.2$ keV	γ, p, α	25, 26, 28, 29
13.222 ± 10	0^+; 0		$\Gamma_{cm} = 40 \pm 13$ keV	α	7, 14, 28
13.224 ± 15	1^-; 0		$\Gamma_{cm} = 80$ keV	p, α	14, 28
13.226 ± 5	3^-; 0		$\Gamma_{cm} = 53 \pm 4$ keV	α	14
13.3075 ± 2.1	1^+		$\Gamma_{cm} = 0.9 \pm 0.1$ keV	γ, p, α	25, 26, 28
13.338 ± 5	7^-; 0	2^-	$\Gamma_{cm} = (8 \pm 3) \times 10^{-2}$ keV	α	6, 7, 8, 14

Table 20.13 (continued)
Energy Levels of ^{20}Ne [a])

E_x (MeV ± keV)	J^π; T	K^π	τ [b]) or Γ	Decay	Reactions
13.341 ± 5	4^+; 0		$\Gamma_{cm} = 26 \pm 3$ keV	α	14
13.414 ± 2	3^-; 0		$\Gamma_{cm} = 24 \pm 3$ keV	α	14, 25, 26, 28
13.426 ± 5	(5^-); 0		$\Gamma_{cm} = 49 \pm 7$ keV	α	14
13.461 ± 10	1^-		$\Gamma_{cm} = 195 \pm 25$ keV	p, α	14, 28
13.484 ± 2	1^+; 1		$\Gamma_{cm} = 6.4 \pm 0.3$ keV	γ, p, α	25, 26, 28, 38
13.507 ± 5	1^-; 0		$\Gamma_{cm} = 24 \pm 8$ keV	p, α	14, 26, 28
13.529 ± 5	2^+; 0		$\Gamma_{cm} = 61 \pm 8$ keV	α	14
13.530 ± 15	(0^+); 0		$\Gamma_{cm} = 76 \pm 32$ keV	α	14
13.573 ± 5	2^+; 0		$\Gamma_{cm} = 12 \pm 5$ keV	α	7, 14, 28
13.586 ± 3	2^+		$\Gamma_{cm} = 9 \pm 1$ keV	p, α	26, 28
13.642 ± 3	0^+; 1		$\Gamma_{cm} = 17 \pm 1$ keV	p, α	7, 26, 28, 29
13.676 ± 2.3	(2^-)		$\Gamma_{cm} = 4.5 \pm 0.2$ keV	γ, p, α	25, 26, 28
13.677 ± 5	5^-; 0		$\Gamma_{cm} = 11 \pm 2$ keV	α	6, 14
13.692 ± 10	7^-; 0	0^-	$\Gamma_{cm} = 310 \pm 30$ keV	α	14
13.736 ± 2.5	7^-; 0	0^-	$\Gamma_{cm} = 7.7 \pm 0.5$ keV	γ, p, α	25, 26, 28
13.744 ± 20	0^+; 0		$\Gamma_{cm} \approx 80$ keV	α	14
13.827 ± 10	3^-; 0		$\Gamma_{cm} = 136 \pm 15$ keV	α	7, 14
13.866 ± 30	1^-; 0		$\Gamma_{cm} \approx 175$ keV	p, α	7, 14, 28
13.881 ± 2.3	2^+; 1		$\Gamma_{cm} = 0.14 \pm 0.05$ keV	γ, p, α	7, 8, 25, 26, 28, 29
13.908 ± 5	2^+; 0		$\Gamma_{cm} = 74 \pm 10$ keV	α	14, 28
13.926 ± 2.3	(0^+)		$\Gamma_{cm} = 3.5 \pm 0.4$ keV	p, α	28
13.928 ± 5	6^+; 0		$\Gamma_{cm} = 65 \pm 3$ keV	α	14, 15, 16
13.948 ± 10	0^+; 0		$\Gamma_{cm} = 79 \pm 15$ keV	α	14
13.965 ± 5	4^+; 0	(0_6^+)	$\Gamma_{cm} = 8.1 \pm 1$ keV	α	14
14.02	1^-		$\Gamma_{cm} \approx 70$ keV	p, α	28
14.063 ± 2.3	2^+		$\Gamma_{cm} \approx 140$ keV	p, α	26, 28
14.115 ± 5	2^+; 0		$\Gamma_{cm} = 42 \pm 6$ keV	α	14
14.128 ± 2	2^-		$\Gamma_{cm} = 4.7 \pm 0.7$ keV	γ, p, α	25, 26, 28
14.150 ± 2.3	2^-		$\Gamma_{cm} = 11.8 \pm 1.0$ keV	γ, p, α	25, 26, 28
14.20	1^+		$\Gamma_{cm} = 14 \pm 1$ keV	γ, p	25, 26
14.270 ± 10	4^+; 0		$\Gamma_{cm} = 92 \pm 9$ keV	α	14
14.304 ± 10	(6^+); 0		$\Gamma_{cm} = 60 \pm 13$ keV	α	6, 7, 14
14.311 ± 5	6^+; 0		$\Gamma_{cm} = 117 \pm 8$ keV	α	6, 7, 14, 15, 16, 18
14.313 ± 15	(3^-); 0		$\Gamma_{cm} \approx 45$ keV	α	14

Table 20.13 (continued)
Energy Levels of ^{20}Ne [a])

E_x (MeV ± keV)	J^π; T	K^π	τ [b]) or Γ	Decay	Reactions
14.370 ± 3			$\Gamma_{cm} \approx 5$ keV	p, α	26, 28
14.454 ± 5	5^-; 0		$\Gamma_{cm} \approx 15$ keV	α	14
14.455 ± 3	$(0^+, 2^+)$; 0		$\Gamma_{cm} = 33 \pm 3$ keV	p, α	14, 26, 28
14.475 ± 6	0^+		$\Gamma_{cm} = 68 \pm 2$ keV	p, α	26, 28
14.597 ± 7	1^-; 0		$\Gamma_{cm} = 116 \pm 5$ keV	p, α	14, 28
14.593 ± 10	4^+; 0		$\Gamma_{cm} = 260 \pm 25$ keV	α	14
14.653 ± 10	(0^+)		$\Gamma_{cm} = 25$ keV	p, α	26, 28
14.699 ± 3.3	(1^+)		$\Gamma_{cm} = 36 \pm 10$ keV	p, α	14, 26, 28
14.731 ± 10	(4^+); 0		$\Gamma_{cm} = 60 \pm 25$ keV	α	14
14.761 ± 5	6^+; 0		$\Gamma_{cm} = 7.3 \pm 4.8$ keV	α	14
14.776 ± 4	(1^-)		$\Gamma_{cm} = 110 \pm 20$ keV	p, α	26, 28
14.807 ± 5	6^+; 0		$\Gamma_{cm} = 86 \pm 7$ keV	α	6, 14, 28
14.816 ± 5	5^-; 0		$\Gamma_{cm} = 117 \pm 13$ keV	α	6, 14
14.839 ± 10	(4^+); 0		$\Gamma_{cm} = 79 \pm 15$ keV	α	14
14.888 ± 10	2^+; 0		$\Gamma_{cm} = 100 \pm 30$ keV	p, α	14, 28
15.047 ± 10	2^+; 0		$\Gamma_{cm} = 66 \pm 20$ keV	p, α	7, 14, 28
15.073 ± 10	5^-; 0		$\Gamma_{cm} = 160 \pm 25$ keV	α	14
15.142 ± 15	(2^+); 0		$\Gamma_{cm} \approx 60$ keV	α	14
15.159 ± 5	6^+; 0		$\Gamma_{cm} = 60 \pm 15$ keV	α	7
15.174 ± 10	5^-; 0		$\Gamma_{cm} = 230 \pm 25$ keV	α	6, 14
15.23			$\Gamma_{cm} = 28$ keV	p, α	28
15.27	(1^-)		$\Gamma_{cm} = 285$ keV	α	4, 6, 7, 14, 15, 16, 18
15.330 ± 5	4^+; 0		$\Gamma_{cm} = 34 \pm 10$ keV	α	4, 6, 7, 14
15.346 ± 2	6^+; 0			α	14
15.366 ± 5	7^-; 0		$\Gamma_{cm} = 110 \pm 10$ keV	α	14, 15, 16, 18, 19
15.436 ± 15	(3^-); 0		$\Gamma_{cm} = 90 \pm 20$ keV	p, α	7, 14, 28
15.5			$\Gamma_{cm} = 55$ keV	p, α	14, 28
15.70 ± 15	(8^-); 0	(2^-)		α	6, 7, 14
15.874 ± 9	8^+		$\Gamma_{cm} = 100 \pm 15$ keV	α	5, 6, 7, 15, 18, 19
15.97	(6^+); 0			α	14
16.01 ± 25	$(2^+; 1)$		$\Gamma_{cm} = 100$ keV	p, α	28
16.139 ± 15			$\Gamma_{cm} = 38$ keV	α	6, 7, 14, 28
16.25				α	6, 14
16.329 ± 11	4^+; 0		$\Gamma_{cm} = 45$ keV	p,α	14, 28

Table 20.13 (continued)
Energy Levels of ^{20}Ne [a])

E_x (MeV ± keV)	J^π; T	K^π	τ [b]) or Γ	Decay	Reactions
16.437 ± 11	$(0,2,4)^+$; 0		$\Gamma_{cm} = 35$ keV	α	14
16.505 ± 15	6^+; 0	(0_6^+)	$\Gamma_{cm} = 24 \pm 4$ keV	α	6, 14
16.559 ± 15	5^-; 0		$\Gamma_{cm} = 90 \pm 30$ keV	α	14
16.581 ± 15	7^-; 0	1^-	$\Gamma_{cm} = 92 \pm 8$ keV	α	7, 14
16.628 ± 20	3^-; 0		$\Gamma_{cm} = 80 \pm 25$ keV	α	14
16.63 ± 20	(7^-)			α	15, 16, 18
16.667 ± 15	4^+; 0		$\Gamma_{cm} = 100 \pm 25$ keV	α	14
16.717 ± 15	5^-; 0		$\Gamma_{cm} \approx 25$ keV	α	6, 7, 14
16.732 ± 5	0^+; 2		$\Gamma_{cm} = 2.0 \pm 0.5$ keV	γ, p, α	24, 25, 26, 28, 56
16.746 ± 25	8^+; 0		$\Gamma_{cm} = 160 \pm 50$ keV	α	14
16.847 ± 15	5^-; 0		$\Gamma_{cm} = 16 \pm 8$ keV	α	14
16.871 ± 200	6^+; 0		$\Gamma_{cm} = 350 \pm 50$ keV	α	14
17.072 ± 20	4^+; 0		$\Gamma_{cm} = 180 \pm 30$ keV	α	14
17.155 ± 15	5^-; 0		$\Gamma_{cm} = 26 \pm 5$ keV	α	14
17.213 ± 15	4^+; 0		$\Gamma_{cm} = 225 \pm 30$ keV	α	14
17.284 ± 15	3^-; 0		$\Gamma_{cm} = 86 \pm 25$ keV	α	14
17.295 ± 15	8^+; 0		$\Gamma_{cm} = 200 \pm 25$ keV	α	4, 14, 15, 16, 18, 19
17.390 ± 15			$\Gamma_{cm} < 10$ keV	α	14
17.430 ± 15	9^-; 0	(0^-)	$\Gamma_{cm} = 220 \pm 25$ keV	α	6, 7, 8, 14
17.541 ± 15	6^+; 0		$\Gamma_{cm} = 86 \pm 9$ keV	α	14
17.55 ± 10	$(2^+; 1)$		$\Gamma_{cm} = 19$ keV	n, p, α	27, 28
17.606 ± 15	5^-; 0		$\Gamma_{cm} = 140 \pm 20$ keV	α	14
17.769 ± 20	4^+; 0		$\Gamma_{cm} \approx 125$ keV	p, α	14, 28
17.851 ± 15	5^-; 0		$\Gamma_{cm} = 200 \pm 30$ keV	α	14
17.91 ± 20	(0^+)			n, p	27
18.005 ± 15	7^-; 0		$\Gamma_{cm} < 10$ keV	α	14
18.024 ± 5	5^-; 0		$\Gamma_{cm} = 34 \pm 7$ keV	α	14
18.083 ± 25	4^+; 0		$\Gamma_{cm} = 140 \pm 60$ keV	α	14
18.125 ± 5	7^-; 0		$\Gamma_{cm} = 29 \pm 6$ keV	α	6, 7, 8, 14
18.286 ± 10	6^+; 0		$\Gamma_{cm} = 190 \pm 300$ keV	α	6, 14
18.430 ± 7	2^+; 2		$\Gamma_{cm} = 9.5 \pm 3$ keV	γ, n, p, α	25, 26, 27, 28, 56
18.430 ± 20	7^-; 0		$\Gamma_{cm} = 185 \pm 40$ keV	α	14
18.494 ± 20	5^-; 0		$\Gamma_{cm} = 130 \pm 30$ keV	α	14
18.538 ± 7	8^+		$\Gamma_{cm} = 138 \pm 33$ keV	α	7
18.621 ± 20	8^+; 0	(0_6^+)	$\Gamma_{cm} = 185 \pm 30$ keV	α	14

Table 20.13 (continued)
Energy Levels of ^{20}Ne [a])

E_x (MeV ± keV)	J^π; T	K^π	τ [b]) or Γ	Decay	Reactions
18.745 ± 25	6^+; 0		$\Gamma_{cm} = 140 \pm 50$ keV	α	14
18.768 ± 20	7^-; 0		$\Gamma_{cm} = 140 \pm 35$ keV	α	14, 15
18.960 ± 25	8^+; 0		$\Gamma_{cm} = 200 \pm 60$ keV	α	14
19.051 ± 15	5^-; 0		$\Gamma_{cm} \approx 90$ keV	α	14
19.15 ± 20	6^+; 0		$\Gamma_{cm} = 200 \pm 50$ keV	α	8, 14
19.284 ± 15	6^+; 0		$\Gamma_{cm} = 140 \pm 25$ keV	α	14
19.298 ± 25	7^-; 0		$\Gamma_{cm} = 430 \pm 60$ keV	α	14, 15
19.443 ± 10	6^+; 0	(0_7^+)	$\Gamma_{cm} = 130 \pm 15$ keV	α	14
19.536 ± 25	6^+; 0		$\Gamma_{cm} = 250 \pm 60$ keV	α	14
19.655 ± 20	6^+; 0		$\Gamma_{cm} = 140 \pm 35$ keV	α	14
19.731 ± 20	8^+; 0		$\Gamma_{cm} = 330 \pm 60$ keV	α	14
19.845 ± 40	6^+; 0		$\Gamma_{cm} = 360 \pm 120$ keV	α	14
19.859 ± 10	5^-; 0		$\Gamma_{cm} = 170 \pm 25$ keV	α	14
19.884 ± 40	7^-; 0		$\Gamma_{cm} \approx 120$ keV	α	14, 15
19.991 ± 30	4^+; 0		$\Gamma_{cm} = 130 \pm 100$ keV	α	14
20.027 ± 15	6^+; 0		$\Gamma_{cm} = 80 \pm 35$ keV	α	14
20.106 ± 25	7^-; 0		$\Gamma_{cm} = 190 \pm 35$ keV	α	14
20.15 ± 150			broad	γ, n	34
20.168 ± 35	6^+; 0		$\Gamma_{cm} = 285 \pm 100$ keV	α	14
20.296 ± 15	7^-; 0		$\Gamma_{cm} = 255 \pm 40$ keV	α	14
20.341 ± 20	5^-; 0		$\Gamma_{cm} = 190 \pm 40$ keV	α	14
20.344 ± 15	7^-; 0		$\Gamma_{cm} = 135 \pm 35$ keV	α	14
20.419 ± 30	6^+; 0		$\Gamma_{cm} = 215 \pm 90$ keV	α	14
20.445 ± 25	6^+; 0		$\Gamma_{cm} = 370 \pm 55$ keV	α	14
20.468 ± 30	5^-; 0		$\Gamma_{cm} = 280 \pm 70$ keV	α	14
20.686 ± 6	9^-; 0	(1^-)	$\Gamma_{cm} = 78 \pm 11$ keV	α	7, 14, 16
20.76 ± 30	7^-; 0		$\Gamma_{cm} = 240 \pm 50$ keV	α	14, 15
20.800 ± 25	5^-; 0		$\Gamma_{cm} = 170 \pm 60$ keV	α	14
20.95 ± 40	7^-; 0		$\Gamma_{cm} = 300 \pm 50$ keV	α	7, 14
21.062 ± 6	9^-; 0	(1^-)	$\Gamma_{cm} = 60 \pm 6$ keV	α	4, 7, 14, 16, 18, 19
21.3 ± 100	7^-; 0		$\Gamma_{cm} = 300$ keV	α	8.3, 14, 15
21.8 ± 100	7^-; 0		$\Gamma_{cm} = 300$ keV	α	7, 8.3, 14, 15
22.3 ± 100	7^-; 0		$\Gamma_{cm} = 500$ keV	α	7, 8.3, 14, 15
22.6 ± 300			broad	α	34
22.8 ± 60	9^-; 0		$\Gamma_{cm} = 500$ keV	α	7, 14

Table 20.13 (continued)
Energy Levels of ^{20}Ne [a])

E_x (MeV ± keV)	J^π; T	K^π	τ [b]) or Γ	Decay	Reactions
22.87 ± 40	9^-; 0		$\Gamma_{cm} = 225 \pm 40$ keV	α	4, 7, 14, 16, 18
23.4 ± 200	8^+; 0		$\Gamma_{cm} = 500$ keV	α	14
23.70 ± 30	(9^-)		$\Gamma_{cm} \leq 200$ keV	α	15, 16
24.21 ± 25	8^+; 0		$\Gamma_{cm} = 350$ keV	α	14, 16
24.9 ± 500			broad	γ, n	34
25.10 ± 50	8^+; 0		$\Gamma_{cm} \approx 200$ keV	α	14, 16
25.67 ± 50			$\Gamma_{cm} = \approx 400$ keV	α	14,16
27.1 ± 100	(9^-)		$\Gamma_{cm} = 700$ keV	α	14, 15, 18
27.5	10^+		broad	γ, n	8.3, 34
28	8^+; 0		$\Gamma_{cm} = 1600$ keV	α	14
28.2 ± 300			$\Gamma_{cm} = 700$ keV	α	14

[a]) See also Tables 20.14 and 20.15. For other states with $E_x > 15.5$ MeV see Tables 20.30 in (78AJ03) and 20.23–25 here and reactions 1, 34, and 36. It is clear that there are many states with low angular momentum and with unnatural parity which have not been located at high E_x.
[b]) See Table 20.20 in (78AJ03).

Table 20.14
Radiative decays in ^{20}Ne [a])

E_i (MeV)	$J_i^\pi; T$	E_f (MeV)	Branch (%)	Γ_γ (meV)
1.63	$2^+; 0$	0	100	0.63 ± 0.04 [b])
4.25	$4^+; 0$	1.63	≈ 100	7.1 ± 0.7 [b])
4.97	$2^-; 0$	0	0.6 ± 0.2	$(8 \pm 3) \times 10^{-4}$ [b])
		1.63	99	0.14 ± 0.02 [b])
				$\delta(\mathrm{M2/E1}) = 0.076 \pm 0.011$
				$\delta(\mathrm{E3/E1}) = 0.043 \pm 0.016$
5.62	$3^-; 0$	0	7.6 ± 1.0	0.018 ± 0.006
		1.63	87.6 ± 1.0	0.21 ± 0.06
		4.97	4.8 ± 1.6	0.012 ± 0.005
5.79	$1^-; 0$	0	18 ± 5	0.8 ± 0.3
		1.63	82 ± 5	3.8 ± 0.8
6.73	$0^+; 0$	0		$\lvert M\rvert^2 = 7.4 \pm 2.0$ fm^2 [d])
		1.63	100	33
7.00	$4^-; 0$	1.63	0.5 ± 0.2	$(7 \pm 3) \times 10^{-3}$ [b])
		4.25	13	0.19 [b])
		4.97	64.5	0.96 [b])
		5.62	22	0.32 [b])
7.16	$3^-; 0$	4.25	60 ± 5	0.97 ± 0.11
		5.79	40 ± 5	0.64 ± 0.10
7.20	$0^+; 0$	0		$\Gamma_\pi = 3.9 \times 10^{-2}$
				6.9 ± 1.4 fm^2 [d])
		1.63	100	4.35 ± 0.75
7.42	2+; 0	0	$\leq 9.4 \pm 1.4$	$\leq 3.0 \pm 0.6$
		1.63	$\geq 90.6 \pm 1.4$ [f])	29 ± 4
		4.25	≤ 7.6	
7.83	$2^+; 0$	0	83 ± 1	57 ± 7
		1.63	17 ± 1	11.7 ± 1.6
		4.25	< 2	< 2
8.46	$5^-; 0$	5.62	100	13 ± 3
8.71	$1^-; 0$	0	87 ± 8	61 ± 16
		1.63	13 ± 8	9 ± 6
8.78	$6^+; 0$	4.25	100	100 ± 15
9.03	$4^+; 0$	1.63	100	340 ± 42
		4.25	< 2	< 6.8
9.12	$3^-; 0$	1.63	50 ± 5	13 ± 2
		4.97	33 ± 5	8.6 ± 1.7
		5.62	17 ± 4	4.4 ± 1.1

Table 20.14 (continued)
Radiative decays in ^{20}Ne [a])

E_i (MeV)	J_i^π; T	E_f (MeV)	Branch (%)	Γ_γ (meV)
9.32 [l])	$(2^-; 0)$	1.63		
9.49	2^+; 0	0		≤ 60
		1.63	(100)	260 ± 100
9.87	3^+; 0	0	< 0.5	
		1.63	78	[g])
		4.25	12 ± 3	
		4.97	≤ 5	
		5.62	≈ 7	
		7.43	≈ 3	
9.94	(1^+); 0	1.63	78 ± 5	
		4.97	22 ± 5	
9.99	4^+; 0	0		≤ 70
		1.63	(100)	900 ± 400
10.27	2^+; 1	0	0.65 ± 0.14	29 ± 8
		1.63	88.9 ± 0.5	4080 ± 440
		4.97	1.3 ± 0.1	60 ± 8
		5.62	2.1 ± 0.2	97 ± 14
		7.43	6.9 ± 0.4	310 ± 40
		7.83	0.22 ± 0.06	8 ± 2
10.61	6^-; 0	7.00	95.5 ± 1.2	29 ± 9 [b])
		8.46	4.5 ± 1.2	1.3 ± 0.4
10.69	4^-, 3^+; 0	4.25	25 ± 4	
		4.97	75 ± 4	
10.88	3^+; 1	1.63	77 ± 5	[h])
		4.25	23 ± 5	
11.09 [c])	4^+; 1	1.63	0.5 ± 0.25	2 ± 1
		4.25 [i])	99.5 ± 0.25	338 ± 40
11.26 [j])	1^+; 1	0	84 ± 5	$(11.2 \pm 2.0) \times 10^3$
		1.63	16 ± 5	$(2.1 \pm 0.7) \times 10^3$
11.27 [c])	1^-; 1	0	55 ± 2	390 ± 47
		1.63	2.5 ± 1	18 ± 7
		4.97	6.5 ± 1	46 ± 9
		8.85	27 ± 1.5	189 ± 24
		9.32	9 ± 1	63 ± 10
11.53	3^+, 4^-; 0	4.25	30 ± 3	
		4.97	70 ± 3	
		7.00	[f])	

Table 20.14 (continued)
Radiative decays in ^{20}Ne [a])

E_i (MeV)	J_i^π; T	E_f (MeV)	Branch (%)	Γ_γ (meV)
11.555	$(3^+; 0)$	1.63		
		7.00		
11.558	$0^+; 0$	1.63	100	
		4.25	< 8	
11.65	$(3^+); 0$	1.63	14 ± 3	
		4.25	86 ± 3	
11.93	$4^+; 0$	1.63	21 ± 11	5.5 ± 3.0
		4.25	79 ± 11	20.5 ± 5.5
11.95	$8^+; 0$	8.78	100	7.7 ± 1.1
12.22 [k])	$2^+; 1$	1.63	(100)	
12.26	$3^-; 1$	1.63	63 ± 1.5	
		5.62	37 ± 1.5	
12.40	$3^-; (1)$	0	≈ 1	
		1.63	≈ 29	80
		4.25	≈ 70	200
12.43	$0^+; 0$	1.63	100	170 ± 50
13.48	$1^+; 1$	1.63	95	
		4.97	5	
13.88	$2^+; 1$	1.63	20	
		4.97	80	
16.73	$0^+; 2$	1.63		
		5.79		
		11.23	(100)	≈ 5000
18.43	$2^+; 2$	12.22	(100)	≈ 300

[a]) For earlier references see Tables 20.19 in (78AJ03) and 20.18 in (83AJ01). See also Tables 20.17 and 20.20 here.
[b]) From τ_m: see Table 20.20 in (78AJ03) and branching ratios.
[c]) See also Table 20.19 in (78AJ03).
[d]) Monopole matrix element.
[e]) See footnote [a]) in Table 2 of (76MA01).
[f]) $\delta(\mathrm{E2/M1}) = -8.36^{+1.0}_{-1.5}$.
[g]) $\Gamma_\gamma(\mathrm{total})/\Gamma = 0.82 \pm 0.27$.
[h]) $\Gamma_\gamma(\mathrm{total})/\Gamma < 0.3$ (77MA07). See also (87FI01).
[i]) $\delta = +0.01 \pm 0.06$.
[j]) (83BE1J): see reaction 35.
[k]) (84CA08).
[l]) (87FI01).

Table 20.15
K^π assignments to states of ^{20}Ne [a])

K^π	J^π	E_x (MeV)	K^π	J^π	E_x (MeV)
0_1^+	0^+	0		6^+	(16.51)
	2^+	1.63		8^+	(18.62)
	4^+	4.25	0_7^+ [b])	0^+	12.43
	6^+	8.78		2^+	(12.96)
	8^+	11.95		6^+	(19.44)
0_2^+	0^+	6.73	0^- [f])	1^-	5.79
	2^+	7.42		3^-	7.16
	4^+	9.99		5^-	10.26
	6^+	(12.59, 13.11)		7^-	13.69
0_3^+	0^+	7.20		9^-	(17.43)
	2^+	7.83	1^-	1^-	8.85
	4^+	9.03		3^-	10.41
	6^+	12.14		5^-	12.71
0_4^+	0^+	8.7		7^-	16.58
	2^+	8.8		9^-	(20.69, 21.06)
	4^+	10.80	2^- [f])	2^-	4.97
	6^+ [c])	(12.59)		3^-	5.62
	8^+ [c])	(17.30)		4^-	7.00
0_5^+	0^+	10.97		5^-	8.46
	2^+ [d])	12.33		6^-	10.61
0_6^+ [b])	0^+	11.55		7^-	13.34
	4^+	(13.97)		8^-	(15.70) [e])
				9^-	17.43

[a]) See Tables 20.19, 20.20, 20.21, 20.22, and 20.23 in (83AJ01) and (84RI01, 84RI07, 85MU14, 86MA48). See also Table 20.15 in (87AJ02).
[b]) See also (92LA01).
[c]) However (87MI07) predict the $J^\pi = 6^+$, 8^+ and 10^+ members of the 0_4^+ band to be at $E_x \approx$ 14–15 MeV [$\Gamma \approx$ 1–2 MeV], $\approx$ 21 MeV [$\Gamma \approx$ 2 MeV] and $\approx$ 29 MeV [$\Gamma \approx$ 29 MeV], suggesting that the 0_4^+ band has a moment of inertia which is very similar to that of the 0^- band.
[d]) For the location of higher J^π members of this band see (84RI01).
[e]) See (70PA1A) and (84RI01).
[f]) See (92HA18).

0.5 ^{9}Be(^{18}O, ^{20}Ne)^{7}He $\quad Q_{\rm m} = -8.502$

Observation of ^{20}Ne in this reaction and measurement of the cross section was reported by (90BEYY).

1. (a) ^{10}B(^{10}B, ^{10}B)^{10}B $\quad E_{\rm b} = 31.144$
   (b) ^{10}B(^{10}B, α)^{16}O $\quad Q_{\rm m} = 26.414$

Excitation functions have been measured for $E(^{10}\mathrm{B}) = 6$ to 30 MeV (reaction (a)) and 6 to 20 MeV (reaction (b)). Large resonant structures are observed in reaction (b), particularly at $E_{\rm x} \approx 38$ MeV (α_0) and 38.6 MeV (α to ^{16}O* (7.0, 10.3, 16.2 (u)), $\Gamma \approx 0.6$ MeV. See also (83KA1E) and (78AJ03). More recently, cross sections for fusion of $^{10}\mathrm{B} + {}^{10}\mathrm{B}$ were measured for $E(^{10}\mathrm{B}) = 1.5$–5 MeV/nucleon, and evidence for fissionlike decay of ^{20}Ne was observed (89SZ01). Mass distributions from the sequential decay of the compound nucleus measured at $E(^{10}\mathrm{B}) \approx 110$ MeV show no evidence for nuclear structure effects (93SZ02).

2. ^{10}B(^{14}N, α)^{20}Ne $\quad Q_{\rm m} = 19.531$

Angular distributions of α-particles to many states of ^{20}Ne below $E_{\rm x} = 10.7$ MeV have been measured at $E(^{14}\mathrm{N}) = 23.5$ to 35 MeV. See also (78AJ03, 83AJ01). Numerical calculations of differential cross sections using CWBA and DWBA are reported by (90OS1B).

3. ^{10}B(^{16}O, ^{6}Li)^{20}Ne $\quad Q_{\rm m} = 0.270$

At $E(^{16}\mathrm{O}) = 19.5$ to 42 MeV angular distributions for the ^{6}Li ions corresponding to transitions to ^{20}Ne* (0, 1.63, 4.25, 4.97, 5.62+5.79, 6.7–7.2) are in good agreement with Hauser-Feshbach calculations. See also (78AJ03, 85ST1B).

4. ^{11}B(^{16}O, ^{7}Li)^{20}Ne $\quad Q_{\rm m} = -3.935$

At $E(^{11}\mathrm{B}) = 115$ MeV, angular distributions are reported to ^{20}Ne* (7.16, 8.78, 10.26, 11.95, 15.4). ^{20}Ne* (8.78, 15.4, 17.3, 21.0$\pm$0.07, 22.78$\pm$0.06) are particularly strongly populated. It is suggested that these five states have $J^{\pi} = 6^{+}$, 7^{-}, (8^{+}), 9^{-}, and 9^{-}: see (83AJ01).

5. ^{12}C(^{9}Be, n)^{20}Ne $\quad Q_{\rm m} = 10.319$

At $E(^{9}\mathrm{Be}) = 16$ and 24 MeV, angular distributions have been measured for ^{20}Ne* (7.3 ± 0.4, 9.2 ± 0.4, 10.9 ± 0.3, 12.2 ± 0.3, 15.7 ± 0.3): see (83AJ01).

6. (a) ^{12}C(^{10}B, d)^{20}Ne $\quad Q_{\rm m} = 5.957$
   (b) ^{12}C(^{11}B, t)^{20}Ne $\quad Q_{\rm m} = 0.760$

At $E(^{12}\mathrm{C}) = 45$ MeV the population of states of ^{20}Ne with $E_{\rm x} = 8.46$, 8.78, 9.03, 10.61, 10.67, 10.99, 11.01, 11.66, 11.94, 12.14, 12.39, 12.58, 12.73, 13.05, 13.17, 13.34 [7^-], 13.69, 13.91, 14.29, 14.36, 14.81, 15.17 [6^+], 15.38 [7^-], 15.71 [(7,8)], 15.89 [(7)], 16.16, 16.22, 16.51 [(8)], 16.73, 17.39 [9^-], 18.18 and 18.32 MeV is reported (76K-L03). [Values in brackets are J^π suggested on basis of Hauser-Feshbach calculations. The underlined states are well resolved: the authors indicate ± 20 keV for such states.] The relative intensities of the groups to ^{20}Ne* (17.39, 15.38) [$J^\pi = 9^-$, 7^-] argue against the existence of a superband: see (78AJ03). See also (83AJ01).

7. ^{12}C(^{12}C, α)^{20}Ne $\quad Q_{\rm m} = 4.617$

Double and triple (α, α, γ) correlations and γ-ray branching measurements [see Table 20.14] lead to the J^π assignments shown in Table 20.16. See Table 20.15 for assignments to rotational bands. Angular distributions for many states have been reported at $E(^{12}\mathrm{C}) = 4.9$ to 51 MeV [see (78AJ03, 83AJ01, 87AJ02)], at 5.2 to 5.8 MeV (88BA12; α_0), and at 69.5 MeV (85XI1B). At $E(^{12}\mathrm{C}) = 38$ to 64 MeV, ^{20}Ne* (7.17, 7.83, 8.54, 8.78, 9.03, 11.95, 12.13, 12.59, 13.90) are strongly populated and subsequently decay to $^{16}\mathrm{O}_{\rm g.s.}$ (87RA02). Alpha decay of the $J^\pi = 6^+$ level at $E_{\rm x} = 15.6$ MeV and the $J^\pi = 8^+$ level at $E_{\rm x} = 18.54$ MeV to the first excited state of ^{16}O was studied by (92LA01). See Table 20.16. For γ-decay measurements see (87FI01), Table 20.16 and (78AJ03). Resonant characteristics of statistical fluctuations in ^{12}C(^{12}C, α)^{20}Ne leading to the 12 lowest ^{20}Ne states were studied by (93GA02).

The yields of various groups of α-particles and their relevance to states of ^{24}Mg, and fusion cross sections, have been studied by many groups: see (78AJ03, 83AJ01, 87AJ02).

Sub-Coulomb cross sections calculated in a statistical framework are discussed in (90KH05). A review of the state of theory and experiments on ^{12}C+^{12}C reactions with formation of molecular states is presented in (87DA1L).

See also (87ER1B, 88GO1G, 88DE18, 91SZ02).

Table 20.16
Excited states of ^{20}Ne from ^{12}C(^{12}C, α)^{20}Ne [a])

E_x (MeV $\pm$ keV) [b])	J^π [c])	Γ_γ/Γ [d])	$\Gamma_{c.m.}$ (keV)	θ_α^2 [e])
1.6329 ± 1.0	2^+			
4.2456 ± 2.5	4^+			
4.9663 ± 2.5	2^-			
5.618 ± 4	3^-			
5.774 ± 6	1^-			
6.725 ± 6	0^+			
7.004 ± 4	4^-			
7.169 ± 6	3^-			
7.196 ± 6	0^+			0.026 [q])
7.435 ± 6	2^+			
7.835 ± 6	2^+			0.015 [q])
8.449 ± 6	5^-			$(1.6 \pm 0.5) \times 10^{-3}$ [r])
8.694 ± 6	1^-			0.0027 [q])
8.779 ± 6	6^+			
8.85	1^-			0.0179 [q])
9.033 ± 6	4^+			0.033 [q]), 0.022 [r])
9.110 ± 6				
9.318 ± 6	2^-	> 0.90		
9.533 ± 6				
9.872 ± 6	1^+, 2^-, 3^+	> 0.8		
9.948 ± 5 [d])	1^+, 2^-, 3^+	> 0.7		
10.024 ± 6				
10.264 ± 6	5^-			
10.407 ± 6	(3^-)			0.078 [q])
10.545 ± 6				
10.609 ± 5	6^-	$\equiv 1$		
10.693 ± 5	4^-; 3^+	> 0.95		
10.840 ± 6	(3^-)			0.0099 [q])
10.917 ± 6	3^+; $T = 0$	> 0.7		
11.013 ± 6				
11.528 ± 5 [d])	$(3^+; 4^-)$	> 0.90		
11.568 ± 10 [d])	$(3^+; T = 0)$	0.75 ± 0.10		
11.653 ± 5 [d])	(3^+)	> 0.90		
11.892 ± 8 [d])		0.16 ± 0.02		
11.949 ± 6	8^+			$(7.6 \pm 2.2) \times 10^{-3}$ [r])
12.014 ± 10 [d])		> 0.10		
12.097 ± 8 [d])		> 0.20		

Table 20.16 (continued)
Excited states of ^{20}Ne from ^{12}C(^{12}C, α)^{20}Ne [a])

E_x (MeV ± keV) [b])	J^π [c])	Γ_γ/Γ [d])	$\Gamma_{c.m.}$ (keV)	θ_α^2 [e])
12.135 ± 5 [f])	6^+			$(4.9 \pm 2.6) \times 10^{-4}$ [r,t])
12.172 ± 8 [d])		> 0.45		
12.219 ± 10 [d])	$2^+; T = 1$	> 0.45		
12.379 ± 8 [d])		0.005 ± 0.001		
12.436 ± 5 [bb])	0^+ [s])		24 ± 1	[r,s])
12.596 ± 5	6^+		50 ± 10	0.09 ± 0.002 [r])
12.730 ± 6	(5^-)			0.129 [q])
12.919 ± 6				
13.010 ± 6				
13.049 ± 6				
13.190 ± 6				
13.277 ± 6				
13.335 ± 6	7^-			$(2.4 \pm 1.0) \times 10^{-4}$ [r,u])
13.441 ± 6	(5^-)			≤ 0.023 [q])
13.569 ± 15				
13.631 ± 15				
13.679 ± 15				
13.845 ± 15				
13.886 ± 15				
13.927 ± 5	6^+		113 ± 7	0.10 ± 0.01 [r])
14.144 ± 15				
14.308 ± 10	6^+		< 50 [r])	< 0.45 [r])
14.60				
14.812 ± 15				
15.034 ± 15	[a])			
15.159 ± 5 [g])	6^+		60 ± 15	$< 8 \times 10 - 4$ [r,v])
15.364 ± 14 [h])	7^-		410 ± 130	
15.438 ± 10 [i])			100 ± 20	
15.691 ± 15				
15.874 ± 8 [j])	8^+		100 ± 15	0.047 ± 0.013 [r,w])
16.139 ± 15				
16.600 ± 15 [k])	7^-		160 ± 30	0.10 ± 0.02 [r,x])
16.717 ± 10			37 ± 10	
17.259 ± 11 [l])	7^- (9^-)		162 ± 20	0.019 ± 0.004 [r,y])
18.153 ± 10 [m])	7^-			
18.538 ± 7 [n])	8^+		138 ± 33	$(3.2 \pm 1.5) \times 10^{-3}$ [r,z])
20.478 ± 11 [o])	(8^+)		250 ± 30	0.11 ± 0.04 [r,aa])

Table 20.16 (continued)
Excited states of ^{20}Ne from ^{12}C(^{12}C, α)^{20}Ne [a])

E_x (MeV ± keV) [b])	J^π [c])	Γ_γ/Γ [d])	$\Gamma_{c.m.}$ (keV)	θ_α^2 [e])
20.704 ± 11 [p])	(9^-)		≈ 120	[r])
20.89 ± 30				
21.05 ± 20			140 ± 50	
21.65 ± 100	$(7^-, 9^-)$		240 ± 50	
22.03 ± 70	(8^+)		630 ± 80	
22.7 ± 70			490 ± 110	
23.2 ± 100			300 ± 100	
23.74 ± 100			230 ± 100	
24.374 ± 30	7^- (5^-)		210 ± 50	

[a]) For complete references see Table 20.21 in (78AJ03). Table 20.19 in (83AJ01) has a number of errors.
[b]) Uncertainties shown for $E_x > 5.7$ MeV are approximate, except for states flagged (d): see footnote (c) in Table 20.21 (78AJ03).
[c]) See discussions in (75ME04), (83HI06), (84LE19) and (87FI01). See also Table 20.14 here.
[d]) (87FI01). ^{20}Ne* (11.89, 12.38) also decay via α_2.
[e]) See also (84LE1B).
[f]) Alpha decay is by α_2 to ^{16}O* (6.13): $\Gamma'_\alpha/\Gamma = (6.0 \pm 0.15)\%$: assuming $\Gamma_\alpha \Gamma'_\alpha/\Gamma = 7.7 \pm 3.8$ eV this leads to $\Gamma_\alpha = 0.128 \pm 0.072$ keV for this 6^+ state: see (78AJ03). (83HI06) report an α_0 branching ratio of $(90 \pm 6)\%$.
[g]) Alpha decay is $(2 \pm 2)\%$ by α_0, $(46 \pm 2)\%$ via α_{1+2} (mainly α_2) and $(52 \pm 2)\%$ via α_{3+4} (mainly α_3) (79YO04). See also (92LA01).
[h]) Alpha decay is $(32 \pm 2)\%$ by α_0, $(58 \pm 2)\%$ via α_{1+2} (mainly α_2) and $(10 \pm 2)\%$ via α_{3+4} (mainly α_3); $\Gamma_{\alpha_0}/\Gamma = 0.3 \pm 0.02$, assuming a single state. The state may correspond to a doublet (79YO04). See also (83HI06).
[i]) Alpha decay is $(20 \pm 5)\%$ by α_0, $(57 \pm 7)\%$ by α_{1+2} and $(23 \pm 4)\%$ by α_{3+4} (83HI06).
[j]) Alpha decay is $(9 \pm 2)\%$ by α_0, $(79 \pm 2)\%$ via α_{1+2} (mainly α_2) and $(12 \pm 4)\%$ via α_{3+4} (mainly α_3) (79YO04); $(24 \pm 5)\%$ via α_0, $(51 \pm 7)\%$ via α_{1+2}, $(25 \pm 5)\%$ via α_{3+4} (83HI06).
[k]) Alpha decay is $(72 \pm 3)\%$ via α_0, $(20 \pm 3)\%$ via α_{1+2} (mainly α_2) and $(8 \pm 3)\%$ via α_{3+4} (mainly α_3) (79YO04); $(60 \pm 5)\%$ via α_0, $(20 \pm 5)\%$ via α_{1+2} and (20 ± 5) via α_{3+4} (83HI06).
[l]) Alpha decay is $(15 \pm 2)\%$ via α_0, $(50 \pm 6)\%$ via α_{1+2} and $(35 \pm 7)\%$ via α_{3+4} (83HI06). See also (79YO1A).
[m]) Alpha decay is $(71 \pm 6)\%$ via α_0 and $(29 \pm 6)\%$ via α_{1+2} (mainly α_2) (79YO1A).
[n]) Alpha decay is $(1.8 \pm 0.9)\%$ via α_0, $(60 \pm 8)\%$ via α_{1+2} and $(26 \pm 4)\%$ via α_{3+4}. Decay to $^{12}C_{g.s.} + {}^8Be_{g.s.}$ is also observed: the branching ratio is $(12 \pm 1.2)\%$. This may be a member of an excited 8p-4h ($K^\pi = 0_6^+$) band of which ^{20}Ne* (12.44) is the 0^+ band head (83HI06). The results of (92LA01), however, argue against this identification.
[o]) Decay is $(66 \pm 26)\%$ via α_0, $(14 \pm 7)\%$ via α_{1+2} and $(13.2 \pm 2.5)\%$ via $^{12}C + {}^8Be$ (83HI06).
[p]) Decay is $\leq 14\%$ via α_0, $(25 \pm 15)\%$ via α_{1+2}, $(46 \pm 22)\%$ via α_{3+4} and $(4.5 \pm 0.9)\%$ via $^{12}C + {}^8Be$ (83HI06). See also (79YO1A).
[q]) (79YO04).
[r]) θ_α^2 shown are $\theta_{\alpha_0}^2$ (83HI06). See also (87FI01).
[s]) See footnote (f) in Table 20.21 of (83AJ01).

Table 20.16 (continued)
Excited states of ^{20}Ne from ^{12}C(^{12}C, α)^{20}Ne [a])

---

[t]) $\theta^2_{\alpha_2} = 0.66 \pm 0.36$ (83HI06).
[u]) $\theta^2_{\alpha_2} = 0.025 \pm 0.010$ (83HI06).
[v]) $\theta^2_{\alpha_2} = 0.05 \pm 0.013$, $\theta^2_{\alpha_3} = 0.91 \pm 0.23$ (83HI06).
[w]) $\theta^2_{\alpha_2} = 0.94 \pm 0.14$, $\theta^2_{\alpha_3} = 4.2 \pm 0.9$ (83HI06).
[x]) $\theta^2_{\alpha_2} = 0.048 \pm 0.013$, $\theta^2_{\alpha_3} = 0.44 \pm 0.12$ (83HI06).
[y]) $\theta^2_{\alpha_2} = 0.071 \pm 0.013$, $\theta^2_{\alpha_3} = 0.32 \pm 0.08$ [all θ^2_α assume $J^\pi = 7^-$] (83HI06).
[z]) $\theta^2_{\alpha_2} = 0.085 \pm 0.014$, $\theta^2_{\alpha_3} = 0.24 \pm 0.04$, $\theta^2(^{12}\mathrm{C}) = 1.50 \pm 0.21$ (83HI06).
[aa]) $\theta^2_{\alpha_2} = 0.016 \pm 0.008$, $\theta^2(^{12}\mathrm{C}) = 0.24 \pm 0.05$ (83HI06).
[bb]) (92LA01) determined $E_\mathrm{x} = 12.436 \pm 0.004$ MeV, $\theta^2_{\alpha_1} \approx 1.15$.

8. (a) ^{12}C(^{14}N, ^{6}Li)^{20}Ne $\quad Q_\mathrm{m} = -4.181$
(b) ^{12}C(^{14}N, d)^{24}Mg $\rightarrow \alpha + {}^{20}$Ne $\quad Q_\mathrm{m} = 7.480$

Angular distributions of the ^{6}Li ions to many states of ^{20}Ne below 17.5 MeV have been reported for $E(^{14}\mathrm{N}) = 30$ to 78 MeV and $E(^{12}\mathrm{C}) = 67.2$ MeV. At the latter energy ^{20}Ne* (16.67, 17.38, 18.11, 19.16, 19.6) are particularly strongly populated: see (78AJ03). For reaction (b) to $^{20}\mathrm{Ne}_{\mathrm{g.s.}}$ see the angular correlation measurements at $E(^{14}\mathrm{N}) = 30$–42 MeV reported by (88AR24, 94ZU1B), and see the review of (87GO12). Earlier work is cited in (87AJ02). See also (88BE1J, 89BE1T, 92ARZX).

8.3 (a) ^{12}C(^{16}O, ^{8}Be)^{20}Ne $\quad Q_\mathrm{m} = -2.636$
(b) ^{12}C(^{16}O, $\alpha\alpha$)^{20}Ne $\quad Q_\mathrm{m} = -2.545$

Reaction (a) was studied at 150 MeV in a search for high-spin α-cluster resonances in ^{20}Ne. A broad 10^+ resonance was located at 27.5 MeV (88AL07). See also (88CAZV, 94RA04).

Excitation functions in the range $E_\mathrm{cm} = 25.7$–38.6 MeV were measured by (93ES01). See also the comment (93ZH21) and reply (93ES03) on the work. Excitation functions for reaction (a) leading to members of the ^{20}Ne ground state rotational band were measured for $E_\mathrm{cm} = 22$–29 MeV by (95SU06).

A triple coincidence measurement of reaction (b) through the ^{20}Ne 6^+ level at $E_\mathrm{x} = 8.78$ MeV was reported by (89WUZZ). α–α coincidence measurements by (94KU18) at $E_\mathrm{cm} = 26.9$ MeV studied the connection of highly deformed isomeric states in ^{28}Si, ^{24}Mg and ^{20}Ne.

8.5 ^{12}C(^{19}F, ^{20}Ne)^{11}B $\quad Q_{\rm m} = -3.113$

This reaction was studied with the use of molecular orbital theory (88DI08).

9. ^{13}C(^{9}Be, 2n)^{20}Ne $\quad Q_{\rm m} = 5.373$

For cross sections see (86CU02).

10. ^{14}N(^{12}C, ^{6}Li)^{20}Ne $\quad Q_{\rm m} = -4.181$

See reaction 8.

11. ^{14}N(^{14}N, 2α)^{20}Ne $\quad Q_{\rm m} = 7.918$

For yields of 1.63 MeV γ-rays see (82DE39).

11.5 ^{14}N(^{20}Ne, ^{14}N)^{20}Ne

Spectra were measured for $E(^{20}\text{Ne}) = 150$ MeV/nucleon (92EGZZ).

12. ^{16}O(α, γ)^{20}Ne $\quad Q_{\rm m} = 4.730$

Observed resonances in the yield of capture γ-rays over the range $E_\alpha = 0.8$ to 10 MeV are displayed in Table 20.17. For a discussion of ^{20}Ne* (11.28) [$J^\pi = 1^+$; $T = 1$], to which excitation by this reaction is parity forbidden, see (83FI02). See also (84BU01). Total cross sections have been measured in the range $E_{\rm c.m.} =$ 1.7 to 2.35 MeV. Assuming that S does not vary with energy over that interval, the astrophysical factor for non-resonant capture to $^{20}\text{Ne}_{\rm g.s.}$ is 0.26 ± 0.07 MeV $\cdot$ b. An estimate of 0.7 ± 0.3 MeV $\cdot$ b for S at 300 keV is deduced (87HA24). A comment (88BA66) on this work summarizes the status of theoretical descriptions of ^{16}O(α, γ)^{20}Ne and discusses the (87HA24) result in the light of a microscopic calculation. See also Table 20.17. For other papers on astrophysical considerations see (85CA41, 88CA1N, 90BL1K, 91RA1C). For earlier work, see (87AJ02).

A microscopic description of the $\alpha + {}^{16}$O system in a multicluster model is discussed in (94DU09). An anharmonic oscillating model description is presented in (93CSZU).

Table 20.17
Resonances in $^{16}O(\alpha, \gamma)^{20}Ne$ [a])

E_α (MeV ± keV)	$\Gamma_{c.m.}$ (keV)	$\omega\gamma$ [b]) (eV)	E_x (MeV ± keV)	J^π; T
1.116 ± 4	2.6×10^{-6} [d])	$(1.7 \pm 0.3) \times 10^{-3}$	5.627 ± 4	3^-; 0
1.3174 ± 2.2 [c])	$(2.8 \pm 0.3) \times 10^{-2}$ [d])	$(1.7 \pm 0.3) \times 10^{-2}$ [l])	5.7877 ± 3.0	1^-; 0
2.490 ± 8	20 ± 3 [d,m])	$(7.1 \pm 1.2) \times 10^{-2}$ [m])	6.726 ± 6	0^+; 0
3.0359 ± 2.3 [c])	8.2 ± 0.3 [l])		7.1563 ± 0.5	3^-; 0
3.069	4	$(4.4 \pm 0.8) \times 10^{-3}$	7.189 ± 3	0^+; 0
3.359	8	0.146 ± 0.019	7.421 ± 1	2^+; 0
3.868	2.4	0.343 ± 0.035	7.828 ± 3	2^+; 0
(4.647 ± 3)			(8.451 ± 3)	$(5^-; 0)$
4.969 ± 9	2.1 ± 0.8	0.21 ± 0.05	8.708 ± 7	1^-; 0
5.05	< 3	1.35 ± 0.15	8.776 ± 3.2	6^+; 0
5.364	3.2	3.05 ± 0.38	9.024 ± 3	4^+; 0
5.477 ± 4	< 4	0.18 ± 0.02	9.114 ± 3	3^-; 0
5.94 ± 30	29 ± 15	1.3 ± 0.5	9.48 ± 24	2^+; 0
6.61 ± 30	155 ± 30	8 ± 3	10.02 ± 24	(4^+); 0
6.924 ± 7 [k])	≤ 1	19.5 ± 1.5 [e])	10.271 ± 7 [f])	2^+; 1
7.948 ± 4	< 1	30.2 ± 3.5	11.090 ± 3	4^+; 1
8.180 ± 5 [g])	< 1	2.06 ± 0.25 [h])	11.276 ± 4	1^-; 1
8.535 ± 6	1.3 ± 0.8	0.41 ± 0.05	11.559 ± 6	0^+; 0 [j])
8.994 ± 8	< 1	0.23 ± 0.05 [i])	11.926 ± 6	4^+; 0
9.02		0.131 ± 0.0018	11.950 ± 4	8^+; 0
(9.05 ± 50)	< 40		(11.97)	
(9.15 ± 50)	< 40		(12.05)	
9.362 ± 5	< 1	1.41 ± 0.23	12.221 ± 4	2^+; 1
9.406 ± 4	< 1	6.6 ± 0.8 [g])	12.256 ± 3	3^-; 1
9.57 ± 10	33 ± 4	1.94 ± 0.15	12.39	3^-; (1)
9.70 ± 30	≤ 10	0.17 ± 0.05	12.49	

[a]) For complete references see Tables 20.22 in (78AJ03) and 20.20 in (83AJ01). See also Table 20.18 here.
[b]) $\omega\gamma = (2J+1)\Gamma_\alpha\Gamma_\gamma/\Gamma$.
[c]) The strength of the γ-decay of ^{20}Ne* (7.16) to ^{20}Ne* (5.79) (see Table 20.14) is strong evidence that these two states are members of the $K^\pi = 0^-$ band.
[d]) This is also Γ_α.
[e]) Other values are $\omega\gamma = 19.2 \pm 1.9$ eV; $\Gamma_\alpha = 116 \pm 20$ eV; $\Gamma_\gamma = 4.26 \pm 0.23$ eV: see (83AJ01).
[f]) The measurements of the decay of this state lead to $E_x = 4247.9 \pm 1.3$, 4966.0 ± 1.9, 5621.0 ± 3.5, 7423.1 ± 3.0, 7828.1 ± 3.8 and 8776.7 ± 2.3 keV.
[g]) See also Table 20.20 in (83AJ01).
[h]) The γ-decay is partly (see Table 20.14) to a state at $E_x = 9318 \pm 2$ keV. The strength of this transition and the subsequent decay to ^{20}Ne* (1.63) (and not to the ground state) favor 2^- for ^{20}Ne* (9.32). The other M1 transition [$11.27 \rightarrow 8.85$] is also strong suggesting similar structures for ^{20}Ne* (8.85, 9.32) (80FI01).

Table 20.17 (continued)
Resonances in $^{16}O(\alpha, \gamma)^{20}Ne$ [a])

[i]) Also observed as a resonance in the yield of 6.13 MeV γ-rays with $(2J+1)\Gamma_{\alpha_0}\Gamma_{\alpha_2}/\Gamma = 5.2 \pm 0.9$ eV (80FI01).
[j]) From (α, α_0): see (84RI07).
[k]) See also (84RO04).
[l]) Best value including the recent work by (87HA24).
[m]) (87HA24).

13. (a) $^{16}O(\alpha, p)^{19}F$ $Q_m = -8.114$
(b) $^{16}O(\alpha, d)^{18}F$ $Q_m = -16.321$ $E_b = 4.730$

For reaction (a) see (90KOZG).

For reaction (b) see (86KA36). A theoretical study of clustering in Yrast states is described in (95KA1F).

14. (a) $^{16}O(\alpha, \alpha)^{16}O$ $E_b = 4.730$
(b) $^{16}O(\alpha, \alpha\alpha)^{12}C$ $Q_m = -7.162$

Excitation functions have been measured over a wide range of energies for elastically and inelastically scattered α-particles and γ-rays from the decay of $^{16}O^*$ (6.13, 6.92, 7.13) [see (78AJ03, 83AJ01)] and (86LE1H; 1.8 to 4.8 MeV; α_0), (85JA17; 2.0 to 3.6 MeV; α_0), (83CA1F, 85CA09; 9.2 to 13.5 MeV; α_0), (92LA01; 10.2 to 18 MeV; α_1) and (79BI10, 84RI06; 14.6 to 20.4 MeV; $\alpha_0 \rightarrow \alpha_5$). See also (83FR14, 85IS1A) and ^{16}O in (93TI07).

A number of anomalies are observed: see Table 20.18. K^π parameter assignments derived from this and other work are displayed in Table 20.15 (84RI07). See also (83MI22, 90WE1A, 92AR18). Backscattering cross section measurements and other application-related studies are reported in (90LE06, 91LE33, 92DE10, 93CH2C, 93SO19). For reaction (b) see ^{12}C in (85AJ01).

In recent theoretical work related to $^{16}O(\alpha, \alpha)^{16}O$, studies have been reported for: optical potentials in the range $E_\alpha = 0$–150 MeV (93AB02, 95MI1B), quadrupole resonances (93BY03), a single-folding potential model (93LI25, 93YA08), an R-matrix analysis of elastic cross sections in the range $E_\alpha = 2$–9 MeV (94SH35), the orthogonality condition model (87SA55), Yrast structure change of ^{20}Ne (87KA24), microscopic cluster theory (87TA1C), core-plus-alpha states in terms of vibron models (88CS01), distribution of α-particle strength (88LE05), α cluster formation in the cluster-orbital shell model (90HA38), the microscopic complex effective interaction for α-^{16}O (91YA08), and the generator-coordinate description (87RE04, 92KR12).

Table 20.18
Resonances in $^{16}O(\alpha, \alpha)$ [a]

E_α (MeV ± keV)	$\Gamma_{c.m.}$ (keV)	Outgoing particles	Γ_{α_0}/Γ	θ^2 (%)	E_x (MeV ± keV)	J^π
1.3174 ± 2.2	$(2.8 \pm 0.3) \times 10^{-2}$ [b]	α_0			5.7877 ± 2.6	1^-
2.522 ± 2.5 [c]	19.0 ± 0.9	α_0		22	6.751 ± 3	0^+
3.0382 ± 2.0 [b,c]	8.1 ± 0.3 [b]	α_0		36	7.164	3^-
3.082 ± 3.1 [c]	3.4 ± 0.2 [c]	α_0		1.1	7.199 ± 3	0^+
3.372 ± 3.4 [c]	15.1 ± 0.7 [c]	α_0		4.7	7.431 ± 3	2^+
3.885 ± 10	2	α_0		0.6	7.841 ± 8	2^+
4.653 ± 5	0.013 ± 0.004	α_0		0.07	8.455 ± 5	5^-
≈ 4.9	> 800	α_0		≈ 70	≈ 8.7	0^+
5.002	2.5	α_0		0.23	8.734	1^-
5.058 ± 3	0.11 ± 0.02	α_0		8.5 ± 1.5	8.779 ± 3	6^+
≈ 5.1	> 800	α_0		≈ 95	≈ 8.8	2^+
5.11	< 1	α_0			8.82	(5^-)
5.152 ± 5	19	α_0		1.1	8.854 ± 5	1^-
5.395 ± 5	3	α_0		3.9	9.049 ± 5	4^+
5.486 ± 5	3.2	α_0		0.49	9.121 ± 5	3^-
5.955 ± 10	24	α_0		1.4	9.496 ± 8	2^+
6.569 ± 10	97	α_0		17	9.987 ± 8	4^+
6.912 ± 5	141	α_0		66	10.262 ± 5	5^-
6.92 ± 10	≤ 0.3	α_0		$\leq 1.3 \times 10^{-3}$	10.27 ± 10	(2^+)
7.092 ± 5	81	α_0		4.8	10.406 ± 5	3^-
7.276 ± 5	16	α_0		1.8	10.553 ± 5	4^+
7.314 ± 10	24	α_0		0.85	10.583 ± 8	2^+
7.580 ± 100	349	α_0		33	10.80 ± 75	4^+
7.635 ± 5	13	α_0		0.42	10.840 ± 5	2^+
7.636	45	α_0		2.1	10.841	3^-
(7.75)	80	α_0			(10.93)	

Table 20.18 (continued)
Resonances in $^{16}O(\alpha, \alpha)$ [a]

E_α (MeV ± keV)	$\Gamma_{c.m.}$ (keV)	Outgoing particles	Γ_{α_0}/Γ	θ^2 (%)	E_x (MeV ± keV)	J^π
7.80 ± 150	576	α_0		14	10.97 ± 113	0^+
7.860 ± 10	24	α_0		2.0	11.020 ± 8	4^+
7.93 ± 10	≤ 0.5	α_0		≤ 0.05	11.08 ± 10	(4^+)
8.132 ± 30	172	α_0		4.2	11.24 ± 23	1^-
8.16 ± 10	≤ 0.3	α_0		≤ 0.009	11.26 ± 10	(1^-)
8.24 ± 10	40 ± 10	α_0		1.4	11.32 ± 10	2^+
8.528 ± 10	1.0 ± 0.5	α_0		0.03	11.551 ± 8	0^+ [i]
(≈ 8.6)	≈ 500	α_0			(≈ 11.6)	(2^+)
8.930 ± 20	46	α_0		1.1	11.875 ± 15	2^+
8.997 ± 5	0.44 ± 0.15	α_0, $\gamma_{6.13}$		0.04 ± 0.01	11.929 ± 5	4^+
9.026 ± 5	$(35 \pm 10) \times 10^{-3}$	α_0		1.0 ± 0.3	11.952 ± 5	8^+
9.043 ± 10	30 ± 5	α_0		0.72	11.966 ± 8	1^-
9.25 [d]		α_0, $\gamma_{6.13}$		[e]	12.137 ± 5	6^+
9.403 ± 9	155 ± 15	α_0	0.89 ± 0.05	6.8	12.253 ± 10	4^+
9.406 ± 4 [f]	< 1	$\gamma_{6.13}$		[e]	12.256 ± 4	3^-; 1
9.495 ± 13	390 ± 50	α_0	0.92 ± 0.04	8	12.327 ± 10	2^+
9.587 ± 2	37.3 ± 0.9	α_0, $\gamma_{6.13}$	1.00 ± 0.04	1.2	12.401 ± 5	3^-
9.628 ± 5	24.4 ± 0.5	α_0, α_1	0.62 ± 0.15	0.3	12.433 ± 5 [h]	0^+
9.677 ± 8	124 ± 6	α_0	0.88 ± 0.05	2.4	12.472 ± 10	(2^+)
9.818 ± 6	72 ± 9	α_0	0.68 ± 0.05	14	12.585 ± 5	6^+
9.827 ± 14	145 ± 25	α_0	0.78 ± 0.09	2.5	12.592 ± 15	(2^+)
9.978 ± 6	84 ± 8	α_0	1.00 ± 0.05	7.3	12.713 ± 5	5^-
10.015 ± 7	61 ± 12	α_0	0.72 ± 0.09	0.9	12.743 ± 10	(2^+)
10.132 ± 2	30 ± 5	α_0, $\gamma_{6.13}$	0.83 ± 0.09	0.45	12.836 ± 5	1^-
(10.27)	(580)	(α_0)	(0.92)	(21)	(12.95)	(4^+)
10.283 ± 2	38 ± 4	α_0, $\gamma_{6.13}$	1.00 ± 0.08	0.8	12.957 ± 5	2^+

Table 20.18 (continued)
Resonances in $^{16}O(\alpha, \alpha)$ [a]

E_α (MeV ± keV)	$\Gamma_{c.m.}$ (keV)	Outgoing particles	Γ_{α_0}/Γ	θ^2 (%)	E_x (MeV ± keV)	J^π
10.397 ± 1	18 ± 3	α_0, $\gamma_{6.13}$	0.55 ± 0.05	0.4	13.048 ± 5	4^+
(10.419 ± 15)	(305 ± 55)	(α_0)	(0.42 ± 0.03)	(3.2)	(13.066 ± 15)	(3^-, 5^-)
10.456 ± 5 [l]	162 ± 13	α_0			13.095 ± 6	2^+
10.468 ± 5	102 ± 5	α_0	0.52 ± 0.04	11	13.105 ± 5	6^+
10.508 ± 2	48 ± 4	α_0	1.00 ± 0.05	1.2	13.137 ± 5	3^-
10.614 ± 7	40 ± 13	α_0	0.55 ± 0.13	0.4	13.222 ± 10	0^+
10.617 ± 19	≈ 80	α_0	0.22 ± 0.07	0.3	13.224 ± 15	1^-
10.620 ± 2	53 ± 4	α_0	1.00 ± 0.04	1.3	13.226 ± 5	3^-
10.759 ± 6 [c]	(8 ± 3) × 10^{-2}	α_0		0.08 ± 0.03	13.338 ± 5	7^-
10.763 ± 1	26 ± 3	α_0, $\gamma_{6.13}$	0.70 ± 0.05	0.6	13.341 ± 5	4^+
10.854 ± 3	34 ± 5	α_0, $\gamma_{6.13}$	0.46 ± 0.05	0.4	13.414 ± 5	3^-
10.857 ± 4	≈ 16	α_0	0.16 ± 0.06	0.06	13.416 ± 5	(3^-)
10.870 ± 4	49 ± 7	α_0	0.38 ± 0.04		13.426 ± 5	(5^-)
10.913 ± 8	195 ± 25	α_0	0.99 ± 0.05	3.2	13.461 ± 10	1^-
10.971 ± 4	24 ± 8	α_0	0.36 ± 0.07	0.15	13.507 ± 5	1^-
10.999 ± 4	61 ± 8	α_0	0.72 ± 0.05	0.8	13.529 ± 5	2^+
11.000 ± 15	76 ± 32	α_0	0.52 ± 0.13	0.6	13.530 ± 15	(0^+)
11.054 ± 3	12 ± 5	α_0	0.19 ± 0.06	0.04	13.573 ± 5	2^+
11.183 ± 1	11 ± 2	α_0	0.33 ± 0.05	0.2	13.677 ± 5	5^-
11.202 ± 12	310 ± 30	α_0, $\gamma_{6.13}$	0.51 ± 0.03	84	13.692 ± 10	7^-
11.267 ± 26	≈ 80	α_0	0.33 ± 0.12	0.4	13.744 ± 20	0^+
11.371 ± 9	136 ± 15	α_0	0.73 ± 0.04	2.1	13.827 ± 10	3^-
11.420 ± 34	≈ 175	α_0	0.21 ± 0.06	0.6	13.866 ± 30	1^-
11.473 ± 5	74 ± 10	α_0	0.75 ± 0.06	1.0	13.908 ± 5	2^+
11.498 ± 5	65 ± 3	α_0	0.86 ± 0.04	6.9	13.928 ± 5	6^+
11.522 ± 7	79 ± 15	α_0	1.0 ± 0.1	1.3	13.948 ± 10	0^+

Table 20.18 (continued)
Resonances in $^{16}O(\alpha, \alpha)^{a)}$

E_α (MeV ± keV)	$\Gamma_{c.m.}$ (keV)	Outgoing particles	Γ_{α_0}/Γ	θ^2 (%)	E_x (MeV ± keV)	J^π
11.544 ± 2	8.1 ± 1	α_0	0.46 ± 0.05	0.11	13.965 ± 5	4^+
(11.607 ± 19)	(≈ 80)	(α_0)	(0.19 ± 0.05)	(0.25)	(14.015 ± 15)	(1^-)
(11.663 ± 19)	(150 ± 50)	(α_0)	(0.24 ± 0.05)	(0.6)	(14.060 ± 15)	(2^+)
11.732 ± 4	42 ± 6	α_0, 7.9 47.1	0.71 ± 0.06	0.5	14.115 ± 5	2^+
11.925 ± 7	92 ± 9	α_0	0.64 ± 0.04	1.6	14.270 ± 10	4^+
11.968 ± 8	60 ± 13	α_0, 6.13, 7.9 47.1	0.31 ± 0.05	1.9	14.304 ± 10	(6^+)
11.977 ± 6	117 ± 8	α_0	0.82 ± 0.04	9.6	14.311 ± 5	6^+
11.979 ± 15	≈ 45	α_0	0.13 ± 0.06	0.1	14.313 ± 15	(3^-)
12.148 ± 28	≈ 95	α_0	0.18 ± 0.06 *)	0.3	14.448 ± 25	$(0^+, 2^+)$
12.156 ± 4	≈ 15	α_0	0.09 ± 0.04	0.05	14.454 ± 5	5^-
12.322 ± 25	140 ± 50	α_0	0.45 ± 0.08	0.9	14.587 ± 20	1^-
12.329 ± 13	260 ± 25	α_0, 7.9 47.1	0.79 ± 0.04	5.3	14.593 ± 10	4^+
12.447 ± 11	90 ± 30	α_0	0.35 ± 0.06	0.6	14.687 ± 10	(3^-)
12.502 ± 10	60 ± 25	α_0	0.25 ± 0.06	0.4	14.731 ± 10	(4^+)
12.539 ± 2	7.3 ± 4.8	α_0	0.18 ± 0.05	0.1	14.761 ± 5	6^+
12.597 ± 4	86 ± 7	α_0	0.95 ± 0.04	6.5	14.807 ± 5	6^+
12.608 ± 5	117 ± 13	α_0	0.69 ± 0.04	3.1	14.816 ± 5	5^-
12.637 ± 8	79 ± 15	α_0	0.45 ± 0.05	0.9	14.839 ± 10	(4^+)
12.699 ± 12	100 ± 30	α_0	0.44 ± 0.06	0.7	14.888 ± 10	2^+
12.897 ± 10	66 ± 20	α_0	0.31 ± 0.06	0.3	15.047 ± 10	2^+
12.930 ± 12	160 ± 25	α_0	0.40 ± 0.04	2.3	15.073 ± 10	5^-
13.016 ± 20	≈ 60	α_0	≈ 0.12	0.11	15.142 ± 15	(2^+)
13.056 ± 10	230 ± 25	α_0	0.70 ± 0.04	5.5	15.174 ± 10	5^-
13.237 ± 29	280 ± 40	α_0	0.39 ± 0.04	20	15.319 ± 25	7^-
(13.238 ± 10)	(130 ± 20)	(α_0)	(0.99 ± 0.08)		(15.319 ± 10)	(1^-)
13.251 ± 6	34 ± 10	α_0	0.29 ± 0.05	0.2	15.330 ± 5	4^+

Table 20.18 (continued)
Resonances in $^{16}O(\alpha, \alpha)$ [a]

E_α (MeV ± keV)	$\Gamma_{c.m.}$ (keV)	Outgoing particles	Γ_{α_0}/Γ	θ^2 (%)	E_x (MeV ± keV)	J^π
(13.266 ± 12)	(50 ± 25)	(α_0)	(0.69 ± 0.17)		(15.342 ± 10)	(0^+)
13.27 [f]		α_1			15.346 ± 2	6^+
13.296 ± 5	110 ± 10	α_0, 7612, 7612+7.1	0.71 ± 0.04	14	15.366 ± 5	7^-
13.384 ± 15 [d]	85 ± 35	α_0	0.26 ± 0.05	0.4	15.436 ± 15	(3^-)
13.58		α_0, 7612, 7612+7.1			15.59	
13.73		α_0, 7612, 7612+7.1			15.71	(6^+)
14.05		α_0, 7612, 7612+7.1			15.97	(6^+)
14.26		7612, 7612+7.1			16.14	
14.40		7612			16.25	
14.501 ± 15	45	α_0, α_{1+2}			16.329 ± 11	4^+
14.636 ± 15 [e]	35	α_0, α_{1+2}, α_3			16.437 ± 11	$(0, 2, 4)^+$
14.721 ± 15	24 ± 4	α_0, α_{1+2}, α_3, α_4	0.36 ± 0.03	0.38 ± 0.07	16.505 ± 15	6^+
14.789 ± 18	90 ± 30	α_0	0.16 ± 0.03	0.37 ± 0.13	16.559 ± 15	5^-
14.816 ± 15	92 ± 8	α_0, α_3	0.45 ± 0.03	4.1 ± 0.5	16.581 ± 15	7^-
14.875 ± 22	80 ± 25	α_0	0.18 ± 0.04	0.22 ± 0.08	16.628 ± 20	3^-
14.924 ± 20	100 ± 25	α_0, (α_3)	0.23 ± 0.03	0.42 ± 0.11	16.667 ± 15	4^+
14.987 ± 18	≈ 25	α_0, α_{1+2}, α_3, α_4	0.08 ± 0.03	≈ 0.05	16.717 ± 15	5^-
15.023 ± 33	160 ± 50	α_0	0.10 ± 0.02	4.8 ± 1.9	16.746 ± 25	8^+
15.149 ± 16	16 ± 8	α_0, α_{1+2}, α_3, α_4	0.11 ± 0.02	0.04 ± 0.02	16.847 ± 15	5^-
15.179 ± 25	350 ± 50	α_0	0.28 ± 0.03	3.9 ± 0.7	16.871 ± 20	6^+
15.430 ± 21	180 ± 30	α_0	0.32 ± 0.03	1.0 ± 0.2	17.072 ± 20	4^+
15.535 ± 15	26 ± 5	α_0, α_{1+2}, α_3, α_4	0.22 ± 0.02	0.13 ± 0.03	17.155 ± 15	5^-
15.607 ± 19	225 ± 30	α_0	0.32 ± 0.02	1.2 ± 0.2	17.213 ± 15	4^+
15.696 ± 20	86 ± 25	α_0, α_{1+2}, α_3, α_4	0.16 ± 0.03	0.20 ± 0.07	17.284 ± 15	3^-
15.710 ± 17	200 ± 25	α_0	0.26 ± 0.02	11.6 ± 1.4	17.295 ± 15	8^+
15.828 ± 15 [f]	< 10	α_{1+2}			17.390 ± 15	

Table 20.18 (continued)
Resonances in $^{16}O(\alpha, \alpha)$ [a]

E_α (MeV ± keV)	$\Gamma_{c.m.}$ (keV)	Outgoing particles	Γ_{α_i}/Γ	θ^2 (%)	E_x (MeV ± keV)	J^π
15.878 ± 18	220 ± 25	α_0	0.24 ± 0.01	48 ± 6	17.430 ± 15	9^-
16.017 ± 16	86 ± 9	α_0, α_{1+2}, α_3, α_4	0.45 ± 0.03	1.3 ± 0.2	17.541 ± 15	6^+
16.099 ± 17	140 ± 20	α_0, α_4	0.36 ± 0.03	1.05 ± 0.15	17.606 ± 15	5^-
16.302 ± 23	≈ 125	α_0	0.13 ± 0.03	≈ 0.3	17.769 ± 20	4^+
16.405 ± 17	200 ± 30	α_0	0.38 ± 0.03	1.6 ± 0.3	17.851 ± 15	5^-
16.598 ± 15 [e]	< 10	α_0, α_{1+2}			18.005 ± 15	7^-
16.622 ± 6	34 ± 7	α_0, α_{1+2}, α_3, α_4	0.34 ± 0.04	0.23 ± 0.06	18.024 ± 5	5^-
16.695 ± 30	140 ± 60	α_0	0.20 ± 0.05	0.4 ± 0.2	18.083 ± 25	4^+
16.748 ± 6	29 ± 6	α_0, α_{1+2}, α_3, α_4	0.46 ± 0.06	0.8 ± 0.2	18.125 ± 5	7^-
16.949 ± 13	190 ± 30	α_0, α_4	0.32 ± 0.02	1.7 ± 0.3	18.286 ± 10	6^+
17.129 ± 24	185 ± 40	α_0, (α_{1+2}), α_3, α_4	0.19 ± 0.02	1.8 ± 0.4	18.430 ± 20	7^-
17.210 ± 21	130 ± 30	α_0, α_3	0.21 ± 0.03	0.5	18.494 ± 20	5^-
17.368 ± 23	185 ± 30	α_0, α_4	0.24 ± 0.03	5.5 ± 1.1	18.621 ± 20	8^+
17.524 ± 29	140 ± 50	α_0, α_{1+2}	0.17 ± 0.04	0.6 ± 0.3	18.745 ± 25	6^+
17.552 ± 24	140 ± 35	α_0	0.22 ± 0.03	1.5 ± 0.4	18.768 ± 20	7^-
17.793 ± 29	200 ± 60	α_0	0.15 ± 0.02	3.2 ± 1.1	18.960 ± 25	8^+
17.906 ± 18	≈ 90	α_0, α_{1+2}	0.18 ± 0.03	≈ 0.3	19.051 ± 15	5^-
18.03 ± 20	200 ± 50	α_0, α_1, (α_2), α_4, α_5	0.38 ± 0.04 [d]	≈ 2	19.15 ± 20	6^+
18.198 ± 17	140 ± 25	α_1, (α_5)	0.12 ± 0.02 [b]		19.284 ± 15	6^+
18.216 ± 30	430 ± 60	α_0	0.36 ± 0.03	6.4 ± 1.1	19.298 ± 25	7^-
18.397 ± 11	130 ± 15	α_1, α_3, α_4	0.38 ± 0.01 [b]		19.443 ± 10	6^+
18.514 ± 29	250 ± 60	α_0, α_2, α_3	0.27 ± 0.04	1.6 ± 0.4	19.536 ± 25	6^+
(18.563 ± 25)	(140 ± 50)	(α_1)	(0.09 ± 0.02) [b]		(19.576 ± 20)	(7^-)
18.662 ± 23	140 ± 35	α_1	0.14 ± 0.02 [b]		19.655 ± 20	6^+
18.757 ± 28	330 ± 60	α_0, (α_2), α_3	0.23 ± 0.02	6.3 ± 1.2	19.731 ± 20	8^+
18.900 ± 48	360 ± 120	α_0	0.18 ± 0.03	1.4 ± 0.5	19.845 ± 40	6^+

Table 20.18 (continued)
Resonances in $^{16}O(\alpha, \alpha)$ [a]

E_α (MeV ± keV)	$\Gamma_{c.m.}$ (keV)	Outgoing particles	Γ_{α_n}/Γ	θ^2 (%)	E_x (MeV ± keV)	J^π
18.918 ± 11	170 ± 25	α_1	0.26 ± 0.02 [h]		19.859 ± 10	5^-
18.949 ± 52	≈ 120	α_0	0.08 ± 0.03	≈ 0.35	19.884 ± 40	7^-
19.083 ± 39	130 ± 100	α_0, α_2 (α_5)	0.11 ± 0.04	0.19 ± 0.04	19.991 ± 30	4^+
19.128 ± 16	80 ± 35	α_1, α_4	0.10 ± 0.04 [h]		20.027 ± 15	6^+
19.227 ± 28	190 ± 35	α_1	0.29 ± 0.03 [h]		20.106 ± 25	7^-
19.304 ± 47	285 ± 100	α_0, α_3	0.18 ± 0.04	1.1 ± 0.4	20.168 ± 35	6^+
19.464 ± 19	255 ± 40	α_1, α_5	0.28 ± 0.03 [h]		20.296 ± 15	7^-
19.521 ± 22	190 ± 40	α_1	0.26 ± 0.03 [h]		20.341 ± 20	5^-
19.524 ± 16	135 ± 35	α_0, α_3	0.25 ± 0.04	1.1 ± 0.3	20.344 ± 15	7^-
19.618 ± 39	215 ± 90	α_0	0.14 ± 0.03	0.6 ± 0.3	20.419 ± 30	6^+
19.651 ± 32	370 ± 55	α_1	0.32 ± 0.03 [h]		20.445 ± 25	6^+
19.679 ± 35	280 ± 70	α_0, α_2	0.20 ± 0.03	0.86 ± 0.25	20.468 ± 30	5^-
19.952 ± 8	78 ± 11	$\alpha_0, \alpha_1, \alpha_2, \alpha_3$	0.33 ± 0.03 [j]	4.5 ± 0.8	20.686 ± 6	9^-
20.04	240 ± 50	$\alpha_0, \alpha_1, \alpha_4$	0.2 [j]	1.8 ± 0.5	20.76 ± 30	7^-
20.095 ± 32	170 ± 60	α_1	0.11 ± 0.02		20.800 ± 25	5^-
20.28	300 ± 50	α_0, α_1	0.23 ± 0.03 [j]	2.1 ± 0.6	20.95 ± 40	7^-
20.423 ± 8 [k]	60 ± 6	α_0, α_3	0.46 ± 0.03	4.1 ± 0.5	21.062 ± 6	9^-
20.7	300	α_0			21.3	7^-
21.3 ± 200	300	α_0			21.8 ± 150	7^-
22.0 ± 200	500	α_0			22.3 ± 150	7^-
22.5 ± 250	500	α_0			22.7 ± 200	9^-
22.65 ± 125	250	α_0			22.84 ± 100	9^-
23.3 ± 250	500	α_0			23.4 ± 200	8^+
24.24 ± 150	350	α_0			24.11 ± 100	8^+
25.4 ± 300	600	α_0			25.0 ± 250	8^+
26.2 ± 200	400	α_0			25.7 ± 150	

Table 20.18 (continued)
Resonances in $^{16}O(\alpha, \alpha)$ [a]

E_α (MeV ± keV)	$\Gamma_{c.m.}$ (keV)	Outgoing particles	Γ_{α_0}/Γ	θ^2 (%)	E_x (MeV ± keV)	J^π
28.1 ± 350	700	α_0			27.2 ± 300	
29	1600	α_0			28	8^+
29.4 ± 350	700	α_0			28.2 ± 300	

[a]) For earlier references see Tables 20.23 in (78AJ03) and 20.21 in (83AJ01). For J^π assignments see Table 20.15 here. The uncertainties in the excitation energies are calculated by taking the uncertainty in E_α in the c.m. [$\frac{4}{5}$ × uncertainty in the lab] and adding the uncertainty in E_b [2 keV], in quadrature, rounding upwards. See (87AJ02).
[b]) $\Gamma_{c.m.} = \Gamma_\alpha$.
[c]) (85JA17).
[d]) Resonances with $9.25 \leq E_\alpha \leq 13.39$ MeV are from (85CA09), except for the states labelled [e]). Certain values are rounded upwards. See also (83CA1F) and Table 20.21 in (83AJ01).
[e]) $(2J+1)\Gamma_{\alpha_0}\Gamma_{\alpha_0}/\Gamma_E = 81 \pm 12$ eV and 14 ± 2 eV, respectively, for $^{20}Ne^*$ (12.14, 12.25) [for the latter see Table 20.17] (80FI01).
[f]) See Table 20.21 in (83AJ01).
[g]) Resonances with $14.6 < E_\alpha < 20.4$ MeV are from the re-analysis of the data of (79BI10) by (84RI06). Certain values are rounded upwards.
[h]) $(\Gamma_{\alpha_0}\Gamma_{\alpha_0})^{1/2}/\Gamma$.
[i]) (84RI07).
[j]) For information on the α_1 strength see (84RI06).
[k]) (92LA01) determine $E_x = 12.436 \pm 0.004$ MeV.
[l]) (92LA01).

15. ^{16}O(^{6}Li, d)^{20}Ne $\quad Q_{\rm m} = 3.255$

Deuteron groups have been observed to many states of ^{20}Ne: see Table 20.19. Angular distributions have been measured for $E(^{6}\text{Li}) = 5.5$ to 75.4 MeV: see (78AJ03, 83AJ01). See also (84MO08). A recent measurement at $E(^{6}\text{Li}) = 22$ MeV by (95MA1A) provided data that were used in a determination of α-particle widths in ^{19}Ne relative to widths in ^{20}Ne. Angular correlations [(d, α_0) to $^{16}\text{O}_{\text{g.s.}}$] have been measured at $E(^{6}\text{Li}) = 60$, 75, and 95 MeV (82AR20, 88ARZU). See also references cited in (87AJ02).

In theoretical work published since the previous review, Hauser-Feshbach theory was applied to this reaction by (87AR13), and angular distributions were analyzed with DWBA formalism by (92RA22). See also (94OS05).

16. ^{16}O(^{7}Li, t)^{20}Ne $\quad Q_{\rm m} = 2.263$

States observed in this reaction are displayed in Table 20.19. Angular distributions have been measured at $E(^{7}\text{Li}) = 15$ to 68 MeV: see (78AJ03, 83AJ01). See also (86CO15).

Angular correlation (τ, α_0) to ^{16}O were measured by (88ARZU). See also references cited in (78AJ03, 83AJ01, 87AJ02).

Theoretical work related to this reaction includes studies on: the form of the α particle potential in direct α-transfer reactions (86GR1C, 88GR1I), a Hauser Feshbach theory application (87AR13), the optical potential (89BE51), clustering phenomena and shell effects (88RA1G), DWBA analysis (92RA22).

17. ^{16}O(^{9}Be, ^{5}He)^{20}Ne $\quad Q_{\rm m} = 2.263$

See (85CU1A).

18. (a) ^{16}O(^{12}C, ^{8}Be)^{20}Ne $\quad Q_{\rm m} = -2.636$
    (b) ^{16}O(^{12}C, 2α)^{20}Ne $\quad Q_{\rm m} = -2.545$
    (c) ^{16}O(^{12}C, α^{12}C)^{12}C $\quad Q_{\rm m} = -7.162$

Angular distributions in reaction (a) have been measured for $E(^{16}\text{O}) = 27.1$ to 53.0 MeV and for $E(^{12}\text{C}) = 22.7$ to 78 MeV [see (78AJ03, 83AJ01)] as well as at $E(^{12}\text{C}) = 109$ MeV (84MU04, 85MU14; ^{20}Ne* (1.63, 4.25, 5.79, 7.16, 8.78, 10.26, 11.95, 12.59, 15.34, 15.87, 17.30, 21.08, 22.87); $\sigma(\theta)$ at several angles; EFR-DWBA

Table 20.19
States of ^{20}Ne from ^{16}O(^{6}Li, d), ^{16}O(^{7}Li, t) and ^{16}O(^{12}C, ^{8}Be) [a]

E_x (MeV ± keV)			$\Gamma_{c.m.}$ (keV)	Γ_{α_0}/Γ	S [b]	J^π
(^{6}Li, d)	(^{7}Li, t)	(^{12}C, ^{8}Be)				
0	0	0			1.00	0^+
1.63	1.63	1.63			0.41	2^+
4.25	4.25	4.25			0.22	4^+
4.97						2^-
5.62					0.06	3^-
5.79	5.79	5.79			0.54	1^-
6.73					0.56	0^+
7.00						4^-
7.16	7.16	7.16			0.26	3^-
7.43					0.13	2^+
8.46					0.04	5^-
8.78	8.78	8.78			0.20	6^+
10.3 ± 100	10.26	10.26	145 ± 40	1	0.15	5^-
10.7 ± 100						4^+
11.95	11.95	11.95		0.85 ± 0.15	0.51	8^+
12.14					0.05	6^+
12.6 ± 100	12.591 ± 10	12.59	110 ± 40	0.80 ± 0.10		6^+
13.9	13.904 ± 20		≈ 100			6^+
14.3	14.310 ± 20	14.3 [d])	< 100			6^+
15.35 ± 100	15.336 ± 15	15.34	380 ± 60	0.90 ± 0.10		7^-
15.9 ± 100		15.87	< 250			7^-
16.7 ± 100	16.63 ± 20	16.63	190 ± 40	0.90 ± 0.10		7^- [e])
17.35 ± 100	17.30 ± 20	17.30	220 ± 40	≥ 0.40 ± 0.10		8^+ [e])
18.7 ± 100						7^-
19.4 ± 100			400			7^-
19.9 ± 100			400			7^-
	20.67 ± 40	20.5 [d])				
20.8 ± 100						7^- (6^+)
	21.08 ± 30	21.08	100 ± 50	0.65 ± 0.15		9^-
21.3 ± 100			300			8^+
21.8 ± 100			300			8^+
22.3 ± 100			300			8^+
	22.87 ± 40	22.87	225 ± 40	0.90 ± 0.10		9^-
23.5 ± 100	23.70 ± 30		≤ 200			9^- (8^+)
	24.21 ± 25		≈ 500			

Table 20.19 (continued)
States of ^{20}Ne from ^{16}O(^{6}Li, d), ^{16}O(^{7}Li, t) and ^{16}O(^{12}C, ^{8}Be) [a])

E_x (MeV ± keV)			$\Gamma_{c.m.}$ (keV)	Γ_{α_0}/Γ	S [b])	J^π
(^{6}Li, d)	(^{7}Li, t)	(^{12}C, ^{8}Be)				
	25.10 ± 50		≤ 200			
	25.67 ± 50		≈ 500			
27.1 ± 100 [c])		27.0 [d])				9^-
28.1 ± 100 [c])						10^+
(29.4) [c])						(10^+)
((33.4))						$((10^+))$

[a]) For complete references see Tables 20.24 in (78AJ03) and 20.22 in (83AJ01).
[b]) Relative α-particle spectroscopic factors (DWBA). Other S_α values have also been reported.
[c]) (82AR20, 88AL07).
[d]) (83SH26).
[e]) An admixture of 6^+ or 8^+ in the d-α angular correlation involving ^{20}Ne* (16.6) and a doublet $(8^+ + 7^-)$ at $E_x = 17.4$ MeV have been suggested. See also Table 20.18.

analysis). See also (88CAZY). Γ_{α_0}/Γ are displayed in Table 20.19: see (83AJ01, 87AJ02) and (83SH26). Spectroscopic factors were extracted in a direct reaction study reported by (89OS02). Evidence for 10^+ strength at $E_x = 27.5$ MeV is reported by (88AL07). See also (83DEZW). For discussion of ^{28}Si states reached in this reaction see (93ES01, 93ES03, 93ZH21). See also the discussion of instrumentation development for ^{8}Be detection reported in (91SU15). For reaction (b) see (78AJ03) and (86CA19). For reaction (c) and for a discussion of ^{24}Mg states reached in this reaction see (83SH26, 84MU04). See also (85BE37, 86BE19, 87SU03).

19. ^{16}O(^{13}C, ^{9}Be)^{20}Ne $\qquad Q_m = -5.918$

At $E(^{13}C) = 105$ MeV angular distributions to ^{20}Ne* (1.63, 4.25, 8.78, 11.95, 15.34, 21.0) have been studied by (79BR1B): the first four states are the 2^+, 4^+, 6^+, and 8^+ members of the 0^+_1 band; the two higher states $[J^\pi = 7^-, 9^-]$ belong to the 0^- band for which the band head is ^{20}Ne* (5.79). In addition, distributions are reported to ^{20}Ne* (12.59, 15.9, 17.3) $[J^\pi = 6^+, 8^+, 8^+]$ (79BR03). See also (85MU14). Spectroscopic factors were extracted in a direct reaction study reported by (89OS02). For fusion cross sections see (86PA10).

20. ^{16}O(^{16}O, ^{12}C)^{20}Ne $\qquad Q_m = -2.432$

Angular distributions have been reported to a number of states of ^{20}Ne at $E(^{16}\mathrm{O}) = 23.9$ to 95.2 MeV [see (78AJ03, 83AJ01)] and recently at $E(^{16}\mathrm{O}) = 26$, 28, and 30 MeV (86CA24). (83ME13) have studied the quasi-elastic spectrum at $E(^{16}\mathrm{O}) = 50$, 60, 68, and 72 MeV. For excitation functions see (86CA24; ^{20}Ne* (0, 1.63)). See also (82KO1C, 84ME10, 85ST1B, 82KO1D, 84AP03, 84KO13).

Studies of the direct-reaction mechanism for this reaction have been carried out by (88GA1L, 88GA19, 89OS02, 90OS03). See also (88AU03) and references cited in (87AJ02).

21. (a) ^{17}O(^{3}He, ^{3}He)^{17}O $E_\mathrm{b} = 21.164$
    (b) ^{17}O(^{3}He, α)^{16}O $Q_\mathrm{m} = 16.434$

The excitation function for α_0 shows a resonance corresponding to ^{20}Ne* (28.): see (78AJ03). Measurements of A_y at $E(^{3}\mathrm{He}) = 33$ MeV, have been reported for the elastic scattering [reaction (a)] (83LE03) and for many α-groups [see ^{16}O in (93TI07)] (82KA12). For the earlier work and for other channels see (83AJ01, 87AJ02).

22. ^{17}O(α, n)^{20}Ne $Q_\mathrm{m} = 0.587$

Neutron emission from this reaction was measured for $E_\alpha = 5.15$ and 5.49 MeV by (87SM1B). Excitation functions were measured at astrophysical energies and S-factor curves were determined by (95KU1H). See also work cited in (78AJ03). In a recent theoretical study, the three-cluster generator coordinate method was applied to low energy cross section by (93DE32).

23. (a) ^{17}O(^{11}B, ^{8}Li)^{20}Ne $Q_\mathrm{m} = -6.045$
    (b) ^{17}O(^{12}C, ^{9}Be)^{20}Ne $Q_\mathrm{m} = -5.115$

At $E = 115$ MeV the 8^+ state at $E_\mathrm{x} = 11.95$ MeV is strongly populated in both reactions: see (83AJ01).

24. ^{18}O(^{3}He, n)^{20}Ne $Q_\mathrm{m} = 13.120$

Angular distributions have been measured for $E(^{3}\mathrm{He}) = 2.8$ to 18.3 MeV. States of ^{20}Ne observed in this reaction are displayed in Table 20.23 of (83AJ01). These include a state at $E_\mathrm{x} = 16.730 \pm 0.006$ MeV, $\Gamma < 20$ keV: $J^\pi = 0^+$, $T = 2$.

Table 20.20
Resonances in ^{19}F(p, γ)^{20}Ne [a])

E_p (keV)	Γ_{lab} (keV)	Γ_{γ_0} (eV)	Γ_{γ_1} (eV)	^{20}Ne* (MeV)	J^π; T
340		< 0.07	0.28 ± 0.06	13.171	
484		≈ 0.05	0.42	13.308	
597 ± 1	30 ± 3	< 0.6	12	13.415	
671 ± 1	6.0 ± 0.7	1.0×10^{-2}	2.2	13.485	1^+
874				13.678	
935				13.736	
980				13.779	
1091	0.8		1.1	13.884	2^+; 1
1280				14.063	
1320	4.0			14.101	
1350				14.130	
1370				14.149	
1420	15.7			14.196	
4090 ± 5				16.732 [b])	0^+; 2
5879 ± 7	10 ± 3	$\Gamma_\gamma \approx 0.3$ eV		18.430	2^+; 2

[a]) For earlier references see Tables 20.26 in (78AJ03) and 20.24 in (83AJ01). See also Table 20.14 here.
[b]) Decays $\approx 100\%$ to the $E_x = 11.23$ MeV J^π; $T = 1^+$; 1 state with $\Gamma_\gamma \approx 5$ eV. See discussion under reaction 25.

25. ^{19}F(p, γ)^{20}Ne $\qquad Q_m = 12.844$

The previous review (87AJ02), observed that over the range $E_p = 2.9$ to 12.8 MeV, the γ_0 and γ_1 yields are dominated by the E1 giant resonance ($\Gamma \approx 6$ MeV) with the γ_1 giant resonance displaced upward in energy. Strong well-correlated structures are observed with characteristic widths $\Gamma \approx 175$ keV. Angular distributions taken over the energy range do not vary greatly with energy. They are incompatible with γ_0 and γ_1 coming from the same levels in ^{20}Ne. The 90° γ_0 yield for $E_p = 3.5$ to 10 MeV has been measured: the results are interpreted in terms of four primary doorway states at $E_x = 16.7$, 17.8, 19.1 and 20.2 MeV. See also (85WA1L; $E_p = 5.9$ to 10.3 MeV; E2 strength; prelim.). See also (86OUZZ).

More recently, polarized and unpolarized angular distributions were measured for $E_p = 16.1$–23.0 MeV (88KU08). Data for (p, γ_1) were also presented and a doorway state calculation was discussed. Cross section and analyzing powers for (p, $\gamma_0\gamma_1$) were measured in the range $E_p = 3.5$–13.3 MeV by (88WA13) in a study of the E2 strength in ^{20}Ne. See also the review of giant resonance work in (88HA12).

The yield curve for 11.2 MeV γ-rays [from the decay of ^{20}Ne* (11.23), $J^\pi = 1^+$, $T = 1$, to the ground state] displays a resonance at $E_p = 4.090 \pm 0.005$ MeV [^{20}Ne* (16.73)]. The 11.2 MeV γ-rays are isotropic which is consistent with the presumed 0^+ character of this lowest $T = 2$ state in ^{20}Ne: $\Gamma_p\Gamma_\gamma/\Gamma \approx 0.5$ eV. Since Γ_p/Γ (from the elastic scattering) is ≈ 0.1, $\Gamma_\gamma \approx 5$ eV. For $E_p = 5.65$ to 6.21 MeV, the γ_0 and γ_1 yields are not resonant but the yield of 10.6-MeV γ-rays is resonant at 5.879 ± 0.007 MeV [$\Gamma_{c.m.} = 9.5 \pm 3$ keV, $\Gamma_{p_0}\Gamma_\gamma/\Gamma \approx 0.05$ eV; $\Gamma_\gamma \approx 0.3$ eV]. The 10.6 MeV γ-ray is due to the cascade decay of ^{20}Ne* (18.43), $J^\pi = 2^+$, $T = 2$ via ^{20}Ne* (12.22) to the 2^+ state at 1.63 MeV. For the upper limits to the strengths of the transitions to various states of ^{20}Ne from the 0^+ and 2^+ $T = 2$ states, see (83AJ01). Internal pair conversion of the GDR at $E_x \approx 18$ MeV was observed by (89MOZY). Resonances observed in the capture reaction are displayed in Table 20.20. For references see (78AJ03, 83AJ01). See also the astrophysics-related work in (87RO1D, 88CA1N). A study of absolute thick-target yields for elemental analysis at $E_p = 7$, 9 MeV is reported in (87RA23).

26. (a) ^{19}F(p, p)^{19}F $E_b = 12.844$
    (b) ^{19}F(p, p′)^{19}F*
    (c) ^{19}F(p, d)^{18}F $Q_m = -8.207$

The elastic scattering has been studied in the range $E_p = 0.5$ to 7.5 MeV and 24.9 to 46.3 MeV [see (78AJ03)] and at $E_p = 1.5$ to 3.5 MeV (85OU01, 86OUZZ, 86OU01). See also the measurements for $E_p = 0.85$–1.01 MeV at $\theta_{lab} = 165°$ by (89KN01), and the work reported in (94CO12) in which a ^{19}F radioactive beam was used in scattering off polyethelyne targets. The observed anomalies are displayed in Table 20.21.

Resonances for inelastic scattering [p_1 and p_2] are listed in Table 20.22. In general the resonances observed are identical with those reported from other ^{19}F + p reactions, although the relative intensities differ greatly. Cross sections for production of 110 and 197 keV γ-rays are reported for $E_p = 0.5$ to 4.3 MeV by (86CH1T). See also (83LE28; astrophysics) and (86BA1N). For reaction (c) see (86KA1U; applied) and ^{18}F.

27. ^{19}F(p, n)^{19}Ne $Q_m = -4.020$ $E_b = 12.844$

Observed resonances are displayed in Table 20.30 of (78AJ03). See also (84BA1R, 85CA41). Polarization transfer coefficient for $E_p = 120$, 160 MeV at $\theta = 0°$ were measured by (90HUZY). Total cross sections for production of ^{19}Ne measured by the activation method are reported by (90WA10).

Table 20.21
Levels of ^{20}Ne from ^{19}F(p, p_0) [a])

E_p (keV)	Γ_{lab} (keV)	l	J^π; T	Γ_p/Γ	θ_p^2 (%)	^{20}Ne* (MeV)
340	2.9	0	1^+	0.016	3.8	13.171
483			1^+			13.307
598	37	1	2^-	0.0012	0.38	13.416
669	7.5	0	1^+	0.98	9.6	13.483
843	23	0	0^+	0.996	10.8	13.649
873	5.2	1	2^- [b])	0.21	1.5	13.677
935	8.0	0	1^+	0.17	0.44	13.736
1346	4.5	1	2^- [b])	0.067	0.07	14.126
1372	15	1	2^- [b])	0.17	0.52	14.151
1422	14.6	0	1^+	0.85	0.92	14.198
1710 [c])	90	0	0^+	0.8		14.472
1896 [c])	25	0	0^+	0.3		14.648
1943 [c])	40	0	(1^+)	0.5		14.693
2030 [c])	70	1	(1^-)	0.75		14.776
2763 [c])		2				15.472
2970 [c])		2				15.668
4094 ± 3	2.1 ± 0.5	0	0^+; 2	0.062 ± 0.004		16.735
5879 ± 7 [d])	10 ± 3	2	2^+; 2	≈ 0.2		18.430

[a]) For references see Table 20.27 in (78AJ03). For θ^2 see Table 20.28 in (78AJ03).
[b]) 1^- not excluded by elastic scattering alone.
[c]) (85OU01, 86OU01; R-matrix analysis). Weak resonances at $E_p = 1.75$ and 1.78 MeV are also suggested.
[d]) Resonance also observed in p_1, p_3, p_4 and p_5 yields.

Table 20.22
Resonances in ^{19}F(p, p′)^{19}F* [a])

E_p (keV)	J^π; T	Γ_{lab} (keV)	Γ_{p_1} (eV)	Γ_{p_2} (eV)	$\theta^2_{p_1}$ (%)	$\theta^2_{p_2}$ (%)	E_x in ^{20}Ne (MeV)
340	1^+	2.9	< 0.5	< 0.1	< 15		13.171
483	1^+	2.2	< 1.3	< 1.2			13.307
598	2^-	37	< 100	< 60	< 28	< 145	13.416
669	1^+	7.5	46	< 0.5	0.6	< 0.4	13.483
720		≈ 30	< 10000	< 10000			13.532
780		≈ 10	< 400	≈ 9000			13.589
831		8.3	< 6	≈ 2300			13.637
845	0^+	23	≈ 50	< 10	≈ 0.14	< 0.92	13.650
873	2^-	5.2	< 2	570	< 0.07	2.7	13.677
900		4.8	< 30	≈ 2200			13.703
935	1^+	8.0	3000	< 20	5.0	< 0.8	13.736
1092 [b])	2^+	0.8	173	592			13.885
1137		3.7	< 40	≈ 2100			13.928
≈ 1250		≈ 80	≈ 70000	< 4000			14.03
1290		19	< 600	≈ 900			14.073
1346	2^-	4.5	300	600	0.92	0.24	14.126
1372	2^-	15	700	1400	1.93	0.56	14.151
1422	1^+	14.6 ± 1	2200	≤ 35	0.56	≤ 0.11	14.198
1610		≈ 5					14.377
1660							14.424
1700							14.462
2763 [c])							15.472
2970 [c])							15.668
5879 [d])	2^+; 2		r				18.430

r = resonant.
[a]) For references see Tables 20.29 in (78AJ03) and 20.26 in (83AJ01).
[b]) $\Gamma_{p_0} = 29$ eV.
[c]) Reported in $p_{1\to4}$ yield (86OU01).
[d]) Resonance also observed in p_3, p_4, and p_5 yields.

28. ^{19}F(p, α)^{16}O $Q_{\rm m} = 8.114$ $E_{\rm b} = 12.844$

Many resonances occur in this reaction. They are displayed in Tables 20.23, 20.24, and 20.25 depending on whether they are observed in the α_0 yield [20.23], in the α_1 [or α_π] yield to ^{16}O* (6.05) [20.24] or in the α_2, α_3, and α_4 yields [or in the yield of the γ-rays from ^{16}O* (6.13, 6.92, 7.12) [20.25]]. See also tables 2 and 3 in (93DA23) which list a number of new resonances for $E_{\rm p} = 0.3$–3.0 MeV. Resonances for α_0 and α_1 are required to have even J, even π or odd J, odd π, while the α_2, α_3, and α_4 resonances are all odd-even or even-odd, with the exception of the $T = 2$ resonance.

Listings of the earlier yield studies are given in (72AJ02, 78AJ03, 83AJ01). A detailed discussion of the evidence leading to many of the J^π assignments is given in (59AJ76). For values of θ^2 see Table 20.28 in (78AJ03). Recent measurements are reported by (85OU01; 1.5 to 2.1 MeV; $\alpha_0 \rightarrow \alpha_3$) and (84IN04; 4.15 to 13 MeV; $\alpha_0 \rightarrow \alpha_5$). In the latter work there are no marked correlations between the different channels.

Longitudinally and transversely polarized protons with $E_{\rm p} \approx 0.67$ MeV have been used to study ^{20}Ne* (13.48) [$J^\pi = 1^+$; $T = 1$] via a parity- (and isospin-) forbidden α-transition. The state is not excited. The upper limits for the process, and their significance in the determination of f_π, the weak pion-nucleon coupling constant, are discussed by (83KN01, 86KN1C, 90KN01). See also (83AJ01, 84KN1A).

Internal pair conversion for ^{19}F(p, α_π) of the 18 MeV GDR in ^{20}Ne was studied by (89MOZY) at $E_{\rm p} = 5.2$ MeV.

A DWBA analysis for energies below the Coulomb barrier is used to determine the astrophysical S-factor in (91HE16). See also (93YA18).

Application-related work is reported in (87EV01, 89MC04, 89MC03, 89TA1N). See also the earlier work cited in (87AJ02).

29. ^{19}F(d, n)^{20}Ne $Q_{\rm m} = 10.620$

Levels of ^{20}Ne derived from this reaction are displayed in Tables 20.31 in (72AJ02) and 20.34 in (78AJ03). See also (83LI1D).

30. ^{19}F(^{3}He, d)^{20}Ne $Q_{\rm m} = 7.350$

Levels of ^{20}Ne observed in this reaction are displayed in Tables 20.35 in (78AJ03) and 20.32 in (87AJ02). Deuteron angular distributions have been studied at $E(^3\text{He}) =$ 9.5 to 21 MeV: see (78AJ03).

Table 20.23
Resonances for ground-state α-particles (α_0) in ^{19}F(p, α_0) [a])

E_p (keV)	Γ_{lab} (keV)	θ_α^2 (%) [a])	J^π; T	^{20}Ne* (MeV)
400	100		1^-	13.228
400	100		0^+	13.228
650 ± 20	200		1^-	13.465
710	35	0.6	(1^-)	13.522
733	66	1.0	2^+	13.544
777 ± 2	9 ± 1	0.02	2^+	13.586
842 ± 2	18 ± 1	0.16 [b])	(2^+) [c])	13.648
≈ 860	120	2.1	1^-	13.66
≈ 930	≈ 180	2.9	0^+	13.73
≈ 1080	≈ 200	3.4	1^-	13.87
1115	50	0.55	2^+	13.907
1160	≈ 70	1.1	0^+	13.950
1235	≈ 70	1.2	1^-	14.021
≈ 1250	≈ 150	2.7	2^+	14.03
1350 ± 3	36 ± 1		2^+	14.130
1652 ± 5	90 ± 5		1^-	14.417
1713 ± 6	72 ± 2		0^+	14.475
1842 ± 7	122 ± 5		1^-	14.597
1901 ± 10	25 [d])		0^+	14.653
2110	75		$(2^+, 4^+)$	14.85
2310	90		(2^+)	15.04
2550	300		(1^-)	15.27
2590	300		(0^+)	15.31
2680	80			15.39
2730	60			15.44
2820	160			15.53
2940				(15.64)
3120	170			(15.81)
3340	105			16.02
3680	(100)			16.34
3860				16.51
3980	135			16.63
4130	100			16.77
4360	100			16.99
4460	95			17.08
4690	65			17.30
4900	90			17.50
4990	40			17.59
5879 ± 7	10 ± 3	[d])	2^+; 2	18.430

Table 20.23
Resonances for ground-state α-particles (α_0) in ^{19}F(p, α_0) [a])

[a]) For earlier references and additional comments see Tables 20.31 in (78AJ03) and 20.28 in (83AJ01). See also (85OU01, 86OU01).
[b]) $\Gamma_{\alpha_0} \approx 0.06$ keV.
[c]) $J = 0$ from ^{19}F(p, p); possibly $T = 0$.
[d]) $\Gamma_{\alpha_0} \approx 0.3$ keV.

Table 20.24
Nuclear pair resonances (α_π) in ^{19}F(p, α_π) [a])

E_p (keV)	Γ_{lab} (keV)	σ (mb)	θ_α^2 (%)	J^π	^{20}Ne* (MeV)
710	35	≈ 0.2	2	1^-	13.522
780	≈ 10	≈ 0.2	0.15	2^+	13.589
842	23	3.4	0.27	2^+ [c])	13.648
1115	50	1.5	3.6	2^+	13.907
1236	≈ 70	3	1.0	1^-	14.022
1367	30	6.0	0.29	2^+	14.146
1640	60			1^-	14.41
1720	95	≈ 18		0^+	14.48
1850	170			1^-	14.60
1896	25			0^+	14.65
2080 [b])	60	12.1		(2^+)	14.82
2170 [b])	70	12.2		(0^+)	14.91
2330 [b])	70	17.0		(2^+)	15.06
2600	100				15.32
2680	100				15.39
2820	125				15.53
3120	145				15.81
3340	100				16.02
(3500)	(80)				(16.17)
(3590)	(115)				(16.26)
3960	200				16.61
4360	95				16.99
4690	< 150				17.30
4900	115				17.50
4990	40				17.59
5170	220				17.76

[a]) For references see Tables 20.32 on (78AJ03) and 20.29 in (83AJ01). See also (85OU01, 86OU01).
[b]) (80CU1B): see also for partial widths.
[c]) See footnote (c) in Table 20.23.

Table 20.25
Resonances for 6–7 MeV γ-rays (α_2, α_3, α_4) in ^{19}F(p, α) [a])

E_p (keV)	Γ_{lab} (keV)	Γ_{α_2} (eV)	Γ_{α_3} (eV)	Γ_{α_4} (eV)	J^π; T	^{20}Ne* (MeV)
223.99 ± 0.07 [b])	0.99 ± 0.02	1000	< 2.5	< 2.5	2^-	13.067
340.46 ± 0.04 [b,c])	2.34 ± 0.04	2800	16	75	1^+	13.1713
483.91 ± 0.10 [b])	0.90 ± 0.03	700	19	190	1^+	13.3075
594 ± 3	25 ± 3					13.412
667.5 ± 2	6.7 ± 0.3					13.482
832.1 ± 1						13.638
872.11 ± 0.20 [d])	4.53 ± 0.16	2200	620	180	2^-	13.6762
935.4 ± 1.3	8.1 ± 0.5	2900	110	720	1^+	13.736
1087.7 ± 1	0.15 ± 0.05					13.881
1135.6 ± 1						13.926
1280 ± 1						14.063
1347.1 ± 1	4.9 ± 0.7	2250	650	1200	2^-	14.128
1371.0 ± 1	12.4 ± 1.0	6650	700	300	2^-	14.150
1603 ± 2						14.370
1692 ± 2	35 ± 3				$(1, 2)^-$	14.455
1949 ± 2.5	40 ± 10				$(0, 1)^+$	14.699
2030 ± 3.0	120 ± 20					14.776
2320	85					15.05
2510	30					15.23
2630	90					15.35
2800	60					15.51
3020	30					15.72
3190	80					15.88
3490	40					16.16
3920	30					16.57
4000	110					16.65
4090					0^+; 2	16.73
4290	50					16.92
4490	30					17.11
4570	30					17.19
4710	30					17.32
4780	35					17.39
4990	20					17.59
5070	35					17.66
5200	70					17.79

[a]) See Tables 20.33 in (78AJ03) and 20.30 in (83AJ01) for earlier references and for additional comments. See also (85OU01, 86OU01), and see tables 2 and 3 in (93DA23).
[b]) (85UH01). See also (77FR1A).
[c]) (82BE29): $\sigma = 88 \pm 3$ mb, $\omega\gamma = 22.3 \pm 0.8$ eV.
[d]) (82BE29): $\sigma = 440 \pm 13$ mb, $\omega\gamma = 570 \pm 30$ eV.

The excitation energy difference (ΔE_x) between the 1^+ and 1^-, $T = 1$ states ^{20}Ne* (11.26, 11.27) is 11.1 ± 0.7 keV (83FI02). $\Gamma_\gamma/\Gamma_\alpha = 0.88 \pm 0.05$ for ^{20}Ne* (12.22) [2^+; $T = 1$] (84CA08). Using $(2J+1)\Gamma_\alpha\Gamma_\gamma/\Gamma = 1.41 \pm 0.23$ eV (80FI01), $\Gamma_\alpha = 0.32 \pm 0.06$ eV for ^{20}Ne* (12.22) (84CA08). The value of Γ_γ/Γ of ^{20}Ne* (12.22) implies $B(\mathrm{M1}) = 0.07$ W.u. for the transition from ^{20}Ne* (18.43) [2^+; $T = 2$]. This is much weaker than other isovector M1 transitions in ^{20}Ne and a factor of five lower than predicted by shell model calculations: see (84CA08).

In recent work at $E(^3\mathrm{He}) = 25$ MeV, differential cross sections were measured (94VE04) for ^{20}Ne levels at $E_x = 0$, 1.634 MeV. DWBA calculations were carried out and absolute values of C^2S were extracted and compared with shell model calculations.

31. ^{19}F(α, t)^{20}Ne $\qquad Q_m = -6.970$

Angular distributions have been measured at $E_\alpha = 18.5$ and 28.5 MeV: see (78AJ03, 83AJ01). The double differential cross section was measured at $E_\alpha = 30.3$ MeV in a study of the reaction mechanism involving excitation of the 0^+, 2^+ and 4^+ states at $E_x = 0$, 1.63, 4.25 MeV (95IG1A).

32. ^{19}F(^{7}Li, ^{6}He)^{20}Ne $\qquad Q_m = 2.869$

Angular distributions have been studied at $E(^7\mathrm{Li}) = 34$ MeV to a number of states of ^{20}Ne. C^2S values are consistent with those reported in the (d, n) and (^{3}He, d) reactions: see (78AJ03).

33. ^{20}F(β^-)^{20}Ne $\qquad Q_m = 7.025$

The decay is primarily to ^{20}Ne* (1.63) with a half-life of 11.163 ± 0.008 sec (92WA04): see reaction 1 in ^{20}F. Besides the principal decay to ^{20}Ne* (1.63) [$\log f_0 t = 4.97$], ^{20}F also decays to ^{20}Ne* (4.97) [$J^\pi = 2^-$] with a branching ratio of $(0.0082 \pm 0.0006)\%$ (87AL06) [$\log f_0 t = 7.20 \pm 0.03$; D.E. Alburger and E.K. Warburton, see (87AJ02)]. The upper limit for the ground-state decay is 0.001% [$\log f_0 t > 10.5$]. For other values and earlier references see Table 20.36 in (78AJ03). The energy of the γ-ray from ^{20}Ne* (1.63) is 1633.602 ± 0.015 keV. E_γ for the $4.97 \rightarrow 1.63$ transition is 3332.54 ± 0.19 keV which gives $E_x = 4966.51 \pm 0.20$ keV based on $E_x = 1633.674 \pm 0.015$ keV for the first excited state. The shape of the β-spectrum is in good agreement with the predictions of CVC (83AJ01, 87AJ02,

89HE11). $\beta - \gamma$ angular correlations reported by (88RO10) are close to the expectations based on CVC theory. For earlier work see (78AJ03, 83AJ01, 87AJ02). The ^{20}F(β^-)^{20}Ne decay is thought to play a part in heavy element nucleosynthesis (88AP1A). See also 89MA1U, 89TA26).

34. (a) ^{20}Ne(γ, n)^{19}Ne $\quad Q_{\rm m} = -16.864$
    (b) ^{20}Ne(γ, 2n)^{18}Ne $\quad Q_{\rm m} = -28.491$
    (c) ^{20}Ne(γ, α)^{16}O $\quad Q_{\rm m} = -4.730$

The photoneutron cross section (bremsstrahlung photons) shows peaks at $E_{\rm x} = 17.78 \pm 0.05$, 19.00 ± 0.05, 20.15 ± 0.15 [main peak of the GDR], 22.6 ± 0.3, 24.9 ± 0.5 and 27.5 MeV [the latter three states are broad]: the integrated cross section to 28.5 MeV is 58 ± 6 MeV $\cdot$ mb [exhausting $\approx 20\%$ of the dipole sum]. The cross section for (γ, Tn) using monoenergetic photons shows a structure at 18 MeV and some fluctuations atop the broad giant dipole resonance, $\sigma_{\rm max} \approx 7$ mb. The double photoneutron cross section, $\sigma(\gamma, 2{\rm n})$, is dominated by a single peak at $E_\gamma \approx 20.5$ MeV, $\sigma_{\rm max} \approx 1.1$ mb. For references see (78AJ03, 83AJ01) and see the atlas of photoneutron cross sections with monoenergetic photons (88DI02). The significance of reaction (c) to astrophysics is discussed by (82SA1A, 84FO1A).

35. ^{20}Ne(γ, γ)^{20}Ne

The first 1^+; $T = 1$ state in ^{20}Ne is measured at $E_{\rm x} = 11262.3 \pm 1.9$ keV. The branchings to ^{20}Ne* (0, 1.63) are (84 ± 5) and $(16 \pm 5)\%$, respectively (83BE19). See also (84BE26).

36. (a) ^{20}Ne(e, e′)^{20}Ne
    (b) ^{20}Ne(e, e′p)^{19}F $\quad Q_{\rm m} = -12.844$
    (c) ^{20}Ne(e, e′α)^{16}O $\quad Q_{\rm m} = -4.730$

The ^{20}Ne charge radius, $\langle r^2 \rangle_{1/2} = 3.004 \pm 0.025$ fm. Form factors for many excited states of ^{20}Ne with $E_{\rm x} < 8$ MeV have been reported: see (78AJ03).

At $E_{\rm e} = 39$ and 56 MeV, the 180° inelastic scattering is dominated by the transition to a $J^\pi = 1^+$, $T = 1$ state at $E_{\rm x} = 11.22 \pm 0.05$ MeV with $\Gamma_{\gamma_0} = 11.2^{+2.1}_{-1.8}$ eV. A subsidiary peak is observed corresponding to a state 0.35 ± 0.03 MeV higher [if $J^\pi = 1^+$ or 2^+, $\Gamma_{\gamma_0} = 0.65 \pm 0.18$ or 0.40 ± 0.13 eV]. A number of small peaks are also reported corresponding to $E_{\rm x} \approx 12.0$, 12.9, 13.9, 15.8, 16.9, 18.0

and 19.0 MeV. Prominent electric dipole peaks are reported at E_x = 17.7, 19.1, 20.2, and 23 MeV, in addition to weaker structures between 12.5 and 15 MeV; and prominent electric quadrupole peaks are observed at E_x = 13.0, 13.7, 14.5, 15.0, 15.4 and 16.2 MeV and there is broad quadrupole excitation between 16 and 25 MeV. The GDR cross section integrated from 11 to 25 MeV contains about 65% of the dipole EWSR while over 90% of the isoscalar quadrupole EWSR is exhausted by the strength in the region 10–25 MeV.

For $11 < E_x < 24$ MeV only two isovector M2 transitions appear: these are to ^{20}Ne* (11.62, 12.10) with B(M2, k)↑= 64 ± 13 and 56 ± 13 μ_N^2fm^2 [orbital contributions are non-negligible]. The M1 transition to ^{20}Ne* (11.26) is also observed but that to ^{20}Ne* (13.48) is not: it is < 0.2 μ_N^2 (85RA08). For reaction (b) see (78AJ03).

Reaction (c) has been studied in order to obtain the (γ, α_0) cross section in the giant resonance region: the cross section at 90° for E_x = 15 to 24 MeV is dominated by an E1 resonance [1^-; $T = 1$, with an admixture of $T = 0$ which permits the α_0 decay] at E_x = 20 MeV; lesser E1 structures are reported at E_x = 16.7, 17.1, 21 and 22 MeV. A relatively strong 2^+; $T = 0$ resonance appears at E_x = 18.5 MeV, and evidence is reported for increasing E2 strength below 16 MeV. For references to the early work see (78AJ03, 87AJ02). For more recent work see the reviews on nuclear dipole excitations (87BE1G) and status of the shell model (88BR1P). Other more recent theoretical work includes studies of large basis space effects in electron scattering form factors (90AM01), correlated charge form factors and densities for s-d shell nuclei (90MA63), electron scattering multipoles for symplectic shell model application (92RO08), mass number dependence of the difference between electron- and muon-scattering charge radii (89AN12), electron scattering from ^{20}Ne in a microscopic boson model (88KU07, 88KU22, 88KU17), and studies of (e, e′γ) reactions and electromagnetic currents in rotational nuclei (90GA09). See also (88BR1D, 88ZH1F, 90MO1J).

36.5 (a) ^{20}Ne($\pi^{\pm}$, $\pi^{\pm\prime}$)^{20}Ne
(b) ^{20}Ne($\pi^{\pm}$, X)

Inelastic pion scattering experiments at T_π = 120 MeV and 180 MeV indicate a broad 2^+ member of the $K^\pi = 0_4^+$ band in ^{20}Ne (89BU14, 95BU01). They report $E_x = 9.00 \pm 0.18$ MeV, Γ = 0.8 MeV B(E2↑) = 40.9 ± 2.0 e^2fm^4. Several other states in the first four $K^\pi = 0^+$ bands were studied by (95BU01). See Table 20.25.5.

For reaction (b), spectra have been measured and analyzed for initial pion momenta of 6.2 GeV/c (91AM1B, 92KI1C).

37. ^{20}Ne(n, n′)^{20}Ne

Table 20.25.5
Ground-state transition strengths in ^{20}Ne from ^{20}Ne($\pi^{\pm}$, $\pi^{\pm\prime}$) [a])

E_x (MeV) [b])	J^{π} [b])	K^{π} [b])	$B(E\lambda)(e^2\mathrm{fm}^{2\lambda})$ [c])
1.63	2^+	0_1^+	322.9 ± 1.8
4.24	4^+	0_1^+	42400 ± 600
8.78	6^+	0_1^+	$2.2 \pm 0.9 \times 10^6$
7.42	2^+	0_2^+	2.9 ± 0.4
9.99	4^+	0_2^+	5000 ± 600
7.83	2^+	0_3^+	16.6 ± 0.5
9.03	4^+	0_3^+	9800 ± 900
9.00	2^+	0_4^+	40.9 ± 2.0
10.79	4^+	0_4^+	6000 ± 300

[a]) See table 1 of (95BU01).
[b]) See (87AJ02).
[c]) (95BU01) notes that all $B(E\lambda)$'s were obtained by fitting 180 MeV π^+ and π^- data simultaneously with the constraint $M = M_n = M_p$ where $B(E\lambda) = |M_p|^2$. The errors given are statistical only.

An evaluation of neutron-induced reaction cross sections of ^{20}Ne for E_n = 1–30 MeV is presented in (91RE10). See also (93DE32) and earlier work cited in (78AJ03).

38. (a) ^{20}Ne(p, p′)^{20}Ne
    (b) ^{20}Ne(p, p′α)^{16}O $\qquad Q_m = -4.730$

Angular distributions of elastically scattered protons and of a number of inelastic groups have been measured for E_p = 2.15 to 65 MeV [see (78AJ03, 83AJ01)] and at E_p = 0.8 GeV (84BL14, 88BL13; to ^{20}Ne* (0, 1.63, 4.25, 8.7) (u); also A_y). The latter work confirms the large hexadecapole deformation of ^{20}Ne. At E_p = 201 MeV, probable 1^+ states at $E_x = 11.25 \pm 0.01$, 13.51 ± 0.03 and 15.72 ± 0.05 MeV are reported by (87WI1C): There does not appear to be any quenching of the M1 strength. In addition 2^- states are observed at 11.58 and 12.08 MeV with $B(\mathrm{M2}) = 64 \pm 13$ and 56 ± 13 μ_N^2 as is a state of unknown J^{π} at $E_x \approx 17$ MeV (87WI03). See also (90CR1B), the measurements at E_p = 6.4–7.7 MeV (92WI13), measurements at E_p = 60–180 MeV (93PLZY), and the earlier work cited in (78AJ03). For reaction (b) see (84CA09, E_p = 101.5 MeV), (92WI13, E_p = 6.4–7.7 MeV), and the earlier experimental and theoretical work cited in (87AJ02). See also (93MU1D).

Theoretical work reported since the previous compilation includes relativistic DWBA calculations on inelastic scattering at E_p = 200–800 MeV (88JO02), a large-

basis-space microscopic-model analysis of 800-MeV inelastic scattering (91AM1A), studies with a coalescence model of hypernuclear formation and mesonic atom production (89WA14) in high energy collisions (88WA1H, 89SA1R), analysis of 800-MeV inelastic scattering with the Dirac formalism (90PH01, 90PH02, 92DE31). See also the microscopic three-cluster study of 21-nucleon systems presented in (93DE32).

38.5 ^{20}Ne(p, $\pi^{\pm}$)

Experimental data on multiplicity, correlations, and inclusive spectra of mesons and other particles produced in p + ^{20}Ne reactions at $E_{\rm p} = 300$ GeV are presented in (92YU1A) and compared with model predictions.

39. ^{20}Ne($\overline{\rm p}$, $\overline{\rm p}$)^{20}Ne

For references to work on antiproton interactions see Table 20.12.5, (^{20}Ne – general).

40. (a) ^{20}Ne(d, d′)^{20}Ne
(b) ^{20}Ne(t, t′)^{20}Ne

Angular distributions of deuterons have been reported at $E_{\rm d} = 10.0$ to 52 MeV [see (78AJ03, 83AJ01)] and at $E_{\rm d} = 52$ MeV (87NU01). Differential cross sections for elastic and inelastic scattering of tritons (reaction b) were measured at $E_{\rm t} =$ 33.4 MeV by (92HA12) and analyzed by the coupled channels method. Potential parameters, deformation lengths and multipole moments were deduced. See also the calculations for these data described in (92HA18) in which spin, parity and band assignments are discussed. The calculations suggest the assignments of $K^{\pi} = 2^{-}$, 2^{-} and 0^{-} respectively to the $J^{\pi} = 2^{-}$, 3^{-}, 3^{-} states at $E_{\rm x} = 4.97$, 5.62 and 5.79 MeV. See also (78AJ03, 87AJ02).

41. ^{20}Ne(^{3}He, ^{3}He′)^{20}Ne

Angular distributions have been measured at $E(^{3}\text{He}) = 10$ to 35 MeV and at 68 MeV: see (78AJ03). See references cited in (78AJ03). More recently differential cross section for elastic and inelastic scattering of ^{3}He were measured at

$E(^3\mathrm{He}) = 33.4$ MeV by (92HA12) and analyzed by the coupled channels method. Comparisons were made with triton scattering. Calculations for these data were described in (92HA18) in which spin, parity and band assignments are discussed. Elastic scattering measurements at $E(^3\mathrm{He}) = 30$ and 45 MeV are described in (92NAZQ).

42. (a) $^{20}\mathrm{Ne}(\alpha,\ \alpha')^{20}\mathrm{Ne}$
    (b) $^{20}\mathrm{Ne}(\alpha,\ 2\alpha)^{16}\mathrm{O}$ $\qquad Q_\mathrm{m} = -4.730$

Angular distributions have been measured at $E_\alpha = 3.8$ to 155 MeV [see references cited in (78AJ03)]. More recently measurements were made at $E_\alpha = 54.1$ MeV (87AB03), $E_\alpha = 50$ MeV (91FR02) and at $E_\alpha = 3.8$–11 MeV (91AB05). Inelastic cross sections were measured at $E_\alpha = 5.6$–11.0 MeV (92DA10), $E_\alpha = 50$ MeV (91FR02), and $E_\alpha = 50.5$ MeV (87BU1E).

For reaction (b) see references cited in (83AJ01, 87AJ02) and the measurements at $E_\alpha = 155$ MeV of cross sections and decay branching ratios for several excited states of ^{20}Ne up to the giant quadrupole resonance by (87SU09).

Theoretical studies related to these reactions include: $\alpha + {}^{20}\mathrm{Ne}$ structures of ^{24}Mg in a microscopic three-cluster ($\alpha + \alpha + {}^{16}\mathrm{O}$ model (87DE40), distributions of α-particle strengths in light nuclei (88LE05), target clustering and exchange effects in internuclear interactions (88LE06), stationary-state currents in nuclear reactions (88MA30), a DWIA analysis of $^{20}\mathrm{Ne}(\alpha,\ 2\alpha)^{16}\mathrm{O}$ at $E_\alpha = 140$ MeV (88SH05), distortion effects in a microscopic $^{16}\mathrm{O} + 2\alpha$ description of ^{24}Mg (89DE32), evidence for a parity dependence in the $\alpha + {}^{20}\mathrm{Ne}$ interactions (89MI12), an l-dependent representation of a Majorana potential (90CO38), a strong-absorption model analysis of α scattering (92RA21), a calculation of quasimolecular states in $^{20}\mathrm{Ne}(\alpha,\ \alpha)$ (92GR15), optical model analysis of $^{20}\mathrm{Ne}(\alpha,\ \alpha)$ at $E_\alpha = 22.9$ MeV (93AOZZ).

43. $^{20}\mathrm{Ne}(^7\mathrm{Li},\ ^7\mathrm{Li}')^{20}\mathrm{Ne}$

Angular distributions have been studied at $E(^7\mathrm{Li}) = 36$, 68, and 89 MeV: see (83AJ01).

44. $^{20}\mathrm{Ne}(^9\mathrm{Be},\ ^9\mathrm{Be}')^{20}\mathrm{Ne}$

For pion production see (85FR1C).

45. (a) ^{20}Ne(^{10}B, ^{10}B)^{20}Ne
(b) ^{20}Ne(^{11}B, ^{11}B)^{20}Ne

Elastic angular distributions have been measured at $E(^{10}\mathrm{B}) = 65.9$ and $E(^{11}\mathrm{B}) = 115$ MeV: see (83AJ01).

46. (a) ^{20}Ne(^{12}C, ^{12}C$'$)^{20}Ne
(b) ^{20}Ne(^{12}C, α^{8}Be)^{20}Ne $\qquad Q_{\mathrm{m}} = -7.366$

Elastic angular distributions have been obtained at $E(^{12}\mathrm{C}) = 22.2$ to 77.4 MeV and at $E(^{20}\mathrm{Ne}) = 65.9$, 74 and 75.2 MeV [see (78AJ03, 83AJ01)] as well as at $E(^{20}\mathrm{Ne}) = 72.6$, 74.0 and 75.2 MeV (82SH29). Elastic and inelastic scattering differential cross sections at $E(^{20}\mathrm{Ne}) = 390$ MeV were measured by (93BO28).

For yield, fusion, total reaction cross section and fragmentation studies see the references cited in (87AJ02). More recently fragmentation studies at $E(^{20}\mathrm{Ne}) =$ 540–1096 MeV/nucleon were reported by (90WE1A) and at $E(^{20}\mathrm{Ne}) = 400$, 800 MeV/nucleon by (88DU01). See also (87AN1B, 94FU01). For pion production and for reaction (b) see references cited in (87AJ02).

Theoretical studies carried out since the previous compilation include: resonances, heavy-ion radioactivity and new predictions for medium mass collective systems (89CI1C), cascade model study of Λ particle productions in central collisions of light nuclei (88IW1A), comparison of quantized ATDHF and GCM theory applied to the $^{12}\mathrm{C} + {}^{20}\mathrm{Ne}$ system (90SL01).

47. ^{20}Ne(^{16}O, ^{16}O$'$)^{20}Ne

Angular distributions have been studied at $E(^{20}\mathrm{Ne}) = 50$ and 94.8 MeV involving $^{16}\mathrm{O}_{\mathrm{g.s.}}$ and ^{20}Ne* (0, 1.63, 4.25) [see (83AJ01)], at $E(^{16}\mathrm{O}) = 25.6$ to 44.5 MeV (elastic; also to ^{20}Ne*(1.63) at 31.3, 33.3 and 44.5 MeV)) and at $E(^{20}\mathrm{Ne}) = 66.8$, 115, 137 and 156 MeV (elastic) [see (87AJ02) for references]. Yield and fusion cross section measurements have also been reported in several references cited in (87AJ02). Excitation functions at $\theta_{\mathrm{cm}} = 90^{\circ}$ for $E_{\mathrm{cm}} = 21.5$–31.2 MeV were measured by (88HE06) and at $\theta_{\mathrm{lab}} = 13^{\circ}$ for $E_{\mathrm{cm}} = 22.8$ to 38.6 MeV by (89SA14). Measurements at projectile energies of 3.6 MeV/nucleon are reported in (87AN1B), and at 4.2 and 4.5 GeV/nucleon by (88BO1D, 88BE2A).

Theoretical studies related to this reaction reported since the previous review include: calculation within the framework of the cascade model (88IW1A), molecular orbital theory for elastic and inelastic scattering (89HE1I), derivation of the

parity-independent interaction for $^{16}O + ^{20}Ne$ (89GA1L), optical model analysis of resonant structure in $^{16}O+^{20}Ne$ (91GA14), and local representation of a deep parity- and L-dependent $^{16}O + ^{20}Ne$ potential (93AI02).

48. $^{20}Ne(^{20}Ne, ^{20}Ne')^{20}Ne$

Elastic angular distributions are reported at $E(^{20}Ne) = 68$, 117, 140, and 156 MeV (83SH25). For yield and fusion measurements see references cited in (83AJ01, 87AJ02). High-spin shape isomers for sd-shell nuclei were studied at E_{cm} near 1.6 times the Coulomb barrier for $^{20}Ne + ^{20}Ne$ by (93BAZZ). Studies of the average number of interacting protons in $^{20}Ne + ^{20}Ne$ collisions of 36 GeV/nucleon were reported by (87AN1B).

Theoretical work related to the reaction includes: a study of mesonic atom production by a coalescence model (89WA14), a formulation of the mesonic atom production probability with a coalescence model (89SA1R), hypernucleus production by heavy ions by a coalescence process (89BA2N, 89WA14, 89BA1E).

49. (a) $^{20}Ne(^{24}Mg, ^{24}Mg')^{20}Ne$
    (b) $^{20}Ne(^{26}Mg, ^{26}Mg')^{20}Ne$

Elastic angular distributions for reaction (a) have been measured at $E(^{20}Ne) =$ 50, 60, 80, 90, and 100 MeV [see (83AJ01)] at 40 MeV (83NA04; S_α for the system $^{20}Ne + ^{24}Mg \ = 0.08 \pm 0.02$) and at $E_{lab} = 55$, 80 and 160 MeV/nucleon (87BE1V). For yield and fusion cross sections for reactions (a) and (b) see references cited in (87AJ02). See also the review of high energy gamma production in heavy ion collisions (89NI1D).

50. $^{20}Ne(^{27}Al, ^{27}Al')^{20}Ne$

Elastic angular distributions are reported at $E(^{20}Ne) = 55.7$, 63, 125, and 151 MeV (83NG01). For yield, fusion and evaporation residue studies see references cited (87AJ02) and the study at $E(^{20}Ne = 217$, 194 and 384 MeV (88GR12, 89BA17, 90BA18). A search for incomplete deep inelastic collisions at $E(^{20}Ne) = 216$ MeV is reported by (88ZH12). Neutral pion production was studied at $E(^{20}Ne) = 4$ GeV by (88JU02, 89FO07, 89FO1G). A description of those data by the cooperative model is discussed in (89GH01). See also the calculation of total reaction cross sections presented in (88JO02).

51. (a) ^{20}Ne(^{28}Si, ^{28}Si′)^{20}Ne
(b) ^{20}Ne(^{29}Si, ^{29}Si′)^{20}Ne

See (83DU13).

52. ^{20}Ne(^{40}Ca, ^{40}Ca′)^{20}Ne

Angular distributions have been studied at $E(^{20}\text{Ne}) = 44.1$ to 70.4 MeV and at 151 MeV: see (83AJ01). For an evaporation residue study see (82MO15). For yield and fusion measurements see (83AJ01). The breakup of ^{20}Ne at $E(^{20}\text{Ne}) = 92$, 149 and 213 MeV involves ^{20}Ne* (5.79, 6.73, 7.16, 8.78, 10.26, 11.95) (86SH30).

See also the references cited in (87AJ02) and see the Monte Carlo simulation method calculation for nuclear transfer (88CH28), and the study of alpha clustering and shell effects related to this reaction (89PU1C).

53. ^{20}Na(β^+)^{20}Ne $\qquad Q_\text{m} = 13.887$

^{20}Na has a half-life of 447.9 ± 2.3 msec: see reaction 1 in ^{20}Na. It decays to a number of states of ^{20}Ne, principally ^{20}Ne* (1.63): see Table 20.26. The ratio of the mirror decays ^{20}Na(β^+)^{20}Ne* (1.63) and ^{20}F(β^-)^{20}Ne* (1.63), $(ft)^+/(ft)^- = 1.03 \pm 0.02$. β–γ correlation measurements, as in the decay of ^{20}F, lead to an upper limit for the second-class contribution to the correlation which is consistent with zero: see (83AJ01). A more recent measurement (88RO10) concluded that the β–γ angular correlations in $A = 20$ are close to and may be in agreement with conserved vector current theory. β–ν–α triple correlation coefficient measurements for the transitions via the α-unstable 2^+ states shown in Table 20.26 lead to values of the isospin mixing amplitudes [and to a determination of the vector weak coupling constant] (83CL1A, 89CL02). See also references cited in (87AJ02) and the measurements of (92KUZO, 92KUZQ).

53.5 ^{21}Ne(e, e′n)^{20}Ne $\qquad Q_\text{m} = -6.761$

A general expression of the polarized spectral function for the (e, e′n) transitions is used by (94CA27) to model this reaction.

54. ^{21}Ne(p, d)^{20}Ne $\qquad Q_\text{m} = -4.537$

Table 20.26
Decay of ^{20}Na [a])

Decay to ^{20}Ne* (keV)	J^π	Branching ratio (%)	ft [b]) (s)	$\log ft$
1633.674 ± 0.015	2^+	79.44 ± 0.27	$(9.802 \pm 0.068) \times 10^4$	4.99
4966.51 ± 0.20	2^-	0.157 ± 0.022	$(9.3 \pm 1.3) \times 10^6$	6.97
6706 ± 47		0.0032 ± 0.0007	$(1.41 \pm 0.32) \times 10^8$	8.15
7421.9 ± 1.2	2^+	15.96 ± 0.22	$(1.588 \pm 0.026) \times 10^4$	4.20
7833.4 ± 1.5	2^+	0.583 ± 0.010	$(3.019 \pm 0.058) \times 10^5$	5.48
8058 ± 8	$(1^-, 2^+, 3^-)$	0.0119 ± 0.0009	$(1.198 \pm 0.092) \times 10^7$	7.08
9196 ± 30	2^+	0.0625 ± 0.0064	$(6.63 \pm 0.73) \times 10^5$	5.82
9483 ± 3	2^+	0.241 ± 0.005	$(1.190 \pm 0.028) \times 10^5$	5.08
9873 ± 4	3^+	0.028 ± 0.014	$(5.9 \pm 3.0) \times 10^5$	5.77
10274 ± 3	2^+	2.877 ± 0.042	$(2.983 \pm 0.061) \times 10^3$	3.48
10578 ± 4	2^+	0.0883 ± 0.0027	$(5.71 \pm 0.20) \times 10^4$	4.76
10840 ± 4	2^+	0.174 ± 0.005	$(1.705 \pm 0.058) \times 10^4$	4.23
10884 ± 3	3^+	0.117 ± 0.042	$(2.3 \pm 0.8) \times 10^4$	4.36
10941 ± 9	2^+	0.0119 ± 0.0015	$(2.00 \pm 0.26) \times 10^5$	5.30
11116 ± 9	2^+	0.0087 ± 0.0011	$(1.81 \pm 0.24) \times 10^5$	5.26
11262.3 ± 1.9	1^+	0.205 ± 0.026	$(5.30 \pm 0.68) \times 10^3$	3.72
11295 ± 5	2^+	0.0263 ± 0.0017	$(3.78 \pm 0.26) \times 10^4$	4.58
11856 ± 8	2^+	0.0016 ± 0.0004	$(9.9 \pm 2.5) \times 10^4$	4.99

[a]) (89CL02). See table 3 of that work for references and details.
[b]) Allowed decay assumed.

See (78AJ03).

55. ^{21}Ne(d, t)^{20}Ne $\qquad Q_\mathrm{m} = -0.504$

The $T = 1$ states observed in this reaction, and the analog states observed in ^{20}F in the (d, ^{3}He) reaction, are displayed in Table 20.16 of (78AJ03). $T = 0$ states are presented in Table 20.38 of (78AJ03).

56. ^{22}Ne(p, t)^{20}Ne $\qquad Q_\mathrm{m} = -8.643$

Angular distributions have been reported at $E_\mathrm{p} = 26.9$ to 43.7 MeV: see (78AJ03, 83AJ01). The angular distributions of the tritons to the ground state of ^{20}Ne and

to the first 0^+, $T = 2$ state [$E_x = 16.722 \pm 0.025$ MeV] have been fitted by $L = 0$ and the tritons to ^{20}Ne* (18.4) by $L = 2$. The latter is the first 2^+, $T = 2$ state. The 0^+, $T = 2$ state [^{20}Ne* (16.73)] decays by $\alpha_0[(6 \pm 5)\%]$, $\alpha_1 + \alpha_2[(35 \pm 12)\%]$, $\alpha_3 + \alpha_4[(29 \pm 12)\%]$, $p_0 + p_1 + p_2[(14 \pm 9)\%]$ and $p_3 + p_4 + p_5[(13 \pm 8)\%]$ [measured branching ratios in percent are given in the brackets] to the final states in ^{16}O and ^{19}F. See (78AJ03) for references and additional information.

57. ^{23}Na(p, α)^{20}Ne $\qquad Q_m = 2.377$

Angular distributions have been measured at $E_p = 10.0$ and 45.5 MeV: see (72AJ02). High resolution measurement at $E_p = 1.08$–4.15 MeV were carried out in a study of 94 resonances in ^{24}Mg by (87VA24) at $E_p = 6.25$–6.55 MeV. A study of ^{24}Mg resonances excited by protons in the range $E_p = 6.25$–6.55 MeV is described in (90MI24, 91MI24). Detailed-balance tests of time reversal invariance are reported in (94DR01, 93MI19, 93MI25). See also (87PA06, 89KA06) which describe analyzing power measurements for this reaction. Measurements of the cross section at $E_p \leq$ 350 keV were carried out by (89GO1N). Astrophysical implications are discussed. See also references to earlier work cited in (87AJ02).

58. ^{23}Na(^{3}He, ^{6}Li)^{20}Ne $\qquad Q_m = -1.642$

See (78AJ03).

58.3 ^{24}Mg(γ, α) ^{20}Ne $\qquad Q_m = -9.316$

Cross sections for this reaction were calculated by (87KA30) in a study of molecular structure of highly-excited states.

58.7 ^{24}Mg(n, nα)^{20}Ne $\qquad Q_m = -9.316$

Production cross sections for ^{20}Ne were measured at $E_n = 5.20$, 7.00, 16.20 and 19.05 MeV (90LA09). Cross sections were calculated with preequilibrium emission and constant-temperature evaporation models by (93KH09).

59. ^{24}Mg(p, pα)^{20}Ne $\qquad Q_m = -9.316$

See (84CA09). See also (78AJ03).

60. ^{24}Mg(d, ^{6}Li)^{20}Ne $\quad Q_{\rm m} = -7.841$

Angular distributions have been studied to many states of ^{20}Ne at $E_{\rm d} = 28$ to 80 MeV [see (78AJ03, 83AJ01)] and at $E_{\rm d} = 54.2$ MeV (84UM04; to ^{20}Ne* (0, 1.63, 4.25, 5.62)). Table 20.35 in (83AJ01) displays the observed states and S_α obtained from several analyses. For newer values of S_α see (84UM04, 86OE01). See also (84PA18, 86PAZJ). Measurements at several different incident energies were reported by (88BA1L, 88RA20). Data were analyzed with finite-range DW-BA calculations, and spectroscopic factors were obtained with different potentials. Comparisons with spectroscopic factors from ^{24}Mg(^{3}He, ^{7}Be)^{20}Ne were made.

61. ^{24}Mg(^{3}He, ^{7}Be)^{20}Ne $\quad Q_{\rm m} = -7.730$

Angular distributions have been studied at $E(^{3}\text{He}) = 25.5$ and 70 MeV: see (78AJ03). See also (83AJ01) and (86RA15). Measurements at $E(^{3}\text{He}) = 41$ MeV were reported by (88RA20, 88RA27). Data were analyzed with finite-range DW-BA calculations and spectroscopic factors were obtained with different potentials. Comparisons with spectroscopic factors from ^{24}Mg(d, ^{6}Li)^{20}Ne were made.

62. ^{24}Mg(α, ^{8}Be)^{20}Ne $\quad Q_{\rm m} = -9.407$

See (83AJ01).

63. ^{24}Mg(^{12}C, ^{16}O)^{20}Ne $\quad Q_{\rm m} = -2.154$

The angular distribution for the ground state transition has been measured at $E(^{12}\text{C}) = 40$ MeV (82LI16) and at $E_{\rm cm} = 25.2$ MeV (90LE12). Coupled-channels calculations were used to study the back angle anomaly. The backward angle yield in the inverse reaction was studied at $E(^{24}\text{Mg}) = 90$–126 MeV by (90GL01). See also (83AJ01, 89OB1C).

63.3 ^{24}Mg(^{16}O, ^{20}Ne)^{20}Ne $\quad Q_{\rm m} = -4.586$

Excitation functions were measured at $\theta_{cm} = 90°$, $E_{cm} = 25$–34 MeV by (89LE19). Data were compared with calculations involving the coupling to higher orders between elastic and α-transfer channels. The effect of the dynamic α-transfer polarization potential in discussed in (89FI03).

64. ^{28}Si(α, ^{12}C)^{20}Ne $\quad Q_m = -12.026$

See (83AJ01).

64.3 ^{28}Si(^{16}O, ^{24}Mg)^{20}Ne $\quad Q_m = -5.255$

This reaction was studied at $E_{cm} = 31.57$ MeV by (89PO1J).

^{20}Na

(Figs. 20.4 and 20.5)

GENERAL: See table 20.26.5.

$$\mu = 0.3694 \pm 0.0002 \text{ nm (75SC1A)}$$

Table 20.26.5
^{20}Na – General

Reference	Description
Review:	
87RA1D	Nuclear processes and accelerated particles in solar flares
89RA17	Compilation of exp. data on nuclear moments for ground & excited states of nuclei
Other articles:	
87BA1T	Spin-isospin excitations in nuclei with relativistic heavy ions
89KU15	Exp. determination of ^{19}Ne(p, γ)^{20}Na reaction rate; breakout problem from hot CNO cycle
90DE34	^{20}F & ^{20}Na nuclei and the ^{19}Ne(p, γ)^{20}Na reaction in a microscopic three-cluster model
90PO04	New method of determining masses & quantum characteristics of light nuclei
92AV03	The proton neutron interaction and mass calcs. for nucl. with $Z > N$
93BR12	Nature of the ^{20}Na 2646-keV level and the stellar reaction rate for ^{19}Ne(p, γ)^{20}Na

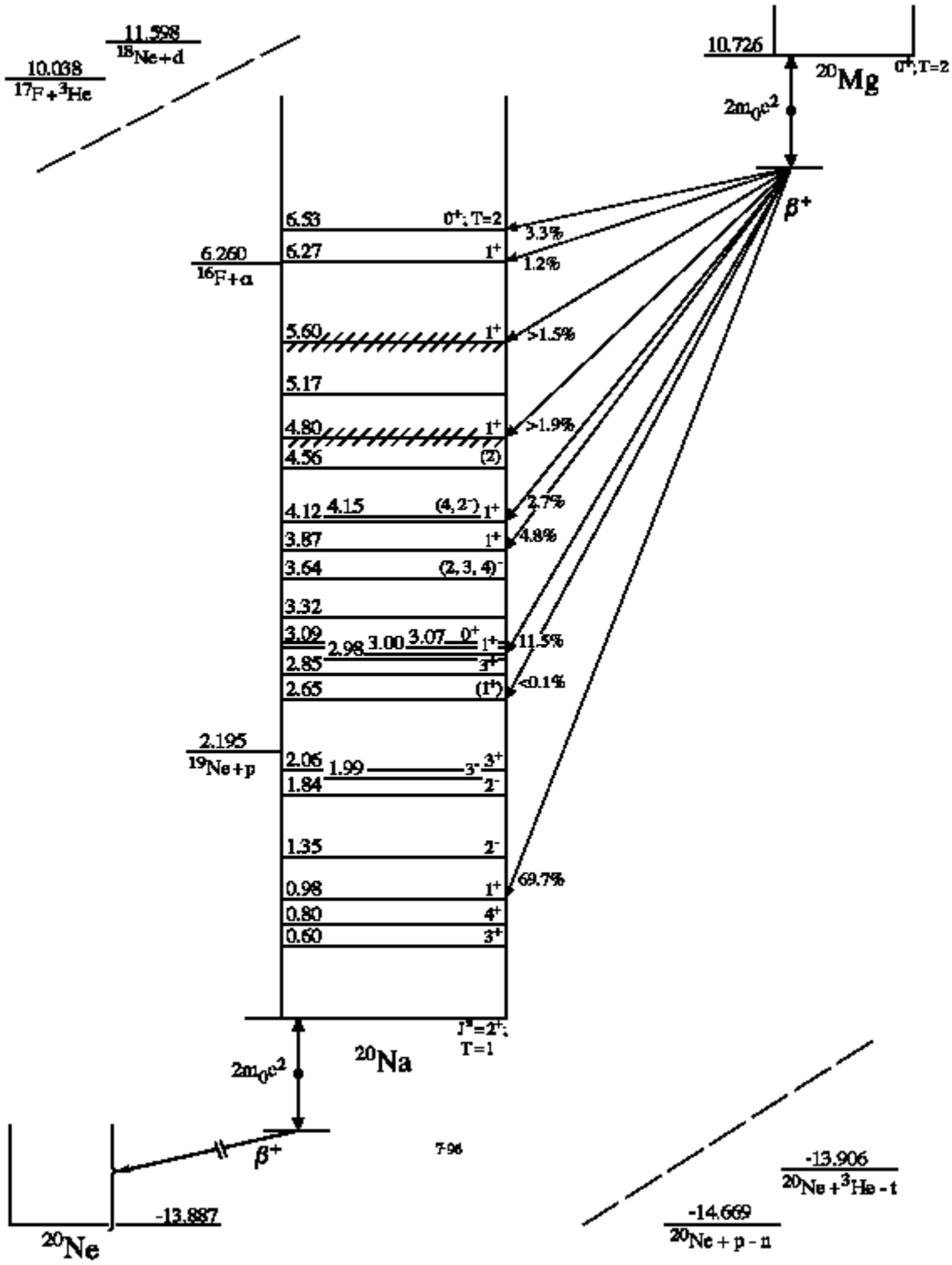

Figure 4: Energy levels of ^{20}Na. For notation see fig. 1.

Table 20.27
Energy Levels of ^{20}Na

E_x (MeV ± keV)	J^π; T	$\tau_{1/2}$ or $\Gamma_{c.m.}$	Decay	Reactions
0	2^+; 1	$\tau_{1/2} = 447.9 \pm 2.3$ ms	β^-	1, 4, 5
0.596 ± 8	3^+		(γ)	4, 5
0.802 ± 7	4^+		(γ)	4, 5
0.98425 ± 0.10	1^+		(γ)	4, 5, 6
1.346 ± 8	2^-		(γ)	4, 5
1.837 ± 7	2^-		(γ)	4, 5
1.992 ± 8	3^-		(γ)	4, 5
2.057 ± 12	3^+		(γ)	5
2.645 ± 6	(1^+)		(γ, p)	4, 5
2.849 ± 6	3^+			4, 5
2.983 ± 7	> 3			5
3.001 ± 2	1^+	$\Gamma = 19.8 \pm 2$ keV [a])	p	3, 3.5, 6
3.067 ± 2	(0^+)			3, 4, 5
3.086 ± 2	0^+	$\Gamma = 35.9 \pm 2$ keV [a])	p	3.5
3.315 ± 9				5
3.642 ± 16	$(2, 3, 4)^-$			4, 5
3.871 ± 9	1^+		p	4, 5, 6
4.123 ± 16	1^+		p	6
4.150 ± 60	$(4, 2^-)$			5
4.560 ± 60	(2)			5
≈ 4.800	1^+		p	6
5.170 ± 60				5
≈ 5.600	1^+			5, 6
6.266 ± 30	1^+		p	6
6.534 ± 13	0^+		p	6

[a]) From (94CO12). See Table 20.27.3.

1. ^{20}Na(β^+)^{20}Ne $\qquad\qquad$ $Q_{\rm m} = 13.887$

^{20}Na decays by positron emission to ^{20}Ne* (1.63) and to a number of other excited states of ^{20}Ne: see Table 20.26 and reaction 53 in ^{20}Ne. The half-life of ^{20}Na is 447.9 ± 2.3 msec [weighted mean of values quoted in (78AJ03, 83CL1A, 89CL02)]; $J^\pi = 2^+$: see (87AJ02). See also (92KUZO, 92KUZQ) and (93BL10; instrumentation). The beta delayed alpha decay of ^{20}Na has been studied by (89CL02) [see reaction 1.3]. See also (93XU1A).

1.3 ^{12}C(^{10}B, nn)^{20}Na $\qquad\qquad$ $Q_{\rm m} = -10.936$

Extensive measurements of the decay of ^{20}Na nuclei produced in the ^{12}C(^{10}B, nn) reaction were reported by (89CL02). Measurements included β^+ spectra, β delayed alphas, $\beta\nu\alpha$ triple correlation coefficients, branching ratios, ^{20}Ne level energies and the ^{20}Na half-life. Isospin mixing and the weak-vector coupling constant were deduced.

1.7 ^{12}C(^{14}N, ^{6}He)^{20}Na $\qquad\qquad$ $Q_{\rm m} = -21.576$

An 82-MeV ^{14}N beam was used by (93BAZX) to study ^{20}Na states up to $E_{\rm x} = 4.5$ MeV. The cross section for the $E_{\rm x} = 2.646$ MeV level was determined and the results suggest that state is not the mirror of the 1^+ 3.173 MeV state in ^{20}F as had been proposed. The results are consistent with the suggestion that the 2.646 MeV level is the mirror of the 2.966 MeV $J^\pi = 3^+$ state in ^{20}F. See also reactions 3 and 5.

2. ^{19}F(p, π^-)^{20}Na $\qquad\qquad$ $Q_{\rm m} = -140.611$

Angular distributions and analyzing powers have been studied at $E_{\rm p} = 199.6$ MeV to ^{20}Na* (0.74, 1.85, 3.01, 4.11) [probably unresolved]: it is suggested that the latter two have $J = 6$ or 7 (87CA1H).

3. ^{19}Ne(p, γ)^{20}Na $\qquad\qquad$ $Q_{\rm m} = 2.195$

The dominant process for the breakout from the HCNO cycle during hot hydrogen burning in stars in considered to be ^{15}O(α, γ)^{19}Ne(p, γ)^{20}Na [see references in the following discussion]. Thus the ^{19}Ne(p, γ)^{20}Na reaction rate at stellar temperatures is of considerable importance. The nuclear levels above the ^{19}Ne(p, γ) threshold are critical for calculation of the reaction rates and have been the object of several experimental studies by the ^{20}Ne(^{3}He, t) reaction (88LAZY, 89KU1D, 89KU15, 89SMZZ, 90LA05, 92SM03) as well as by ^{20}Ne(p, n)^{20}Na (89KU15). See reactions 4, 5, 6 and table 20.27.5.

The ^{20}Na state at $E_x = 2.646$ MeV is presumed to be the strongest (p, γ) resonance and it has been the object of several studies [see refs. mentioned above as well as (92GO10, 92KU07, 90DE34). Work by (93BAZX, 93BR12, 93CL1B) strongly suggests that the state has $J^\pi = 3^+$ (the analog of the ^{20}F 3^+ state at $E_x = 2.969$ MeV) rather than 1^+ as had been assumed in earlier work. More recent work described in (94PA42, 94HU1D) determined a 90% confidence-level upper limit of 18 meV for the resonance strength of this level and provides arguments against the $J^\pi = 3^+$ assignment.

3.5 ^{19}Ne(p, p)^{19}Ne

Resonances in ^{20}Na above the proton threshold were studied with radioactive ^{19}Ne beams scattered off polyethelene targets by (94CO12). Analysis by extended Breit Wigner, R-matrix and K-matrix formalism is described. Results are summarized in Table 20.27.3

Table 20.27.3
Resonances in ^{1}H(^{19}Ne, ^{19}Ne)^{1}H [a])

J^π	Formalism	E_r (keV)	γ or g (MeV$^{1/2}$)	Γ (keV)	E_x (MeV)
1^+	BW	797		19.8	2.996
	R	797	0.92	19.8 [b])	
	K	797	15.6	19.8	
0^+	BW	887		35.9	3.086
	R	887	1.00	35.9 [c])	
	K	887	15.8	35.9	

[a]) From Table I of (94CO12). Resonance energies (E_r) and widths (Γ) of the ^{20}Na resonances in the c.m. system; E_r, E_x and Γ are affected by a ± 2 keV uncertainty; γ and g are, respectively, R-matrix and K-matrix reduced widths amplitudes; Γ_F is the R-matrix formal width.
[b]) $\Gamma_F = 28.8$ keV ($R = 4.5$ fm).
[c]) $\Gamma_F = 55.2$ keV ($R = 4.5$ fm).

4. ^{20}Ne(p, n)^{20}Na $\qquad Q_{\rm m} = -14.669$

Early work on this reaction is described in (87AJ02). More recently ^{20}Na levels up to $E_{\rm x} = 3.636$ MeV were studied at $E_{\rm p} = 35$ MeV by (89KU15). See table 20.27.5.

The ^{20}Ne reaction at $E_{\rm p} = 136$ MeV was used in measurements of Gamow Teller strength (91AN01) and in a study of isovector stretched-state excitation (92TA04).

A review of spin-isospin response in nuclei based on charge exchange reaction data is presented in (89RA1G). See also (87EL14). An analysis leading to total Gamow Teller strength is described in (88MA53).

5. ^{20}Ne(^{3}He, t)^{20}Na $\qquad Q_{\rm m} = -13.906$

Early work on this reaction is summarized in (87AJ02). See also (87EL14). More recent measurements include those at $E(^{3}\text{He}) = 55.33$ MeV (88KU23, 89KU15), at $E(^{3}\text{He}) = 25.5$ MeV (88LAZY, 90LA05), at $E(^{3}\text{He}) = 29.7$ MeV (89SMZZ, 92SM03) and at $E(^{3}\text{He}) = 33.4$ MeV (90CL06, 93CL1B). Energy levels and spin parity assignments obtained from these experiments are displayed in Table 20.27.5. See also (89AR1H, 89KU1D). A major concern of this work was the ^{20}Na level at $E_{\rm x} = 2.646$ MeV, which is presumed to be the strongest (p, γ) resonance in ^{19}Ne(p, γ) [see reaction 3]. Detailed comparison of data on ^{20}Ne(^{3}He, t)^{20}Na and the analogue reaction ^{20}Ne(t, ^{3}He)^{20}F by (93BR12) and (93CL1B) has led to the conclusion that the 2.646 MeV state in ^{20}Na is to be identified with the $J^{\pi} = 3^{+}$ state at $E_{\rm x} = 2.966$ MeV in ^{20}F. This conclusion is supported by the work of (93BAZX) [see however the discussion of reaction 3].

5.3 ^{20}Ne(^{12}C, ^{12}B)^{20}Na $\qquad Q_{\rm m} = -27.256$

A study of the response of nuclei to spin-isospin excitation displayed through charge exchange reactions such as ^{20}Ne(^{12}C, ^{12}B)^{20}Na is described in (88RO17).

5.5 ^{20}Na(p, γ)^{21}Mg $\qquad Q_{\rm m} = 3.222$

To estimate the stellar reaction rate of ^{20}Na(p, γ)^{21}Mg, the nuclear structure of ^{21}Mg was studied by the ^{24}Mg(^{3}He, ^{6}He)^{21}Mg reaction at 74 MeV by (92KU02).

6. ^{20}Mg(β^{+})^{20}Na $\qquad Q_{\rm m} = 10.726$

Table 20.27.5
Levels in ^{20}Na from ^{20}Ne(p, n) and ^{20}Ne(^{3}He, t)

(p, n) [a]		(^{3}He, t) [a]		(^{3}He, t) [b]		(^{3}He, t) [c]		(^{3}He, t) [d]
E_x (MeV ± keV)	J^π	E_x (MeV ± keV)	J^π	E_x (MeV ± keV)	J^π	E_x (MeV ± keV)	J^π	E_x (MeV ± keV)
0.0	2^+	0.0	$(1, 2, 3)^+$			0.0	2^+	
0.580 ± 15	3^+	0.600 ± 15	$(3, 4, 5)^+$	0.606 ± 13	3^+	0.595 ± 20	3^+	
0.790 ± 15	4^+	0.802 ± 15	$(3, 4, 5)^+$	0.808 ± 11	4^+	0.801 ± 20	4^+	
0.993 ± 15	1^+	0.990 ± 15	$(1, 2, 3)^+$	0.996 ± 12	1^+	0.996 ± 20	$(1^\pm)$	
1.353 ± 15	(2^-)	1.347 ± 15	$(2, 3, 4)^-$	1.338 ± 14	2^-	1.350 ± 20	2^-	
1.843 ± 15	(2^-)	1.832 ± 15	$(2, 3, 4)^-$	1.841 ± 11	$2^\pm$	1.819 ± 26	2^-	
2.016 ± 20	(3^-)	1.967 ± 20	$(2, 3, 4)^-$	1.993 ± 12	3^-	1.992 ± 20	$(3^\pm, 2^-)$	
		2.034 ± 20	$(3, 4, 5)^+$	2.064 ± 16	$(2, 3)^+$	2.10 ± 40	$(3, 4, 5^\pm)$	
2.651 ± 20	1^+	2.637 ± 15	$(0, 1)^+$	2.649 ± 16	1^+	2.64 ± 20	$(1^\pm)$	2.646 ± 9
2.852 ± 20	$(2, 3)^+$	2.842 ± 15	$(3, 4, 5)^+$	2.836 ± 12	3^+	2.86 ± 20	$(3, 4^\pm)$	2.857 ± 9
		2.967 ± 20		2.972 ± 13				2.986 ± 9
3.053 ± 20		3.046 ± 20	$(1, 2, 3)^+$	3.035 ± 15		3.01 ± 20	$(> 3^-, > 4^+)$	3.056 ± 9
				3.100 ± 14				
		3.302 ± 30	$(4, 5, 6)^-$	3.324 ± 11	$(1, 2)^+$	3.29 ± 20	$(2, 3, 4^\pm)$	
3.636 ± 20		3.644 ± 30	$((2, 3, 4)^-)$			3.69 ± 60	$(2, 3^-, 4^\pm)$	
						4.15 ± 60	$(4^\mp, 2^-)$	
						4.56 ± 60	$(2^\pm)$	
						5.17 ± 60		
						5.43 ± 60		

[a] (89KU15).
[b] (90LA05).
[c] (90CL1B).
[d] (92SM03).

Table 20.27.8
Branching in ^{20}Mg(β^+)^{20}Na [a])

E_x(^{20}Na) (keV)	Branch (%) [b])	log ft	B(GT) [c])	J^π
984.25 ± 0.10	69.7 ± 1.2	3.83 ± 0.02	0.579 ± 0.030	1^+
2645	≤ 0.1	≥ 6.24	≤ 0.002	?
3001 ± 2	11.5 ± 1.4	4.08 ± 0.06	0.33 ± 0.05	1^+
3874 ± 15	4.8 ± 0.6	4.17 ± 0.06	0.27 ± 0.04	1^+
4123 ± 16	2.7 ± 0.3	4.33 ± 0.06	0.18 ± 0.03	1^+
≈ 4800 [d])	≥ 1.9 [3.6 ± 0.5]	≤ 4.23 [3.95 ± 0.06]	≥ 0.23 [0.45 ± 0.07]	1^+
≈ 5600 [d])	≥ 1.5 [2.8 ± 0.4]	≤ 3.97 [3.70 ± 0.06]	≥ 0.42 [0.79 ± 0.10]	1^+
6266 ± 30	1.2 ± 0.1	3.72 ± 0.06	0.75 ± 0.11	1^+
6521 ± 30	3.3 ± 0.4	3.13 ± 0.06	B(F) 4.57 ± 0.68	0^+
6770 ± 100	≥ 0.03	≤ 5.01	≥ 0.04	(1^+)
6920 ± 100	≥ 0.01	≤ 5.39	≥ 0.03	(1^+)
7440 ± 100	≥ 0.01	≤ 4.99	≥ 0.04	(1^+)

[a]) From Table 4 of (95PI03). The asterisk symbol indicates broad or unresolved states, for which the branching percentage could be determined only from proton emission to excited ^{19}Ne levels. For those states the numbers in square brackets indicate the estimated branch, log ft and B(GT) values under inclusion of the 3% branching to the ^{19}Ne ground state.
[b]) It is noted in (95PI03) that these branching ratios refer to the number of implanted ^{20}Mg atoms as 100%. For details on branching of the proton decay into ^{19}Ne levels see (95PI03).
[c]) Gamow-Teller strength.
[d]) Unresolved levels.

The ^{20}Mg decay to ^{20}Na has been studied through β-delayed proton and γ-ray measurements. For the earlier work see (79MO1B, 87AJ02). More recent studies are described in (92KU07, 92GO10, 92PI1O, 95PI03). Half-lives measured for this decay are 95 ± 3 ms (95PI03), 82 ± 4 ms (92GO10), 114 ± 17 ms (92KU07), 95^{+80}_{-50} ms (79MO1B). See Table 20.27.8 for β-decay branching ratios and log ft values. A compilation of ^{20}Na levels as observed in beta decay and other experiments is provided in (95PI03), and serves as the basis for Table 20.27 here.

7. ^{27}Al(^{20}Ne, ^{27}Mg)^{20}Na $\qquad Q_m = -16.497$

The Δ resonance is very strongly excited in this reaction at $E(^{20}\text{Ne}) = 950$ MeV/A (86BA1P).

^{20}Mg

(Fig. 20.5)

^{20}Mg has been populated in the ^{24}Mg(α, ^{8}He) reaction at $E_\alpha = 127$ and 156 MeV, in the ^{20}Ne(^{3}He, 3n) reaction at $E(^{3}\text{He}) = 70$ MeV, and more recently in projectile fragmentation reactions. Reviews of proton rich nuclei and methods of production are presented in (89AY1B, 93SO13). See also (90PO04). The super-allowed decay of ^{20}Mg to the first $T = 2$ ($J^\pi = 0^+$) state of ^{20}Na [$E_x = 6.450 \pm 0.020$ MeV (92PI1O)] has been reported in early work (79MO1B, 87AJ02) and more recently by (92KU07, 92PI1O, 92GO10, 95PI03), who also observed β decay to other proton-unstable ^{20}Na states [see ^{20}Na, reaction 6]. Lifetime measurements for ^{20}Mg have given $\tau_{1/2} = 95^{+80}_{-50}$ ms (79MO1B), 114 ± 17 ms (92KU07), 82 ± 4 ms (92GO10), and 95 ± 3 ms (95PI03).

In related theoretical work, shell model calculations for isospin-forbidden β delayed proton emission are described in (90BR26); also see the mass calculation (92AV03).

^{20}Al, etc.

(Not observed)

See (72AJ02, 83ANZQ, 86AN07).

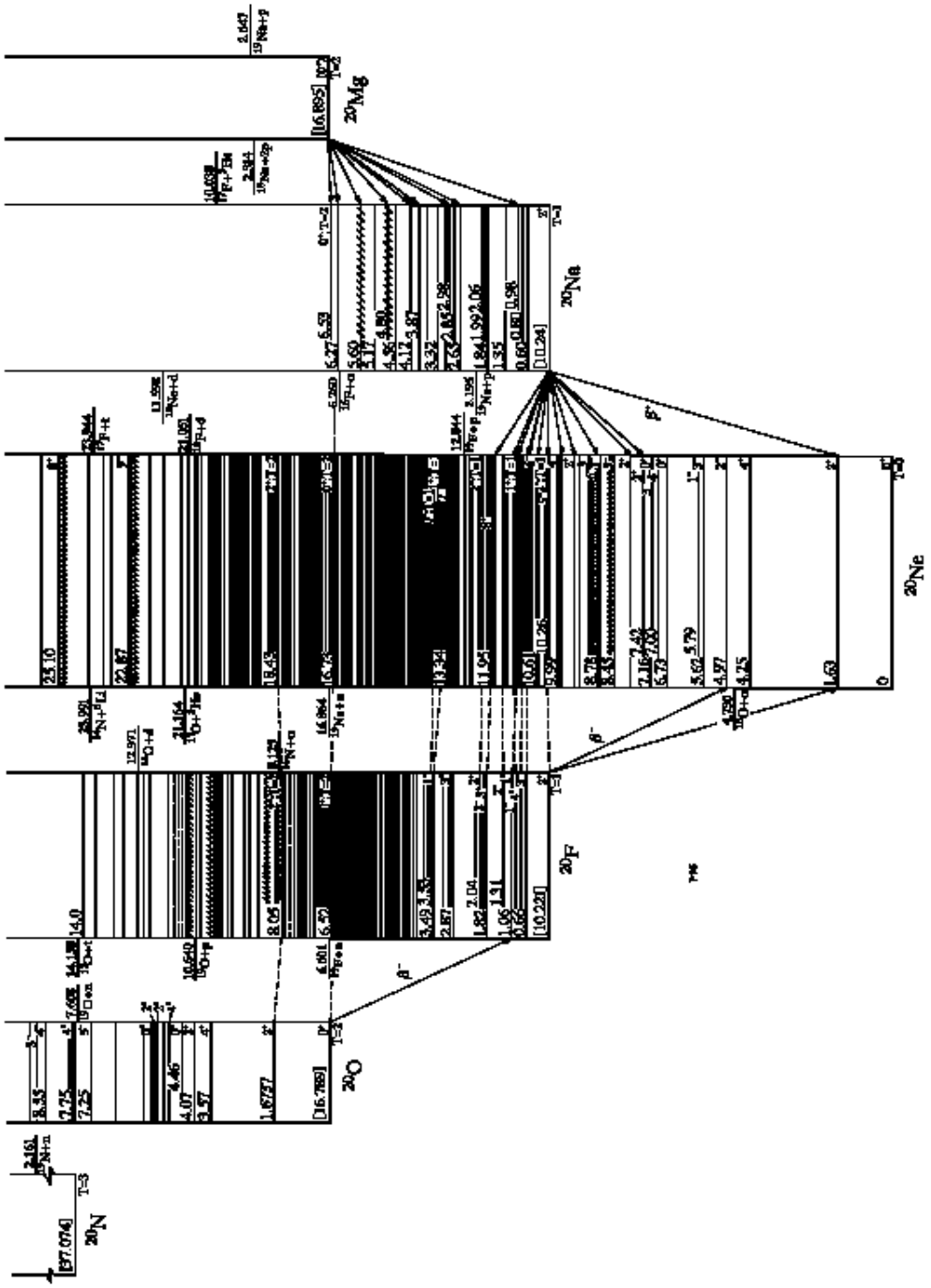

Figure 5: Isobar diagram, $A = 20$. The diagrams for individual isobars have been shifted vertically to eliminate the neutron-proton mass difference and the Coulomb energy, taken as $E_c = 0.60Z(Z-1)/A^{1/3}$. Energies in square brackets represent the (approximate) nuclear energy, $E_N = M(Z,A) - ZM(\mathrm{H}) - NM(\mathrm{n}) - E_c$, minus the corresponding quantity for ^{20}Ne: here M represents the atomic mass excess in MeV. Levels which are presumed to be isospin multiplets are connected with dashed lines.

References

(Closed September 15, 1995)

References are arranged and designated by the year of publication followed by the first two letters of the first-mentioned author's name and then by two additional characters. Most of the references appear in National Nuclear Data Center files and have NNDC key numbers ending in numeric characters. Otherwise, TUNL key numbers were assigned with the last two characters of the form 1A, 1B, etc. In response to many requests for more informative citations, we have, when possible, included up to 10 authors per paper and added the initials of all authors.

59AJ76 F. Ajzenberg and T. Lauritsen, Nucl. Phys. 11 (1959) 1

68SP01 P. Spilling, H. Gruppelaar, H.F. De vries and A.M.J. Spits, Nucl.Phys. A113 (1968) 395

70PA1A A.D. Panagiotou, Phys. Lett. B31 (1970) 361

72AJ02 F. Ajzenberg-Selove, Nucl. Phys. A190 (1972) 1

73MA14 R.L. Macklin and R.R. Winters, Phys. Rev. C7 (1973) 1766

73WA19 E.K. Warburton, P. Gorodetzky and J.A. Becker, Phys. Rev. C8 (1973) 418

74TH01 C. Thibault and R. Klapisch, Phys. Rev. C9 (1974) 793

75HO15 R.E. Horstman, J.L. Eberhardt, H.A. Doubt, C.M.E. Otten and G. Van Middelkoop, Nucl. Phys. A248 (1975) 291

75ME04 L.R. Medsker, H.T. Fortune, R.R. Betts and R. Middleton, Phys. Rev. C11 (1975) 1880

75SC1A Scweickert et al, Nucl. Phys. A246 (1975) 187

76GA1A Garber and Kinsey, BNL 325 (1976)

76KL03 H.V. Klapdor, H. Reiss and G. Rosner, Nucl. Phys. A262 (1976) 157

76MA01 R.E. Marrs, E.G. Adelberger, K.A. Snover and M.D. Cooper, Nucl. Phys. A256 (1976) 1

77CE1A Cerny and Hardy, Ann. Rev. Nucl. Sci. 27 (1977) 333

77FO11 H.T. Fortune and J.N. Bishop, Nucl. Phys. A293 (1977) 221

77FR1A Frey et al, Z. Phys. A281 (1977) 211

77MA07 R.E. Marrs, E.G. Adelberger and K.A.Snover, Nucl. Phys. A277 (1977) 429

78AJ03 F. Ajzenberg-Selove, Nucl. Phys. A300 (1978) 1

78GR06 E.E. Gross, T.P. Cleary, J.L.C. Ford, D.C. Hensley and K.S. Toth, Phys. Rev. C17 (1978) 1665

78LE19 J.C. Legg, D.J. Crozier, G.G. Seaman and H.T. Fortune, Phys. Rev. C18 (1978) 2202

78LEZA C.M. Lederer, V.S. Shirley, E. Browne, J.M. Dairiki, R.E. Doebler, A.A. Shihab-Eldin, L.J. Jardine, J.K. Tuli and A.B. Buyrn, Table of Isotopes 7th ed. (New York: John Wiley & Sons, 1978)

79BI10 J.H. Billen, Phys. Rev. C20 (1979) 1648

79BR03 H.S. Bradlow, W.D.M. Rae, P.S. Fisher, N.S. Godwin, G. Proudfoot and D. Sinclair, Nucl. Phys. A314 (1979) 171

79FO17 H.T. Fortune, L. Bland, R. Middleton, W. Chung and B.H. Wildenthal, Phys. Lett. B87 (1979) 29

79GL12 H. Glattli, G.L. Bacchella, M. Fourmond, A. Malinovski, P. Meriel, M. Pinot, P. Roubeau and A.Abragam, J. Physique 40 (1979) 629

79KO26 L. Koester, K. Knopf and W. Waschkowski, Z. Phys. A292 (1979) 95

79LA04 S. LaFrance, H.T. Fortune, S. Mordechai and R. Middleton, J. Phys. G5 (1979) L59

79LA18 S. LaFrance, H.T. Fortune, S. Mordechai, M.E. Cobern, G.E. Moore, R. Middleton, W. Chung, B.H.Wildenthal, Phys. Rev. C20 (1979) 1673

79MO1B Moltz et al, Phys. Rev. Lett. 42 (1979) 43

79PI01 A.A. Pilt, M.A.M. Shahabuddin and J.A. Kuehner, Phys. Rev. C19 (1979) 20

79YO04 K.C. Young,Jr., R.W. Zurmuhle, J.M. Lind and D.P. Balamuth, Nucl. Phys. A330 (1979) 452

80FI01 L.K. Fifield, M.J. Hurst, E.F. Garman, T.J.M. Symons, F. Watt and K.W. Allen, Nucl. Phys. A334 (1980) 109

81MA04 C.J. Martoff, J.A. Bistirlich, K.M. Crowe, M. Koike, J.P. Miller, S.S. Rosenblum, W.A. Zajc, H.W.Baer, A.H.Wapstra, G.Strassner et al, Phys. Rev. Lett. 46 (1981) 891

82AN12 M.S. Antony, J. Phys. G8 (1982) 1659

82AR20 K.P. Artemov, V.Z. Goldberg, I.P. Petrov, V.P. Rudakov, I.N. Serikov and V.A. Timofeev, Yad.Fiz. 36 (1982) 1345; Sov. J. Nucl. Phys. 36 (1982) 779

82DE30 L.C. Dennis, K.M. Abdo, A.D. Frawley and K.W. Kemper, Phys. Rev. C26 (1982) 981

82DE39 P.A. DeYoung, J.J.Kolata, L.J.Satkowiak and M.A.Xapsos, Phys. Rev. C26 (1982) 1482

82HU06 M. Hugi, J. Lang, R. Muller, J. Sromicki, E. Ungricht, K. Bodek, L. Jarczyk, B. Kamys, A. Strzalkowski and H. Witala, Phys. Rev. C25 (1982) 2403

82KA12 O. Karban, A.K. Basak, P.M. Lewis and S. Roman, Phys. Lett. B112 (1982) 433

82KO1C Kolata, Proc. Fifth Oaxtepec Symp. on Nucl. Phys., 1982, Unam 5, No. 2 (1982) 99

82KO1D Kondo and Tamura, Bad Honnef Symp. 1981, Springer-Verlag(1982) 314

82LI16 R. Lichtenthaler,Jr., A. Lepine-Szily, A.C.C. Villari, W. Mittig, V.J.G. Porto and C.V. Acquadro, Phys. Rev. C26 (1982) 2487

82MA25 G. Mairle, G.J. Wagner, P. Grabmayr, K.T. Knopfle, Liu Ken Pao and H. Riedesel, K. Schindler, V.Bechtold, L.Friedrich, P.Ziegler, Nucl. Phys. A382 (1982) 173

82MO15 H. Morgenstern, W. Bohne, K. Grabisch, D.G. Kovar and H. Lehr, Phys. Lett. B113 (1982) 463

82SA1A Sargood, Phys. Rep. 93 (1982) 61

82SH29 D. Shapira, J.L.C. Ford, Jr. and J. Gomez del Campo, Phys. Rev. C26 (1982) 2470

83AJ01 F. Ajzenberg-Selove, Nucl. Phys. A392 (1983) 1

83ANZQ Y. Ando, M. Uno and M. Yamada, JAERI-M-83-025 (1983)

83BE19 U.E.P. Berg, K. Ackermann, K. Bangert, R. Stock and K. Wienhard, Phys. Rev. C27 (1983) 2981

83CA1F Caskey, Ph.D. Thesis, U. Wisconsin (1983)

83CL1A Clifford et al, Phys. Rev. Lett. 50 (1983) 23

83CS1A Csikai, Florence (1983) 451

83DEZW L.C. Dennis, A.D. Frawle and J.F. Mateja, Bull. Am. Phys. Soc. 28 (1983) 669

83DU13 G.G. Dussel, A.O. Gattone and E.E. Maqueda, Phys. Rev. Lett. 51 (1983) 2366

83FI02 L.K. Fifield, W.N. Catford, S.H. Chew, E.F. Garman, D.M. Pringle, K.W. Allen and J. Lowe, Nucl. Phys. A394 (1983) 1

83FR14 A.D. Frawley, J.D. Fox, L.C. Dennis, K.W. Kemper and N.R. Fletcher, Phys. Rev. C27 (1983) 2482

83HI06 M.M. Hindi, J.H. Thomas, D.C. Radford and P.D. Parker, Phys. Rev. C27 (1983) 2902

83HU12 P. Hungerford, T. von Egidy, H.H. Schmidt, S.A. Kerr, H.G. Borner and E. Monnand, Z. Phys. A313 (1983) 339

83JA09 L. Jarczyk, B. Kamys, Z. Rudy, A. Strzalkowski, H. Witala, M. Hugi, J. Lang, R. Muller, J. Sromicki and H.H. Wolter. Phys. Rev. C28 (1983) 700

83JI04 C. Jiang, S. Han, Q. Guo and Q. Li, Chin. J. Nucl. Phys. 5 (1983) 8

83KA1E Kane, Bull. Am. Phys. Soc. 28 (1983) 661

83KN01 N .Kniest, E. Huttel, J. Gunzl, G. Clausnitzer, P.G. Bizzeti, P.R. Maurenzig and N. Taccetti, Phys. Rev. C27 (1983) 906

83KN05 W. Knupfer and B.C. Metsch, Phys. Rev. C27 (1983) 2487

83LE03 P.M. Lewis, A.K. Basak, J.D. Brown, P.V. Drumm, O. Karban, E.C. Pollacco and S. Roman, Nucl. Phys. A395 (1983) 204

83LE28 J.R. Letaw, R. Silberberg and C.H. Tsao, Astrophys. J. 51 (1983) 271

83LI1D Lister, Brooks and Nelson, Bull. Am. Phys. Soc. 28 (1983) 658

83ME13 M.C. Mermaz, F. Auger and B. Fernandez, Phys. Rev. C28 (1983) 1587

83MI22 F. Michel, J. Albinski, P. Belery, Th. Delbar, Gh. Gregoire, B. Tasiaux and G. Reidemeister, Phys. Rev. C28 (1983) 1904

83NA04 W.J. Naude, H.S. Bradlow, O. Dietzsch, A.A. Pilt, W.D.M. Rae and D. Sinclair, Z. Phys. A311 (1983) 297

83NG01 Nguyen Van Sen, R. Darves-Blanc, J.C. Gondrand and F. Merchez, Phys. Rev. C27 (1983) 194

83SH25 D. Shapira, D. DiGregorio, J. Gomez del Campo, R.A. Dayras, J.L.C. Ford, Jr., A.H. Snell, P.H. Stelson, R.G.Stokstad and F.Pougheon, Phys. Rev. C28 (1983) 1148

83SH26 T. Shimoda, S. Shimoura, T. Fukuda, M. Tanaka, H. Ogata, I. Miura, E. Takada, M.-K. Tanaka, K. Takimoto and K.Katori, J. Phys. G9 (1983) L199

84AP03 B. Apagyi and W. Scheid, J. Phys. G10 (1984) 791

84BA1R Baturin et al, PANIC (1984) I11

84BE26 U.E.P. Berg, K. Ackermann, K. Bangert, C. Blasing, W. Naatz, R. Stock, K. Wienhard, M.K. Brussel, T.E.Chapuran and B.H.Wildenthal, Phys. Lett. B140 (1984) 191

84BL14 G.S. Blanpied, G.A. Balchin, G.E. Langston, B.G. Ritchie, M.L. Barlett, G.W. Hoffmann, J.A. McGill, M.A.Franey, M.Gazzaly and B.H.Wildenthal, Phys. Rev. C30 (1984) 1233
84BR15 T. Bright, D. Ballon, R.J. Saxena, Y. Niv and N. Benczer-Koller, Phys. Rev. C30 (1984) 696
84BU01 V.V. Burov, V.M. Dubovik, S.G. Kadmensky, Yu.M. Tchuvilsky and L.A. Tosunyan, J. Phys. G10 (1984) L21
84CA08 W.N. Catford, E.F. Garman and L.K. Fifield, Nucl. Phys. A417 (1984) 77
84CA09 T.A. Carey, P.G. Roos, N.S. Chant, A. Nadasen and H.L. Chen, Phys. Rev. C29 (1984) 1273
84DE1A P. De Bievre, M. Gallet, N.E. Holden and I.L. Barnes, J. Phys. Chem Ref. Data 13 (1984) 809
84FO1A Fowler, Rev. Mod. Phys. 56 (1984) 149
84IN04 T.Inoue, J. Phys. Soc. Jpn. 53 (1984) 4158
84KN1A Kniest et al, PANIC (1984) H9
84KO13 Y. Kondo and T. Tamura, Phys. Rev. C30 (1984) 97
84LE19 R.J. Ledoux, C.E. Ordonez, M.J. Bechara, H.A. Al-Juwair, G. Lavelle and E.R. Cosman, Phys. Rev. C30 (1984) 866
84ME10 M.C. Mermaz, Nuovo Cim. A81 (1984) 291
84MO08 S. Mordechai and H.T. Fortune, Phys. Rev. C29 (1984) 1765
84MU04 T. Murakami, E. Ungricht, N. Takahashi, Y.-W. Lui, Y. Mihara, R.E. Neese, E. Takada, D.M. Tanner, R.E.Tribble and K.Nagatani, Phys. Rev. C29 (1984) 847
84PA18 G. Palla and W. Oelert, Phys. Rev. C30 (1984) 1331
84RI01 H.T. Richards, Phys. Rev. C29 (1984) 276
84RI06 S.R. Riedhauser, Phys. Rev. C29 (1984) 1961
84RI07 H.T. Richards, G. Caskey, J.H. Billen, S.R. Riedhauser and D.J. Stec, Phys. Rev. C29 (1984) 2332
84RO04 R.G.H. Robertson, P. Dyer, R.C. Melin, T.J. Bowles, A.B. McDonald, G.C. Ball, W.G. Davies and E.D. Earle, Phys. Rev. C29 (1984) 755
84UM04 K. Umeda, T. Yamaya, T. Suehiro, K. Takimoto, R. Wada, E. Takada, S. Shimoura, A. Sakaguchi, S. Murakami, M.Fukada et al, Nucl. Phys. A429 (1984) 88
85AJ01 F. Ajzenberg-Selove, Nucl. Phys. A449 (1985) 1
85AN17 M.S. Antony, J. Britz, J.B. Bueb and V.B. Ndocko-Ndongue, Nuovo Cim. A88 (1985) 265
85BE37 C. Beck, R.M. Freeman, F. Haas, B. Heusch and J.J. Kolata, Nucl. Phys. A443 (1985) 157
85BR29 B.A. Brown and B.H. Wildenthal, At. Data Nucl. Data Tables 33 (1985) 347
85CA09 G.Caskey, Phys. Rev. C31 (1985) 717
85CA41 G.R. Caughlan, W. A. Fowler, M.J. Harris and B.A. Zimmerman, At. Data Nucl. Data Tables 32 (1985) 197
85CU1A Cujec, Lecture Notes in Phys. 219 (1985) 108

85FO07 H.T.Fortune and R.Eckman, Phys. Rev. C31 (1985) 2076
85FR1C K.A. Frankel, J.A. Bistirlich, R. Bossingham, H.R. Bowman, K.M. Crowe, C.J. Martoff, D.L. Murphy, J.O. Rasmussen, J.P. Sullivan, E. Yoo et al, Phys. Rev. C32 (1985) 975
85IS1A Islamov et al, Leningrad (1985) 323
85JA17 R.A.Jarjis, Nucl. Instrum. Methods Phys. Res. B12 (1985) 331
85MU14 T. Murakami, E. Ungricht, Y.-W. Lui, Y. Mihara, E. Takada and R.E. Tribble, Phys. Rev. C32 (1985) 1558
85OU01 S. Ouichaoui, H. Beaumevieille, N. Bendjaballah, A.C. Chami, A. Dauchy, B. Chambon, D. Drain and C. Pastor, Nuovo Cim. A86 (1985) 170
85RA08 C. Rangacharyulu, E.J. Ansaldo, D. Stockhausen, D. Bender, S. Muller, A. Richter, N. Lo Iudice and F. Palumbo, Phys. Rev. C31 (1985) 1656
85ST1B Stokstad, Treatise on Heavy-Ion Sci. 3 (1985) 83
85UH01 M. Uhrmacher, K. Pampus, F.J. Bergmeister, D. Purschke and K.P. Lieb, Nucl. Instr. and Meth. B9 (1985) 234
85WA1L Wang et al, Bull. Am. Phys. Soc. 30 (1985) 1248
85XI1B Y. Xie, G. Wu, Y. Zhu, R. Miao, E. Fong, X. Yin, H. Miao, J. Cai, W. Sheng, S. Sun et al, Phys. Energ. Fortis & Phys. Nucl. 9 (1985) 71
86AN07 M.S. Antony, J. Britz and A. Pape, At. Data Nucl. Data Tables 34 (1986) 279
86BA1M Baba et al, Santa Fe (1986) 223
86BA1N Bauhoff, At. Data Nucl. Data Tables 35 (1986) 429
86BA1P Bachelier et al, Phys. Lett. B172 (1986) 23
86BE19 B. Bendyk, L. Jarczyk, B. Kamys, A. Strzalkowski and H. Witala, Phys. Rev. C34 (1986) 753
86CA19 W.N. Catford, D.M. Pringle, D.G. Lewis, A.E. Smith, E.F. Garman, I.F. Wright and J. Lukasiak, Nucl. Instrum. Methods Phys. Res. A247 (1986) 367
86CA24 B.O. Carragher, J. Carter, R.G. Clarkson, V. Hnizdo and J.P.F. Sellschop, Nucl. Phys. A460 (1986) 341
86CH1T M.A. Chaudhri, Santa Fe 85 (1986) 819
86CO15 S.G. Cooper, J. Phys. G12 (1986) 371
86CU02 B. Cujec, B. Dasmahapatra, Q. Haider, F. Lahlou and R.A. Dayras, Nucl. Phys. A453 (1986) 505
86GR1C K.A. Gridnev, N.Z. Darvish, V.B. Subbotin and S.N. Fadeev, Ivz. Akad. Nauk SSSR, Ser. Fiz. 50 (1986) 1991; Bull. Russ. Acad. Sci. 50:10 (1986) 117
86KA1U Kamanin, P7-86-322, DUBNA (1986) 55
86KA36 Y. Kadota, K. Ogino, K. Obori, Y. Taniguchi, T. Tanabe, M. Yasue and J. Schimizu, Nucl. Phys. A458 (1986) 523
86KN1C Kniest et al, J. Phys. Soc. Jpn. Suppl. 55 (1986) 1034
86LE1H Leavitt, Nucl. Instr. and Meth. B15 (1986) 296
86MA13 J.F. Mateja, A.D. Frawley, R.A. Parker and K. Sartor, Phys. Rev. C33 (1986) 1307

86MA48 D.M. Manley, B.L. Berman, W. Bertozzi, J.M. Finn, F.W. Hersman, C.E. Hyde-Wright, M.V. Hynes, J.J. Kelly, M.A. Kovash, S. Kowalski et al, Phys. Rev. C34 (1986) 1214
86OE01 W. Oelert, Nucl. Phys. A449 (1986) 395
86OU01 S. Ouichaoui, H. Beaumevielle, N. Bendjaballah and A. Genoux-Lubain, Nuovo Cim. A94 (1986) 133
86OUZZ S. Ouichaoui, H. Beaumevieille, N. Bendjaballah and G.J. Costa, Proc.Intern.Nuclear Physics Conference, Harrogate, U.K. (1986) 105
86PA10 C.T. Papadopoulos, R. Vlastou, E.N. Gazis, P.A. Assimakopoulos, C.A. Kalfas, S. Kossionides and A.C. Xenoulis, Phys. Rev. C34 (1986) 196
86PAZJ G. Palla, Proc. Int..Nucl. Phys. Conf., Harrogate, U.K. (1986) 407
86RA15 Md.A. Rahman and H.M. Sen Gupta, Nuovo Cim. A93 (1986) 236
86SA1F Samosvat, Sov. J. Part. & Nucl. 17 (1986) 313
86SC1E Schmid, Hammaren and Grummer, AIP Conf. Proc. 142 (1986) 327
86SE1B N. Seichert, W. Assmann, H. Clement, G. Graw, C. Hategan, H. Kader, F. Merz and P. Schiemenz, J. Phys. Soc. Jpn. Suppl. 55 (1986) 646
86SH30 T. Shimoda, K. Katori, T. Fukuda, H. Ogata, S. Shimoura, M. Tanaka and E. Takada, J. Phys. Soc. Japan 55 (1986) 3021
86TR08 W. Trolenberg, F. Hagelberg, H.J. Simonis, P.N. Tandon, K.-H. Speidel, M. Knopp and J. Gerber, Nucl. Phys. A458 (1986) 95
86WO1A Woosley and Weaver, Ann. Rev. Astron. Astrophys. 24 (1986) 205
87AB03 H. Abele, H.J. Hauser, A. Korber, W. Leitner, R. Neu, H. Plappert, T. Rohwer, G. Staudt, M. Strasser, S. Welte et al, Z. Phys. A326 (1987) 373
87AJ02 F. Ajzenberg-Selove, Nucl. Phys. A475 (1987) 1
87AL06 D.E. Alburger, G. Wang and E.K. Warburton, Phys. Rev. C35 (1987) 1479
87AN1B Ankinia et al (Dubna-Bucharest-Warsaw-Tbilisi-Alma Ata-Moscow Collaboration SKM-200), Yad. Fiz. 45 (1987) 1680; Sov. J. Nucl. Phys. 45 (1987) 1040
87AR13 A.E. Aravantinos and A.C. Xenoulis, Phys. Rev. C35 (1987) 1746
87BA1T D. Bachelier, J.L. Boyard, D. Contardo, V. Datar, P. Dekker, C. Ellegaard, C. Gaarde, J.Y. Grossiord, A. Guichard, T. Hennino et al, Eleventh Int. Conf. on Particles and Nuclei (1987) 268
87BA2G F. Balestra, M.P. Bussa, L. Busso, L. Fava, L. Ferrero, D. Panzieri, G. Piragino, F. Tosello, G. Bendiscioli, A. Rotondi et al, Phys. Lett. B194 (1987) 192
87BAZI D. Bazin, R. Anne, D. Guerreau, D. Guillemaud-Mueller, A.C. Mueller, M.G. Saint-Laurent, W.D. Schmidt-Ott, V. Borrel, J.C. Jacmart, F. Pougheon et al, Contrib. Proc. 5th Int. Conf. Nuclei far from Stability, Rosseau Lake, Canada, (1987) K7
87BE1F B. Berthier, R. Boisgard, J. Julien, J.M. Hisleur, R. Lucas, C. Mazur, C. Ngô, M. Ribrag and C. Cerruti, Phys. Lett. B193 (1987) 417
87BE1G U.E.P. Berg and U. Kneissl, Ann. Rev. Nucl. Part. Sci. 37 (1987) 33
87BE1V P. Belery, P. Cohilis, Th. Delbar, Y. El Masri and Gh. Grègoire, Phys. Rev. C36 (1994) 1335

87BL18 R. Blumel and K. Dietrich, Nucl. Phys. A471 (1987) 453
87BO23 R. Bougault, D. Horn, C.B. Chitwood, D.J. Fields, C.K. Gelbke, D.R. Klesch, W.G. Lynch, M.B. Tsang, Phys. Rev. C36 (1987) 830
87BU07 M. Bürgel, H. Fuchs, H. Homeyer, G. Ingold, U. Jahnke and G. Thoma, Phys. Rev. C36 (1987) 90
87BU1E N.T. Burtebaev, A.D. Duisebaev, V.S. Sadkovskii and G.A. Feofilov, Izv. Akad. Nauk SSSR Ser. Fiz. 51 (1987) 615; Bull. Acad. Sci. USSR 51:3 (1987) 191
87CA1H Cao et al, Phys. Rev. C35 (1987) 625
87CH1J W.H. Chung, Singapore J. Phys. 4 (1987) 15
87CO31 P.D. Cottle and K.W. Kemper, Phys. Rev. C36 (1987) 2034
87DA12 O.D. Dal'karov, V.A. Karmanov and A.V. Trukhov, Sov. J. Nucl. Phys. 45 (1987) 430; Yad. Fiz. 45 (1987) 688
87DA1D O.D. Dal'karov and V.A. Karmanov, Fiz. Elem. Chastits At. Yadra 18 (1987) 1399 Sov. J. Part. Nucl. 18:6 (1987) 599
87DA1L B.V. Danilin and M.V. Zhukov, Fiz. Elem. Chastits At. Yadra 18 (1987) 205 Sov. J. Part. Nucl. 18:2 (1987) 83
87DE1O Detraz, Dubna (1987) 42
87DE40 P. Descouvemont and D. Baye, Nucl. Phys. A475 (1987) 219
87DI07 Th. Diaco, C. Friedli and Lerch, Radiochim. Acta 42 (1987) 1
87DUZU J.P. Dufour, R. Del Moral, F. Hubert, D. Jean, M.S. Pravikoff, A. Fleury, H. Delagrange, A. Mueller, K.-H. Schmidt, E. Hanelt et al, Contrib. Proc. 5th Int. Conf. Nuclei far from Stability, Rosseau Lake, Canada, (1987) D1
87DW1A R. Dwyer and P. Meyer, Astrophys. J. 322 (1987) 981
87EL14 Ellegaard, Can. J. Phys. 65 (1987) 600
87ER1B Erb, Symp. in honor of D. Allan Bromley, Yale Univ. (1987) 54
87EV01 E.J. Evers, J.W. de Vries, G.A.P. Engelbertink and C. van der Leun, Nucl. Instrum. Methods Phys. Res. A257 (1987) 91
87FI01 L.K.Fifield, D.M.Pringle and W.J.Vermeer, Nucl. Phys. A463 (1987) 644
87FU12 R.J. Furnstahl, C.E. Price and G.E. Walker, Phys. Rev. C36 (1987) 2590
87GI05 A. Gillebert, W. Mittig, L. Bianchi, A. Cunsolo, B. Fernandez, A. Foti, J. Gastebois, C. Grègoire, Y. Schutz and C. Stephan, Phys. Lett. B192 (1987) 39
87GO12 M.S. Golovkov and V.Z. Gol'dberg, Ivz. Akad. Nauk SSSR Ser. Fiz. 51 (1987) 129
87HA16 P. Halse, Phys. Rev. C36 (1987) 372
87HA24 K.H. Hahn, K.H. Chang, T.R. Donoghue and B.W. Filippone, Phys. Rev. C36 (1987) 892
87HA41 P. Halse and J.N. Ginocchio, Phys. Rev. C36 (1987) 2611
87HE1D J. Herberz, G. Fricke, T. Hennemann, G. Mallot, M. Reuter, R. Jacot-Guillarmod, C. Piller, L.A. Schaller, L. Schellenberg and W. Reichart, Eleventh Int. Conf. on Particles and Nuclei (1987) 640
87HI08 M. Hino, K. Muto and T. Oda, J. Phys. G13 (1987) 1119

87KA24 H. Kazama, Prog. Theor. Phys. 77 (1987) 1178
87KA2B S.A. Karamyan, Yad. Fiz. 46 (1987) 1338; Sov. J. Nucl. Phys. 46 (1987) 786
87KA30 K. Kato and H. Tanaka, Fizika (Zagreb) Supplement 1 (1987) 11
87KE09 T.J. Kennett, W.V. Prestwich and J.S. Tsai, Can. J. Phys. 65 (1987) 1111
87KR08 A.J. Kreiner and C. Pomar, Phys. Rev. C36 (1987) 436
87LE1G V.E. Lewis and T.B. Ryves, Nucl. Instrum. Methods Phys. Res. A257 (1987) 462
87LI1F X.-Y. Li, S.-H. Yao and Q.-Y. Zhang, High Energy Phys. Nucl. Phys. 11 (1987) 397
87LI26 H. Liu and L. Zamick, Phys. Rev. C36 (1987) 2057
87LI34 Y. Ling and Z. Qui, Chin. J. Nucl. Phys. 9 (1987) 329
87LY04 W.G. Lynch, Nucl. Phys. A471 (1987) 309c
87MI07 F. Michel, G. Reidemeister and S. Ohkubo, Phys. Rev. C35 (1987) 1961
87MU03 Yu.A. Muzychka and B.I. Pustyl'nik, Yad. Fiz. 45 (1987) 90; Sov. J. Nucl. Phys. 45 (1987) 57
87MU16 H. Müther, R. Machleidt and R. Brockmann, Phys. Lett. B198 (1987) 45
87NU01 J. Nurzynski, T. Kihm, K.T. Knopfle, G. Mairle and H. Clement, Nucl. Phys. A465 (1987) 365
87PA06 H. Paetz gen Schieck, N.O. Gaiser, K.R. Nyga, R.M. Prior and S.E. Darden, Nucl. Instrum. Methods Phys. Res. A254 (1987) 616
87PA29 W. Pannert, P. Ring and J. Boguta, Phys. Rev. Lett. 59 (1987) 2420
87PR03 C.E. Price and G.E. Walker, Phys. Rev. C36 (1987) 354
87RA01 S. Raman, C.H. Malarkey, W.T. Milner, C.W. Nestor, Jr. and P.H. Stelson, At. Data Nucl. Data Tables 36 (1987) 1
87RA02 W.D.M. Rae, P.R. Keeling and S.C. Allcock, Phys. Lett. B184 (1987) 133
87RA1D R. Ramaty and R.J. Murphy, Space Sci. Rev. 45 (1987) 213
87RA23 J. Räisänen, T. Witting and J. Keinonen, Nucl. Instrum. Methods Phys. Res. B28 (1987) 199
87RE04 P.-G. Reinhard and K. Goeke, Rep. Prog. Phys. 50 (1987) 1
87RO1D Rolfs, Trautvetter and Rodney, Rep. Prog. Phys. 50 (1987) 233
87SA1P S. Sarkar, K. Kar and V.K.B. Kota, Phys. Rev. C36 (1987) 2700
87SA1Q T. Sakuda and H. Bando, Prog. Theor. Phys. 78 (1987) 1317
87SA55 S.M. Saad, V.B. Subbotin, K.A. Gridnev, E.F. Hefter and V.M. Semjonov, Nuovo Cim. A98 (1987) 529
87SC1J K.W. Schmid and F. Grümmer, Rep. Prog. Phys. 50 (1987) 731
87SE17 H.M. Sen Gupta, M.S. Chowdhury, F. Watt and M.J. Hurst, Nuovo Cim. A98 (1987) 715
87SH23 W. Shen, Y. Zhu, W. Zhan, Z. Guo, S. Yin, W. Qiao and X. Yu, Nucl. Phys. A472 (1987) 358
87SI1E Simenog, Yurmala (1987) 167
87SM1B V.M. Smirnov, N.G. Triumfov, O.S. Tsvetkov and P.P. Chinenov, Atomnaya Energiya 63:2 (1987) 136; Sov. At. Energ. 63 (1987) 645

87SN1A K. Sneppen, Nucl. Phys. A470 (1987) 213
87SO1D L.G. Sobotka, D.G. Sarantites, Z. Li, E.L. Dines, M.L. Halbert, D.C. Hensley, J.C. Lisle, R.P. Schmitt, Z. Majka, G. Nebbia et al, Phys. Rev. C36 (1987) 2713
87SU03 T. Sugimitsu, H. Inoue, H. Fujita, N. Kato, K. Kimura, T. Tachikawa, K. Anai, Y. Ikeda and Y. Nakajima, Nucl. Phys. A464 (1987) 415
87SU07 T. Suomijärvi, B. Berthier, R. Lucas, M.C. Mermaz, J.P. Coffin, G. Guillaume, B. Heusch, F. Jundt and F. Rami, Phys. Rev. C36 (1987) 181
87SU09 C. Sukosd, C. Mayer-Böricke, M. Rogge, P. Turek, K.T. Knöpfle, H. Riedesel, K. Schindler and G.J. Wagner, Nucl. Phys. A467 (1987) 365
87SU13 Y. Suzuki, Nucl. Phys. A470 (1987) 119
87SU1I J.P. Sullivan, Phys. Rev. C36 (1987) 1200
87TA1C Y.C. Tang, AIP Conf. Proc. 162 (1987) 174
87VA24 J.R. Vanhoy, E.G. Bilpuch, C.R. Westerfeldt and G.E. Mitchell, Phys. Rev. C36 (1987) 920
87VI1B V.E. Viola, Nucl. Phys. A471 (1987) 53c
87VI1D Vigdor, Jacobs and Korkmaz, Phys. Rev. Lett. 58 (1987) 840
87WA1P S. Wang, P.B. Price, S.W. Barwick, K.J. Moody and E.K. Hulet, Phys. Rev. C36 (1987) 2717
87WI03 A. Willis, M. Morlet, N. Marty, C. Djalali, G.M. Crawley, A. Galonsky, V. Rotberg and B.A. Brown, Nucl. Phys. A464 (1987) 315
87YI1A S.-Z. Yin, Y.-T. Zhu, W.-Q. Shen, Z.-Y. Guo, W.-L. Zhan, W.-M. Qiao, E.-C. Wu and Z.-H. Zheng, Phys. Energ. Fortis and Phys. Nucl. 11 (1987) 259
88AI1A J. Aichelin, G. Peilert, A. Boohnet, A. Rosenhauer, H. Stöcker and W. Greiner, Phys. Rev. C37 (1988) 2451
88AL07 S.C. Allcock, W.D.M. Rae, P.R. Keeling, A.E. Smith, B.R. Fulton and D.W. Banes, Phys. Lett. B201 (1988) 201
88AP1A J.H. Applegate, Phys. Rep. 163 (1988) 141
88AP1B J.H. Applegate, AIP Conf. Proc. 176 (1988) 988
88AR24 K.P. Artemov, M.S. Golovkov, V.Z. Gold'berg, V.V. Pankratov, V.P. Rudakov, I.N. Serikov and V.A. Timofeev, Yad. Fiz. 48 (1988) 1236; Sov. J. Nucl. Phys. 48 (1988) 784
88ARZU K.P. Artemov, M.S. Golovkov, V.Z. Goldberg, V.P. Rudakov, I.N. Serikov, V.A. Timofeev, J. Schmider, M. Madeya and Ya. Yakel, Program & Theses, Proc. 38th Ann. Conf. Nucl. Spectrosc. Struct. At. Nucl., Baku (1988) 381
88AU03 F. Auger and B. Fernandez, Nucl. Phys. A481 (1988) 577
88BA12 Z. Basrak, W. Tiereth and H. Voit, Phys. Rev. C37 (1988) 1511
88BA16 E.B. Balbutsev and I.N. Mikhailov, J. Phys. G14 (1988) 545
88BA1H J.N. Bahcall and R.K. Ulrich, Rev. Mod. Phys. 60 (1988) 297
88BA1J D. Bazin, R. Anne, D. Guerreau, D. Guillemaud-Mueller, A.C. Mueller, M.G. Saint-Laurent and W.D. Schmidt-Ott, AIP Conf. Proc. 164 (1988) 722
88BA66 D. Baye and P. Descouvemont, Phys. Rev. C38 (1988) 2463

88BA80 E.B. Bal'butsev and I. Piperova, Izv. Akad. Nauk SSSR Ser. Fiz. 52 (1988) 2132; Bull. Acad. Sci. USSR Phys. Ser. 52:11 (1988) 52
88BA82 H. Bando, Nucl. Phys. A478 (1988) 697c
88BE1J Belyaeva and Zelenskaya, Baku (1988) 449
88BE2A Besliu and Jipa, Rev. Roum. Phys. 33 (1988) 409
88BL11 R. Blendowske and H. Walliser, Phys. Rev. Lett. 61 (1988) 1930
88BL13 G.S. Blanpied, B.G. Ritchie, M.L. Barlett, R.W. Fergerson, G.W. Hoffmann, J.A. McGill and B.H. Wildenthal, Phys. Rev C38 (1988) 2180
88BO1D J. Bogdanowicz, Nucl. Phys. A479 (1988) 323c
88BO27 D.H. Boal and J.N. Glosli, Phys. Rev. C38 (1988) 1870
88BR11 B.A. Brown, W.A. Richter, R.E. Julies and B.H. Wildenthal, Ann. Phys. 182 (1988) 191
88BR1D B.A. Brown and B.H. Wildenthal, MSUCL-637 (1988)
88BR1P B.A. Brown and B.H. Wildenthal, Ann. Rev. Nucl. Part. Soc. 38 (1988) 29
88BU01 L. Buchman, J.M. D'Auria and P. McCorquodale, Astrophys. J. 324 (1988) 953
88CA09 M. Carchidi and B.H. Wildenthal, Phys. Rev. C37 (1988) 1681
88CA1G G. Cardella, M. Papa, G. Pappalardo, F. Rizzo, A. De Rosa, G. Inglima, M. Sandoli, G. Fortuna, G. Montagnoli, A.M. Stefanini et al, Nucl. Phys. A482 (1988) 235c
88CA1N G.R. Caughlan and W.A. Fowler, At. Data Nucl. Data Tables 40 (1988) 283
88CAZV D.D. Caussyn, N.R. Fletcher, G.L. Gentry, J.A. Liendo, K.L. Lamkin, J.D. Fox, A.D. Frawley, E.G. Myers and J.F. Mateja, Bull. Am. Phys. Soc. 33:8 (1988) 1562 (AC11)
88CE01 C. Cerruti, J. Desbois, R. Boisgard, C. Ngô, J. Natowitz and J. Nemeth, Nucl. Phys. A476 (1988) 74
88CH28 A.K. Chaudhuri, S. Bhattacharya and K. Krishan, Nucl. Phys. A485 (1988) 181
88CO12 M.E. Colin and C. Friedli, Radiochim. Acta. 43 (1988) 139
88CS01 J. Cseh and G. Lèvai, Phys. Rev. C38 (1988) 972
88CU03 J. Cugnon, P. Deneye and J. Vandermeulen, Phys. Rev. C38 (1988) 795
88CU1A A.C. Cummings, E.R. Christian and E.C. Stone, Bull. Am. Phys. Soc. 33 (1988) 1069
88CU1D J. Cugnon, AIP Conf. Proc. 176 (1988) 378
88DE18 B. Dechant and E. Kuhlmann, Z. Phys. A330 (1988) 93
88DI02 S.S. Dietrich and B.L. Berman, At. Data Nucl. Data Tables 38 (1988) 199
88DI08 J. Ding and G. He, J. Phys. G14 (1988) 1315
88DO17 C. Dorso and J. Randrup, Phys. Lett. B215 (1988) 611
88DU01 P. Dupieux, J.P. Alard, J. Augerat, R. Babinet, N .Bastid, F. Brochard, P. Charmensat, N. De Marco, H. Fanet, Z. Fodor et al, Phys. Lett. B200 (1988) 17
88DU1C J.P. Dufour, R. Del Moral, F. Hubert, D. Jean, M.S. Pravikoff, A. Fleury, H. Delagrange, A.C. Mueller, K.-H. Schmidt, E. Hanelt et al, AIP Conf. Proc. 164 (1988) 344
88EL06 A.J.R. El Hassani, J.-F. Gilot, P.F.A. Goudsmit, H.J. Leisi and St. Thomann, Helv. Phys. Acta 61 (1988) 1130

88ET01 M.C. Etchegoyen, A. Etchegoyen, B.H. Wildenthal, B.A. Brown and J. Keinonen, Phys. Rev. C38 (1988) 1382
88FI01 J. Fiase, A. Hamoudi, J.M. Irvine and F. Yazici, J. Phys. G14 (1988) 27
88FO1E D.J. Forrest and R.J. Murphy, Solar Phys. 118 (1988) 123
88FR02 E. Friedman, A. Gal, G. Kalbermann and C.J. Batty, Phys. Lett. B200 (1988) 251
88GA19 C. Gao, P. Ning and G. He, Nucl. Phys. A485 (1988) 282
88GA1K J. Galin, Nucl. Phys. A488 (1988) 297c
88GA1L C. Gao and G. He, Chin. Phys. 8 (1988) 987
88GO1G Goryonov et al, 38th Meeting on Nucl. Spectroscopy and the Structure of the At. Nucl., Baku, USSR, 12-14 April 1988 (Nauka, 1988) 366
88GR12 K.A. Griffioen, E.A. Bakkum, P. Decowski, R.J. Meijer and R. Kamermans, Phys. Rev. C37 (1988) 2502
88GR1I K.A. Gridnev, N.Z. Darwish, V.B. Subbotin and S.N. Fadeiv, Proc. Indian Natn. Sci. Acad. 54 (1988) 917
88GU12 I.S. Gul'karov, Fiz. Elem. Chastis At. Yadra 19 (1988) 345; Sov. J. Part. Nucl. 19 (1988) 149
88HA12 S.S. Hanna, J. Phys. G14 (1988) S283
88HE06 D.F. Hebbard, J. Nurzynski, T.R. Ophel, P.V. Drumm, Y. Kondo, B.A. Robson and R. Smith, Nucl. Phys. A481 (1988) 161
88HE1I T. Hennino, AIP Conf. Proc. 176 (1988) 663
88HI05 M. Hino, K. Muto and T. Oda, Phys. Rev. C37 (1988) 1328
88IV02 M. Ivascu and I. Silisteanu, Nucl. Phys. A485 (1988) 93
88IW1A H. Iwe and E. Okonov, Phys. Lett. B215 (1988) 465
88JO02 J.I. Johansson, E.D. Cooper and H.S. Sherif, Nucl. Phys. A476 (1988) 663
88JO1B G. A. Jones, Interact. and Struct. in Nucl., Proc. in honor of D.H. Wilkinson, Sussex, 9/87; Adam Hilger Publ. (1988) 9
88JU02 J. Julien, M. Bolore, H. Dabrowski, J.M. Hisleur, V. Bellini, A.S. Figuera, R. Fonte, A. Insolia, G.F. Palama, G.V. Russo et al, Z. Phys. A330 (1988) 83
88KA1Z K. Kato, K. Fukatsu and H. Tanaka, Prog. Theor. Phys. 80 (1988) 663
88KO18 L. Koester, W. Waschkowski, J. Meier, G. Rau and M. Salehi, Z. Phys. A330 (1988) 387
88KU07 R. Kuchta, Nucl. Phys. A483 (1988) 92
88KU08 P.M. Kurjan, J.R. Calarco, G.A. Fisher and S.S. Hanna, Phys. Rev. C37 (1988) 2281
88KU17 R. Kuchta, Phys. Rev. C38 (1988) 1460
88KU22 R. Kuchta, Z. Phys. A331 (1988) 243
88KU23 Kubono et al, Z. Phys. A331 (1988) 359
88LAZY L.O. Lamm, C.P. Browne, J. Görres, S. Graff, M. Wiescher and A.A. Rolleson, Bull. Am. Phys. Soc. 33 (1988) 1563
88LE05 G. Lèvai and J. Cseh, J. Phys. G14 (1988) 467
88LE06 M. LeMere and Y.C. Tang, Phys. Rev. C37 (1988) 1369

88LI10 G.-B. Liu and H.T. Fortune, Phys. Rev. C37 (1988) 1818
88LI28 G.-B. Liu and H.T. Fortune, Phys. Rev. C38 (1988) 2134
88MA1Q L. Majling, J. Zofka, T. Sakuda and H. Bando, PROG. THEOR. PHYS. 79 (1988) 561
88MA1U R.A. Malaney and W.A. Fowler, Astrophys. J. 333 (1988) 14
88MA30 R.S. Mackintosh, A.A. Ioannides and S.G. Cooper, Nucl. Phys. A483 (1988) 173
88MA53 G. Mairle, K.T. Knöpfle and M. Seeger, Nucl. Phys. A490 (1988) 371
88MCZT V. McLane, C.L. Dunford and P.F. Rose, Neutron Cross Sections, Vol. 2 (Academic Press, Inc. 1988)
88ME09 A.C. Merchant and M.P. Isidro Filho, Phys. Rev. C38 (1988) 1911
88MI1I M. Mishra, M. Satpathy and L. Satpathy, J. Phys. G14 (1988) 1115
88MU08 A.C. Mueller, D. Bazin, W.D. Schmidt-Ott, R. Anne, D. Guerreau, D. Guillemaud-Mueller, M.G. Saint-Laurent, V. Borrel, J.D. Jacmart, F. Pougheon et al, Z. Phys. A330 (1988) 63
88MU10 H. Müther, T. Taigel and T.T.S. Kuo, Nucl. Phys. A482 (1988) 601
88PO1E N.A.F.M. Poppelier, J.H. de Vries, A.A. Wolters and P.W.M. Glaudemans, AIP Conf. Proc. 164 (1988) 334
88RA1G W.D.M. Rae, Int. J. Mod. Phys. A3 (1988) 1343
88RA20 Md.A. Rahman, S.N. Rahman, H.M. Sen Gupta, H.-J. Trost, P. Lezoch and U. Strohbusch, Nuovo Cim. A99 (1988) 317
88RA27 Md.A. Rahman, Nuovo Cim. A100 (1988) 419
88RE1F D.V. Reames, R. Ramaty and T.T. von Rosenvinge, Astrophys. J. 332 (1988) L87
88RO10 Rosa et al, Phys. Rev. C37 (1988) 2722
88RO17 Roy-Stephan, Nucl. Phys. A488 (1988) 187c
88RO19 A.S. Rosenthal, Prog. Theor. Phys. 80 (1988) 359
88RO1H M. Roy-Stephan, Nucl. Phys. A488 (1988) 187c
88SH05 N.R. Sharma, B.K. Jain and R. Shyam, Phys. Rev. C37 (1988) 873
88SI1E Simons, Phys. Scr. T22 (1988) 90
88SM1B A.R. Smith, J.C. Hill, J.A. Winger and P.J. Karol, Phys. Rev. C38 (1988) 210
88ST04 B. Strohmaier and S.M. Grimes, Z. Phys. A329 (1988) 431; Erratum Z. Phys. A331 (1988) 114
88UT02 H. Utsunomiya and R.P. Schmitt, Nucl. Phys. A487 (1988) 162
88VI1D D.J. Vieira, J.M. Wouters and the TOFI Collaboration, AIP Conf. Proc. 164 (1988) 1
88WA13 T.R. Wang, W. Haeverli, S.W. Wissink and S.S. Hanna, Phys. Rev. C37 (1988) 2301
88WA1H M. Wakai, H. Bando and M. Sano, Phys. Rev. C38 (1988) 748
88WO09 J.M. Wouters, R.H. Kraus, Jr., D.J. Vieira, G.W. Butler and K.E.G. Löbner, Z. Phys. A331 (1988) 229
88WO1C S.E. Woosley and W.C. Haxton, Nature 334 (1988) 45
88ZH09 J.-K. Zhang and D.S. Onley, Phys. Lett. B209 (1988) 145

88ZH12 Y. Zhu, W. Shen, X. Hu, Y. Xie, W. Zhan, X. Zhu and S. Li, Nucl. Phys. A488 (1988) 409c
88ZH1F Zhao, Li, Chen and Wang, Kexue Tongbao 33 (1988) 1423
89AD1C M. Aderholz, M.M. Aggarwal, H. Akbari, P.P. Allport, P.V.K.S. Baba, S.K. Badyal, M. Barth, J.P. Baton, H.H. Bingham, E.B. Brucker et al, Phys. Rev. Lett. 63 (1989) 2349
89AN12 I. Angeli, Z. Phys. A334 (1989) 377
89AR1H Arima, Tokyo (1988) 407
89AR1R W.D. Arnett, J.N. Bahcall, R.P. Kirshner and S.E. Woosley, Ann. Rev. Astron. Astrophys. 27 (1989) 629
89AY1B J. Äysto and J. Cerny, Treatise on Heavy-Ion Sci. 8 (1989) 207
89BA10 F. Balestra, S. Bossolasco, M.P. Bussa, L. Busso, L. Ferrero, D. Panzieri, G. Piragino, F. Tosello, R. Barbieri, G. Bendiscioli et al, Nucl. Phys. A491 (1989) 541
89BA17 E.A. Bakkum, P. Decowski, K.A. Friffioen, R.J. Meijer and R. Kamermans, Phys. Rev. C39 (1989) 2094
89BA1E H. Bando, M. Sano, J. Zoofka and M. Wakai, Nucl. Phys. A501 (1989) 900
89BA1S F. Balestra, S. Bossolasco, M.P. Bussa, L. Busso, L. Ferrero, D. Panzieri, G. Piragino, F. Tosello, R. Barbieri, G. Bendiscioli et al, Phys. Lett. B217 (1989) 43
89BA2N H. Bando, Nuovo Cim. A102 (1989) 627
89BE17 C. Beck, D.G. Kovar, S.J. Sanders, B.D. Wilkins, D.J. Henderson, R.V.F. Janssens, W.C. Ma, M.F. Vineyard, T.F. Wang, C.F. Maguire et al, Phys. Rev. C39 (1989) 2202
89BE1T Belyaeva, Bogdanova and Zelenskaya, Tashkent (1989) 432
89BE2H D. Bencivenni, V. Castellani, A. Tornambè and A. Weiss, Astrophys. J. Suppl. Ser. 71 (1989) 109
89BE51 T.L. Belyaeva and N.S. Zelenskaya, Ukr. Fiz. Zh. 34 (1989) 1635
89BR1G C. Brechtmann, W. Heinrich and E.V. Benton, Phys. Rev. C39 (1989) 2222
89BU14 M. Burlein, H.T. Fortune, W.M. Amos, T.L. Ekenberg, A. Kotwal, P.H. Kutt, J.M. O'Donnell, J.D. Silk, B. Boyer, A. Fuentes et al, Phys. Rev. C40 (1989) 785
89CA05 O. Castaños and J.P. Draayer, Nucl. Phys. A491 (1989) 349
89CA15 S. Cavallaro, S.Z. Yin, G. Prete and G. Viesti, Phys. Rev. C40 (1989) 98
89CI1C N. Cindro and M. Bozin, Heavy Ions in Nucl. and Atomic Phys., 1988 Mikolajki Summer School on Nucl. Phys. (1989) 239
89CL02 Clifford et al, Nucl. Phys. A493 (1989) 293
89CO22 M.E. Colin, C. Friedli and P. Lerch, Radiochim. Acta. 46 (1989) 13
89CU06 J. Cugnon and J. Vandermeulen, Ann. Phys. 14 (1989) 49
89DE12 Y.D. Devi, V.K.B. Kota and J.A. Sheikh, Phys. Rev. C39 (1989) 2057
89DE32 P. Descouvemont and D. Baye, Phys. Lett. B228 (1989) 6
89ET01 A. Etchegoyen, M.C. Etchegoyan and B.H. Wildenthal, Phys. Rev. C39 (1989) 680
89FI03 R. Lichtenthäler Filho, A. Lèpine-Szily, A.C.C. Villari and O. Portezan Filho, Phys. Rev. C39 (1989) 680

89FI04 J. Fink, V. Blum, P.-G. Reinhard, J.A. Maruhn and W. Greiner, Phys. Lett. B218 (1989) 277
89FI05 D.E. Fields, K. Kwiatkowski, D. Bonser, R.W. Viola, W.G. Lynch, M.J. Pochodzalla, M.B. Tsang, C.K. Gelbke, D.J. Fields and S.M. Austin, Phys. Lett. B220 (1989) 356
89FO07 R. Fonte, A. Insolia, G. Palamá and G.V. Russo, Nucl. Phys. A495 (1989) 43c
89FO1G Fonte, Insolia, Palama and Russo, Sao Paulo (1989) 415
89GA05 C. Gao and Y. Kondo, Phys. Lett. B219 (1989) 40
89GA09 C. García-Recio, M.J. López, J. Navarro and F. Roig, Phys. Lett. B222 (1989) 329
89GA16 Y.K. Gambhir and P. Ring, Pramana 32 (1989) 389
89GA1L Gao and Kondo, Sao Paulo (1989) 317
89GE10 P.M. Gensini, Nuovo Cim. A102 (1989) 1563
89GH01 B. Ghosh and R. Shyam, J. Phys. G15 (1989) L185
89GO1N J. Görres, M. Wiescher and C. Rolfs, Astrophys. J. 343 (1989) 365
89GU1I N. Guessoum and R.J. Gould, Astrophys. J. 345 (1989) 356
89GU1J N. Guessoum, Astrophys. J. 345 (1989) 363
89GU1Q M. Gupta and W.R. Webber, Astrophys. J. 340 (1989) 1124
89HE11 D.W. Hetherington, A. Alousi and R.B. Moore, Nucl. Phys. A494 (1989) 1
89HE1I He and Gao, Sao Paulo (1989) 320
89HE1N R.B.C. Henry, Monthly Notice Royal Astron. Soc. 241 (1989) 453
89HO16 E. Hourani, M. Hussonnois and D.N. Poenaru, Ann. Physique 14 (1989) 311
89HU1E Hubert et al, Proc. 1989 Int. Nucl. Phys. Conf., Sao Paulo, Brasil, 20-26 August 1989 (World Sci., 1989) 147
89JI1A L. Jin, W.D. Arnett and S.K. Chakrabarti, Astrophys. J. 336 (1989) 572
89KA06 O. Karban, W.C. Hardy, K.A. Connell, S.E. Darden, C.O. Blyth, H.D. Choi, S.J. Hall, S. Roman and G. Tungate, Nucl. Instrum. Methods Phys. Res. A274 (1989) 4
89KA37 G. Kalbermann, E. Friedman, A. Gal and C.J. Batty, Nucl. Phys. A503 (1989) 632
89KI13 A. Kiss, F. Deák, Z. Seres, G. Caskey, A. Galonsky, B. Remington and L. Heilbronn, Nucl. Phys. A499 (1989) 131
89KN01 J.M. Knox and J.F. Harmon, Nucl. Instrum. Methods Phys. Res. B44 (1989) 40
89KO13 W. Koepf and P. Ring, Nucl. Phys. A493 (1989) 61
89KU15 S. Kubono, H. Orihara, S. Kato and T. Kajino, Astrophys. J. 344 (1989) 460
89KU1D Kubono et al, Tokyo (1988) 83
89LE16 M. Lewitowicz, Yu.E. Penionzhkevich, A.G. Artukh, A.M. Kalinin, V.V. Kamanin, S.M. Lukyanov, Nguyen Hoai Chau, A.C. Mueller, D. Guillemaud-Mueller, R. Anne et al, Nucl. Phys. A496 (1989) 477
89LE19 A. Lèpine-Szily, R. Lichtenthäler Filho, M.M. Obuti, J. Martins de Oliveira, Jr., O. Portezan Filho, W. Sciani and A.C.C. Villari, Phys. Rev. C40 (1989) 681
89MA1U P. Marage, P.P. Allport, N. Armenise, J.P. Baton, M. Berggren, W. Burkot, M. Calicchio, T. Coghen, A.M. Cooper-Sarkar, O. Erriquez et al, Z. Phys. C43 (1989) 523

89MA45 Z. Majka, V. Abenante, Z. Li, N.G. Nicolis, D.G. Sarantites, T.M. Semkow, L.G. Sobotka, D.W. Stracener, J.R. Beene, D.C. Hensley et al, Phys. Rev. C40 (1989) 2124
89MC03 V.A. McGlone, Nucl. Instrum. Methods Phys. Res. A274 (1989) 601
89MC04 V.A. McGlone, Nucl. Instrum. Methods Phys. Res. B42 (1989) 143
89ME1C R.A. Mewaldt and E.C. Stone, Astrophys. J. 337 (1989) 959
89MI12 F. Michel and G. Reidemeister, Z. Phys. A333 (1989) 331
89MI18 H.G. Miller, B.J. Cole and R.M. Quick, Phys. Rev. Lett. 63 (1989) 1922
89MI1M Miller, Cole and Quick, Sao Paulo (1989) 96
89MOZY C.P. Montoya, R. Butsch, M.G. Herman, D.J. Hofman, M. Thoennessen and P. Paul, Bull. Am. Phys. Soc. 34 (1989) 1155
89NI1D H. Nifenecker and J.A. Pinston, Prog. Part. Nucl. Phys. 23 (1989) 271
89OB1C Obuti et al, Sao Paulo (1989) 324
89OR02 W.E. Ormand and B.A. Brown, Nucl. Phys. A491 (1989) 1
89OR03 N.A. Orr, W.N. Catford, L.K. Fifield, M.A.C. Hotchkis, T.R. Ophel, D.C. Weisser and C.L. Woods, Nucl. Phys. A491 (1989) 443
89OS02 A. Osman and A.A. Farra, J. Phys. G15 (1989) 871
89PA06 D.J. Parker, J.J. Hogan and J. Asher, Phys. Rev. C39 (1989) 2256
89PE04 R. Pepelnik, Nucl. Instrum. Methods Phys. Res. B40/41 (1989) 1205
89PO04 A. Poves, J. Retamosa and E. Moya de Guerra, Phys. Rev. C39 (1989) 1639
89PO05 I.V. Poplavskii, Yad. Fiz. 49 (1989) 408; Sov. J. Nucl. Phys. 49 (1989) 253
89PO1J Portezan, Lepine-Szily, Lichtenthaler and Villari, Sao Paulo (1989) 323
89PU1C Puri, Chattopadhyay and Gupta, Sao Paulo (1989) 322
89QU01 R.M. Quick, H.G. Miller and B.J. Cole, Phys. Rev. C40 (1989) 993
89QU1A J.F.H. Quick, R.M. Quick and H.G. Miller, J. Comput. Phys. 80 (1989) 243
89RA16 S. Raman, C.W. Nestor, Jr. , S. Kahane and K.H. Bhatt, At. Data Nucl. Data Tables 42 (1989) 1
89RA17 P. Raghavan, At. Data Nucl. Data Tables 42 (1989) 189
89RA1G J. Rapaport, Fundamental Symmetries and Nucl. Structure, eds. J.N. Ginocchio & S. P. Rosen, Santa Fe, NM, 1988 (World Sci. 1989) 186
89RI1D Ring, "Fundamental Symmetries and Nucl. Structure," edited by Ginocchio & Rosen, Santa Fe, New Mexico, 1988 (World Sci., 1989) 140
89RO01 G. Royer and J. Mignen, J. Phys. G15 (1989) L1
89RO1G Rosensteel, Sao Paulo (1989) 87
89RU08 J.H. Ruza, T.V. Guseva, Yu.Ya. Tamberg, J.A.C. Alcaras, L.Y. Sabalyauskas and V.V. Vanagus, Ukr. Fiz. Zh. 34 (1989) 1458
89SA10 M.G. Saint-Laurent, R. Anne, D. Bazin, D. Guillemaud-Mueller, U. Jahnke, Jin Gen-Ming, A.C. Mueller, J.F. Bruandet, F. Glasser, S. Kox et al, Z. Phys. A332 (1989) 457
89SA14 A. Sarma and R. Singh, Z. Phys. A333 (1989) 299
89SA1R M. Sano, M. Wakai and H. Bando, Phys. Lett. B224 (1989) 359

89SA26 S. Sarkar and K. Kar, Phys. Rev. C40 (1989) 1826
89SC14 K.W. Schmid, R. Zheng, F. Grümmer and A. Faessler, Nucl. Phys. A499 (1989) 63
89SH1N A. Shor, E.F. Barasch, J.B. Carroll, T. Hallman, G. Igo, G. Kalnins, P. Kirk, G.F. Krebs, P. Linstrom, M.A. McMahan et al, Phys. Rev. Lett. 63 (1989) 2192
89SMZZ M.S. Smith, P.V. Magnus, K.I. Hahn, A.J. Howard, P.D. Parker, A.E. Champagne and Z.Q. Mao, Bull. Am. Phys. Soc. 34 (1989) 1802
89SO1C G. Soff and J. Rafelski, Z. Phys. D14 (1989) 187
89SP01 R.H. Spear, At. Data Nucl. Data Tables 42 (1989) 55
89SZ01 A. Szanto de Toledo, M.M. Coimbra, N. Added, R.M. Anjos, N. Carlin Filho, L. Fante, Jr., M.C.S. Figueira, V. Guimarães and E.M. Szanto, Phys. Rev. Lett. 62 (1989) 1255
89TA1N C. Tan, Y. Xia, H. Yang, X. Sun, J. Liu, Z. Zheng and P. Zhu, Nucl. Instrum. Methods Phys. Res. B42 (1989) 1
89TA26 M. Takahara, M. Hino, T. Oda, K. Muto, A.A. Wolters, P.W.M. Glaudemans and K. Sato, Nucl. Phys. A504 (1989) 167
89TO05 Y. Tosaka, Y. Suzuki and K. Ikeda, Prog. Theor. Phys. 81 (1989) 379
89TO1D F. Tosello, Nuovo Cim. A102 (1989) 663
89VAZN V.V. Vanagas, Ya.Kh. Ruzha, T.V. Guseva and Yu.Ya. Tamberg, Program and Thesis, Proc.39th Ann.Conf.Nucl.Spectrosc.Struct.At.Nuclei, Tashkent (1989) 159
89VO1F V.V. Volkov, Treatise on Heavy-Ion Sci. 8 (1989) 101
89WA14 M. Wakai, H. Bando and M. Sano, Z. Phys. A333 (1989) 213
89WUZZ A.H. Wuosmaa and R.W. Zurmühle, Bull. Am. Phys. Soc. 34 (1989) 1187
89YO02 A. Yokoyama, T. Saito, H. Baba, K. Hata, Y. Nagame, S. Ichikawa, S. Baba, A. Shinohara and N. Imanishi, Z. Phys. A332 (1989) 71
89YO09 W. Yokota, T. Nakagawa, M. Ogihara, T. Komatsubara, Y. Fukuchi, K. Suzuki, W. Galster, Y. Nagashima, K. Furuno, S.M. Lee et al, Z. Phys. A333 (1989) 379
89ZH05 R.-R. Zheng, K.W. Schmid, F. Grümmer and A. Faessler, Nucl. Phys. A494 (1989) 214
89ZU02 M.D. Zubkov and A.V. Pozdnyakov, Yad. Fiz. 49 (1989) 1005; Sov. J. Nucl. Phys. 49 (1989) 625
90AM01 K. Amos and C. Steward, Phys. Rev. C41 (1990) 335
90AR10 M. Arnould and M. Rayet, Ann. Physique 15 (1990) 183
90BA01 B.F. Bayman, S.M. Lenzi and E.E. Maqueda, Phys. Rev. C41 (1990) 109
90BA18 E.A. Bakkum, P. Decowski, K.A. Friggioen, R.J. Meijer and R. Kamermans, Nucl. Phys. A511 (1990) 117

90BEYY A.V. Belozerov, I. Vintsour, R.G. Kalpakchieva, I.V. Kuznetsov, Yu.E. Penionahkevich and Sh. Piskorzh, Prog. & Thesis, Proc. 40th Ann. Conf. Nucl. Spectrosc. Struct. At. Nucl., Leningrad (1990) 359
90BL09 Blunden and Horowitz, Phys. Lett. B240 (1990) 6
90BL1K O. Blaes, R. Blandford, P. Madau and S. Koonin, Astrophys. J. 363 (1990 612

90BO01 W. Bohne, H. Morgenstern, K. Grabisch, T. Nakagawa and S. Proschitzki, Phys. Rev. C41 (1990) R5
90BO04 J. Boger, S. Kox, G. Auger, J.M. Alexander, A. Narayanan, M.A. McMahan, D.J. Moses, M. Kaplan and G.P. Gilfoyle, Phys. Rev. C41 (1990) R801
90BO16 R. Bonetti, E. Fioretto, C. Migliorino, A. Pasinetti, F. Barranco, E. Vigezzi and R.A. Broglia, Phys. Lett. B241 (1990) 179
90BR26 B.A. Brown, Phys. Rev. Lett. 65 (1990) 2753
90CA07 J.A. Caballero and E. Moya de Guerra, Nucl. Phys. A509 (1990) 117
90CH09 S.K. Charagi and S.K. Gupta, Phys. Rev. C41 (1990) 1610
90CH13 H.C. Chiang, E. Oset and P. Fernández de Córdoba, Nucl. Phys. A510 (1990) 591
90CL06 Clarke et al, J. Phys. G16 (1990) 1547
90CO04 B.J. Cole, H.G. Miller and R.M. Quick, Phys. Rev. C41 (1990) 789
90CO1N M.A. Coplan, K.W. Ogilvie, P. Bochsler and J. Geiss, Solar Phys. 128 (1990) 195
90CO38 S.G. Cooper and R.S. Mackintosh, Z. Phys. A337 (1990) 357
90CU01 J. Cugnon, P. Deneye and J. Vandermeulen, Phys. Rev. C41 (1990) 1701
90CU04 J. Cugnon, P. Deneye and J. Vandermeulen, Nucl. Phys. A517 (1990) 533
90DE1I D. Deprospo, M. Kalelkar, M. Lauko and P. Stamer, Bull. Am. Phys. Soc. 35 (1990) 952
90DE34 Descouvemont and Baye, Nucl. Phys. A517 (1990) 143
90DE45 J. Deutsch, M. Lebrun and R. Priells, Nucl. Phys. A518 (1990) 149
90DI12 V.I. Dimitrov and B. Slavov, Phys. Lett. B252 (1990) 1
90FO04 S. Fortier, S. Gales, S.M. Austin, W. Benenson, G.M. Crawley, C. Djalali, J.S. Winfield and G. Yoo, Phys. Rev. C41 (1990) 2689
90GA09 C. García-Recio, T.W. Donnelly and E. Moya de Guerra, Nucl. Phys. A509 (1990) 221
90GA10 Y.K. Gambhir, P. Ring and A. Thimet, Ann. Phys. 198 (1990) 132
90GL01 A. Glaesner, W. Dünnweber, M. Bantel, W. Hering, D. Konnerth, R. Ritzka, W. Trautmann, W. Trombik and W. Zipper, Nucl. Phys. A509 (1990) 331
90GU02 D. Guillemaud-Mueller, J.C. Jacmart, E. Kashy, A. Latimier, A.C. Mueller, F. Pougheon, A. Richard, Yu.E. Penionzhkevich, A.G. Artukh, A.V. Belozyorov et al, Phys. Rev. C41 (1990) 937
90GU08 H.-Å. Gustafsson, B. Jakobsson, A. Kristiansson, A. Oskarsson, M. Westenius, P. Arve, J. Helgesson, L. Westerberg, K. Aleklett, A.J. Kordyasz et al, Phys. Lett. B241 (1990) 322
90GU10 I.S. Gul'karov, Yad. Fiz. 51 (1990) 97; Sov. J. Nucl. Phys. 51 (1990) 61
90GU35 I.S. Gul'karov, V.I. Kuprikov, V.N. Tarasov and M.M. Mansurov, Izv. Akad. Nauk SSSR, Ser. Fiz. 54 (1990) 2207; Bull. Acad. Sci. USSR 54:11 (1990) 120
90GUZV I.S. Gulkarov, V.I. Kuprikov and V.N. Tarasov, Prog. & Thesis, Proc. 40th Ann. Conf. Nucl. Spectrosc. Struct. At. Nucl., Leningrad (1990) 163
90HA07 W.C. Haxton, Nucl. Phys. A507 (1990) 179c
90HA38 S. Hara, K.T. Hecht and Y. Suzuki, Prog. Theor. Phys. 84 (1990) 254

90HE1G R.S. Henderson, B.W. Pointon, O. Häusser, A. Celler, R.L. Helmer, K.P. Jackson, B.W. Larson, C.A. Miller and M.C. Vetterli, Nucl. Instrum. Methods Phys. Res. A286 (1990) 41
90HUZY W. Huang, C.D. Goodman, G.C. Kiang, Y. Wang, T. Carey, R. Byrd, L. Rybarcyk, T. Taddeucci, D. Marchlenski, E. Sugarbaker et al, Bull. Am. Phys. Soc. 35 (1990) 1059
90KH05 S.A. Khan and W.P. Beres, Phys. Rev. C42 (1990) 1768
90KN01 N. Kniest, E. Huttel, E. Pfaff, G. Reiter and G. Clausnitzer, Phys. Rev. C41 (1990) R1336
90KOZG F. Komori, S. Katsumoto, S. Kobayashi, S. Ikehata, N. Ikeda, O. Hashimoto, T. Fukuda, T. Nomura and T. Yamazaki, Inst. Nucl. Study, Univ. Tokyo, 1989 Ann. Rept. (1990) 27
90LA05 Lamm et al, Nucl. Phys. A510 (1990) 503
90LA09 B. Lavielle, H. Sauvageon, P. Bertin and G. Haouat, Phys. Rev. C42 (1990) 305
90LA1M M. Lauko, D. Deprospo, M .Kalelkar and P. Stamer, Bull. Am. Phys. Soc. 35 (1990) 952
90LE06 J.A. Leavitt, L.C. McIntyre, Jr., M.D. Ashbaugh, J.G. Oder, Z. Lin and B. Dezfouly-Arjomandy, Nucl. Instrum. Methods Phys. Res. B44 (1990) 260
90LE12 A. Lèpine-Szily, M.M. Obuti, R. Lichtenthäler Filho, J.M. Oliveira, Jr. and A.C.C. Villari, Phys. Lett. B243 (1990) 23
90LO11 R.J. Lombard, J. Phys. G16 (1990) 1311
90MA1Z R.A. Malaney, Wksp. on Primordial Nucleosynthesis, Chapel Hill, NC, 1989 (World Sci., 1990) 49
90MA63 S.E. Massen, J. Phys. G16 (1990) 1713
90MI24 T.N. Mikhaleva, Izv. Akad. Nauk. SSSR, Ser. Fiz. 54 (1990) 586; Bull. Acad. Sci. USSR 54:3 (1990) 207
90MO1J Moya de Guerra, PANIC XII (1990) Paper I-82
90MU06 A.C. Mueller, D. Guillemaud-Mueller, J.C. Jacmart, E. Kashy, F. Pougheon, A. Richard, A. Staudt, H.V. Klapdor-Kleingrothaus, M. Lewitowicz, R. Anne et al, Nucl. Phys. A513 (1990) 1
90MU1H R.J. Murphy, G.H. Share, J.R. Letaw and D.J. Forrest, Astrophys. J. 358 (1990) 298
90NA1E T. Nakagawa, T. Asami and T. Yoshida, JAERI-M 90-099
90OS03 A. Osman and A.A. Farra, Nuovo Cim. A103 (1990) 1693
90OS1B A. Osman and S.S. Abdel-Aziz, Ind. J. Pure Appl. Phys. 28 (1990) 226
90PH01 D.L. Pham and R. de Swiniarski, Z. Phys. A335 (1990) 37
90PH02 D.L. Pham and R. de Swiniarski, Nuovo Cim. A103 (1990) 375
90PO04 I.V. Poplavskii, Yad. Fiz. 51 (1990) 1258; Sov. J. Nucl. Phys. 51 (1990) 799
90PR1B S. Prasad, S.N. Chatterjee and B.N. Roy, Indian J. Pure Appl. Phys. 28 (1990) 40
90RE06 J. Retamosa, J.M. Udías, A. Poves and E. Moya de Guerra, Nucl. Phys. A511 (1990) 221
90SC1N D.N. Schramm and J.W. Truran, Phys. Rep. 189 (1990) 89

90SH12 S.D. Sharma and A. Sharma, J. Phys. G16 (1990) 701
90SI1A R. Silberberg and C.H. Tsao, Astrophys. J. 352 (1990) L49
90SI1D R. Silberberg and C.H. Tsao, Phys. Rep. 191 (1990) 351
90SK04 L.D. Skouras and J.C. Varvitsiotis, Nucl. Phys. A513 (1990) 239
90SL01 B. Slavov, F. Grümmer, K. Goeke, R. Gissler, V.I. Dimitrov and Ts. Venkova, J. Phys. G16 (1990) 395
90ST08 A. Staudt, E. Bender, K. Muto and H.V. Klapdor-Kleingrothaus, At. Data Nucl. Data Tables 44 (1990) 79
90TH1C F.-K. Thielemann, M.-A. Hashimoto and K. Nomoto, Astrophys. J. 349 (1990) 222
90TH1E F.-K. Thielemann and M. Wiescher, Wksp. on Primordial Nucleosynthesis, Chapel Hill, NC, 1989, (World Sci, 1990) 92
90VA14 V. Vanagas, O. Katkevicius, J.A. Castilho Alcarás, J. Tambergs and J. Ruza, Fizika 22 (1990) 101
90WA10 S. wa Kitwanga, P. Leleux, P. Lipnik and J. Vanhorenbeeck, Phys. Rev. C42 (1990) 748
90WE1A W.R. Webber, J.C. Kish and D.A. Schrier, Phys. Rev. C41 (1990) 520
90WE1I W.R. Webber, A. Soutoul, P. Ferrando and M. Gupta, Astrophys. J. 348 (1990) 611
90YA08 T. Yamada, Phys. Rev. C42 (1990) 1432
90YE02 S.J. Yennello, K. Kwiatkowski, S. Rose, L.W. Woo, S.H. Zhou and V.E. Viola, Phys. Rev. C41 (1990) 79
90ZH01 D.-C. Zheng, L. Zamick and N. Auerbach, Ann. Phys. 197 (1990) 343
91AB05 R. Abegg and C.A. Davis, Phys. Rev. C43 (1991) 2523
91AJ01 F. Ajzenberg-Selove, Nucl. Phys. A523 (1991) 1
91AM1A K. Amos, L. Berge, C. Steward and R. de Swiniarski, Aust. J. Phys. 44 (1991) 217
91AM1B A.I. Amelin, I.L. Kiselevich, S.V. Lapushkin, V.I. Mikhailichenko, S.Yu. Panitkin, A.K. Ponosov, N.O. Poroshin, F.M. Sergeev and M.Yu. Tel'nov, Yad. Fiz. 54 (1991) 1021; Sov. J. Nucl. Phys. 54 (1991) 616
91AN01 Anderson et al, Phys. Rev. C43 (1991) 50
91BA18 F. Balestra, Yu.A. Batusov, G. Bendiscioli, S. Bossolasco, F.O. Breivik, M.P. Bussa, L. Busso, K.M. Danielsen, C. Guaraldo, I.V. Falomkin et al, Nucl. Phys. A526 (1991) 415
91BA25 E.B. Bal'butsev, I.V. Molodtsova and I. Piperova, Yad. Fiz. 53 (1991) 670; Sov. J. Nucl. Phys. 53 (1991) 419
91BA49 F. Balestra, G. Bendiscioli, V. Filippini, A. Rotondi, P. Salvini, A. Zenoni, S. Bossolasco, M.P. Bussa, L. Busso, L. Fava et al, Phys. Scr. 44 (1991) 323
91BO45 D. Bonatsos, L.D. Skouras, P. Van Isacker and M.A. Nagarajan, J. Phys. G17 (1991) 1803
91CI08 A. Cieply, M. Gmitro, R. Mach and S.S. Kamalov, Phys. Rev. C44 (1991) 713
91CI11 A. Cieply, M. Gmitro and R. Mach, Czech. J. Phys. B41 (1991) 1091
91CS01 J. Cseh, G. Levai and K. Kato, Phys. Rev. C43 (1991) 165

91DU05 J. Dukelsky, A. Poves and J. Retamosa, Phys. Rev. C44 (1991) 2872
91FR02 J. Fritze, R. Neu, H. Abele, F. Hoyler, G. Staudt, P.D. Eversheim, F. Hinterberger and H. Müther, Phys. Rev. C43 (1991) 2307
91GA14 C. Gao, Y. Kondo and B.A. Robson, Nucl. Phys. A529 (1991) 234
91GO21 P.F.A. Goudsmit, H.J. Leisi and E. Matsinos, Phys. Lett. B271 (1991) 209
91HE16 H. Herndl, H. Abele, G. Staudt, B. Bach, K. Grün, H. Scsribany, H. Oberhummer and G. Raimann, Phys. Rev. C44 (1991) R952
91HI23 P.Z. Hien, T.K. Mai, T.X. Quang, N.V. Loc and T.N. Thuy, J. Radioanal. Nucl. Chem. 153 (1991) 169
91IG1A M. Igashira, H. Kitazawa, S. Kitamura, H. Anze and M. Horiguchi, AIP Conf. Proc. 238 (1991) 624
91KH09 D.E. Kharzeev and M.G. Sapozhnikov, Nuovo Cim. A104 (1991) 1509
91LE33 J.A. Leavitt and L.C. McIntyre Jr., Nucl. Instr. and Meth. B56/57 (1991) 734
91LI33 G. Li, D.T. Khoa, T. Maruyama, S.W. Huang, N. Ohtsuka, A. Faessler and J. Aichelin, Nucl. Phys. A534 (1991) 697
91MA1D P. Marage, M. Aderholz, P.P. Allport, N. Armenise, J.P. Baton, M. Berggren, W. Burkot, V. Burtovoy, M. Calicchio, E.F. Clayton et al, Z. Phys. C49 (1991) 385
91MA41 E. Maglione and L.S. Ferreira, Phys. Lett. B262 (1991) 179
91MI24 T.N. Mikhaleva, Izv. Akad. Nauk SSSR, Ser. Fiz. 55:1 (1991) 120; Bull. Acad. Sci. USSR, Phys. Ser. 55 (1991) 112
91MU19 A.C. Mueller and R. Anne, Nucl. Instrum. Methods Phys. Res. B56/57 (1991) 559
91OM03 Kh.M. Omar, S.S. Saad and N.Z. Darwish, Appl. Radiat. Isot. 42 (1991) 823
91OR01 N.A. Orr, W. Mittig, L.K. Fifield, M. Lewitowicz, E. Plagnol, Y. Schutz, W.L. Zhan, L. Bianchi, A. Gillibert, A.V. Belozyorov et al, Phys. Lett. B258 (1991) 29
91PI09 C.N. Pinder, C.O. Blyth, N.M. Clarke, D. Barker, J.B.A. England, B.R. Fulton, O. Karban, M.C. Mannion, J.M. Nelson, C.A. Ogilvie et al, Nucl. Phys. A533 (1991) 25
91PO11 V. Potbhare and N. Tressler, Nucl. Phys. A530 (1991) 171
91PO14 B.W. Pointon, O. Häusser, R. Henderson, A. Celler, K. Hicks, K.P. Jackson, R. Jeppesen, B. Larson, J. Mildenberger, A. Trudel et al, Phys. Rev. C44 (1991) 2430
91RA1C C.M. Raiteri, M. Busso, R. Gallino and G. Picchio, Astrophys. J. 371 (1991) 665
91RE02 P.L. Reeder, R.A. Warner, W.K. Hensley, D.J. Vieira and J.M. Wouters, Phys. Rev. C44 (1991) 1435
91RE10 G. Reffo, M.H. Mac Gregor and T. Komoto, Nucl. Instrum. Methods Phys. Res. A307 (1991) 380
91SU15 T. Sugimitsu and N. Hori, Nucl. Instrum. Methods Phys. Res. A309 (1991) 218
91SZ02 A. Szczurek, A. Budzanowski, L. Jarczyk, A. Magiera, K. Möhring, R. Siudak and T. Srokowski, Z. Phys. A338 (1991) 187
91WA11 K.-X. Wang, G.-Z. Liu, D.F. Collinson, D.H. Feng and C.-L. Wu, Phys. Rev. C43 (1991) 2268
91YA08 Yamaguchi, Phys. Rev. C44 (1991) 1171

91ZH02 J.-K. Zhang and D.S. Onley, Phys. Rev. C43 (1991) R942

91ZH05 Z.Y. Zhu, H.J. Mang and P. Ring, Phys. Lett. B254 (1991) 325

91ZH06 J.-K. Zhang and D.S. Onley, Nucl. Phys. A526 (1991) 245

92AN1F A.N. Antonov, E.N. Nikolov, I.Z. Petkov, P.E. Hodgson and G.A. Lalazissis, Bulg. J. Phys. 19 (1992) 11

92AR11 K.P. Artemov, M.S. Golovkov, V.V. Pankratov and V.P. Rudakov, Sov. J. Nucl. Phys. 55 (1992) 326

92AR18 K.P. Artemov, M.S. Golovkov, V.Z. Goldberg, V.V. Pankratov, A.E. Pakhomov, I.N. Serikov and V.A. Timofeev, Sov. J. Nucl. Phys. 55 (1992) 1460

92ARZX K.P. Artemov, V.Z. Goldverg, M.S. Golovkov, V.P. Rudakov, I.N. Serikov, V.A. Timofeev, R.W. Zurmuhle, D.R. Benton, Z. Liu, S.P. Barrow, et al, Proc. Int. Conf. Nuclear Structure and Nuclear Reactions at Low and Intermediate Energies, Dubna (1992) 49

92AV03 M.P. Avotina, K.I. Erokhina and I.Kh. Lemberg, Sov. J. Nucl. Phys. 55 (1992) 1777

92BE14 A.N. Behkami and Z. Kargar, J. Phys. G18 (1992) 1023

92CA05 J.A. Carr, S.D. Bloom, R. Petrovich and R.J. Philpott, Phys. Rev. C45 (1992) 1145

92CA19 N. Canosa, R. Rossignoli and H.G. Miller, Phys. Rev. C45 (1992) 3027

92CA1J R. Canal, J. Isern and J. Labay, Astrophys. J. 398 (1992) L49

92CH39 M.S. Chowdhury, M.A. Zaman and H.M. Sen Gupta, Phys. Rev. C46 (1992) 2273

92CS03 J. Cseh and W. Scheid, J. Phys. G18 (1992) 1419

92DA10 C.A. Davis, Phys. Rev. C45 (1992) 2693

92DE10 W. De Coster, B. Brijs, J. Goemans and W. Vandervorst, Nucl. Instrum. Methods Phys. Res. B64 (1992) 417

92DE31 De Swiniarski, Pham and Raynal, Z. Phys. A343 (1992) 179

92EGZZ Egelhof et al, Univ. Mainz, 1991 Ann. Rep. (1992) 20

92FR01 G. Fricke, J. Herberz, Th. Hennemann, G. Mallot, L.A. Schaller, L. Schellenberg, C. Piller and R. Jacot-Guillarmod, Phys. Rev. C45 (1992) 80

92GO10 J. Görres, M. Wiescher, K. Scheller, D.J. Morrissey, B.M. Sherrill, D. Bazin and J.A. Winger, Phys. Rev. C46 (1992) R833

92GR11 Grimes, Z. Phys. A343 (1992) 125

92GR15 C. Grama, N. Grama and I. Zamfirescu, Rev. Roum. Phys. 37 (1992) 161

92GU02 Gutekunst and Muther, Phys. Lett. B277 (1992) 227

92HA12 P.R. Hayes, N.M. Clarke, K.I. Pearce, M.B. Becha, R.S. Mackintosh, J.B.A. England, L. Zybert, G.M. Field and S. Roman, Nucl. Phys. A540 (1992) 171

92HA18 P.R. Hayes and N.M. Clarke, J. Phys. G18 (1992) 1119

92HA1N S. Hara, K. Ogawa and Y. Suzuki, Prog. Theor. Phys. 88 (1992) 329

92HJ01 M. Hjorth-Jensen, E. Osnes and H. Muther, Ann. Phys. 213 (1992) 102

92JI04 M.F. Jiang, R. Machleidt, D.B. Stout and T.T.S. Kuo, Phys. Rev. C46 (1992) 910

92JO07 C.W. Johnson, S.E. Koonin, G.H. Land and W.E. Ormand, Phys. Rev. Lett. 69 (1992) 3157

92KI1C I.L. Kiselevich, V.I. Mikhailichenko, S.Yu. Panitkin, A.K. Ponosov, F.M. Sergeev and M. Yu. Tel'nov, Sov. J. Nucl. Phys. 55 (1992) 2100
92KN06 O.M. Knyaz'kov and Yu.A. Matusov, Bull. Russ. Acad. Sci. Phys. 56 (1992) 1756
92KR12 M. Kruglanski and D. Baye, Nucl. Phys. A548 (1992) 39
92KU02 S. Kubono, N. Ikeda, Y. Funatsu, M.H. Tanaka, T. Nomura, H. Orihara, S. Kato, M. Ohura, T. Kubo, N. Inabe et al, Nucl. Phys. A537 (1992) 153
92KU07 S. Kubono, N. Ikeda, Y. Funatsu, M.H. Tanaka, T. Nomura, H. Orihara, S. Kato, M. Ohura, T. Kubo, N. Inabe et al, Phys. Rev. C46 (1992) 361
92KUZO S. Kubono, Y. Funatsu, N. Ikeda, M.H. Tanaka, T. Nomura, H. Orihara, S. Kato, M. Ohura, T. Kubo, N. Inabe et al, RIKEN-91 (1992) 39
92KUZQ S. Kubono, Y. Funatsu, N. Ikeda, M.H. Tanaka, T. Nomura, H. Orihara, S. Kato, M. Ohura, T. Kubo, N. Inabe et al, RIKEN-91 (1992) 11
92LA01 C.M. Laymon, K.D. Brown and D.P. Balamuth, Phys. Rev. C45 (1992) R576
92MA29 A. Majhofer and Z. Szymanski, Acta. Phys. Pol. B23 (1992) 701
92ME09 A.C. Merchant and W.D.M. Rae, Phys. Rev. C46 (1992) 2096
92ME11 A.C. Merchant and W.D.M. Rae, Nucl. Phys. A549 (1992) 431
92MU01 M.G. Mustafa, M. Blann, A.V. Ignatyuk and S.M. Grimes, Phys. Rev. C45 (1992) 1078
92PI1O A. Piechaczek, M.F. Mohar, R. Anne, V. Borrel, J.M. Core, D. Guillemaud-Mueller, M. Ishihara, H. Keller, S. Kubono, V. Kunze et al, IOP Conf. Ser. 132, Proc. of the Sixth Int. Conf. on Nucl. Far From Stability and the Ninth Int. Conf. on At. Masses and Fundamental Constants, Bernkastel-Kues, Germany, 19-24 July, 1992 (1993) 851
92PY1A P. Pyykkö, Z. Naturforsch A47 (1992) 189
92QU02 R.M. Quick, B.J. Cole and H.G. Miller, Nuovo Cim. A105 (1992) 913
92RA21 MD.A. Rahman, S.C. Paul, H.M. Sen Gupta and M. Rahman, Nuovo Cim. A105 (1992) 851
92RA22 M.A. Rahman, M. Mecking and U. Strohbusch, Nuovo Cim. A105 (1992) 859
92RE1I P.L. Reeder, H.S. Miley, W.K. Hensley, R.A. Warner, H.L. Seifert, D.J. Vieira, J.M. Wouters and Z.Y. Zhou, IOP Conf. Ser. 132, Proc. of the Sixth Int. Conf. on Nucl. Far From Stability and the Ninth Int. Conf. on At. Masses and Fundamental Constants, Bernkastel-Kues, Germany, 19-24 July, 1992 (1993) 623
92RO06 R. Rossignoli, R.M. Quick and H.G. Miller, Phys. Lett. B277 (1992) 18
92RO08 P. Rochford and J.P. Draayer, Ann. Phys. 214 (1992) 341
92RO09 Romanov and Grechukhin, Z. Phys. D22 (1992) 667
92RO16 G. Rosensteel, Phys. Rev. C46 (1992) 1818
92SM03 M.S. Smith, P.V. Magnus, K.I. Hahn, A.J. Howard, P.D. Parker, A.E. Champagne and Z.Q. Mao, Nucl. Phys. A536 (1992) 333
92TA04 N. Tamimi, B.D. Anderson, A.R. Baldwin, T. Chittrakarn, M. Elaasar, R. Madey, D.M. Manley, M. Mostajabodda'vati, J.W. Watson, W.M. Zhang et al, Phys. Rev. C45 (1992) 1005

92WA04 T.F. Wang, R.N. Boyd, G.J. Mathews, M.L. Roberts, K.E. Sale, M.M. Farrell, M.S. Islam and G.W. Kolnicki, Nucl. Phys. A536 (1992) 159
92WA22 E.K. Warburton and B.A. Brown, Phys. Rev. C46 (1992) 923
92WI13 J.F. Wilkerson, T.M. Mooney, R.E. Fauber, T.B. Clegg, H.J. Karwowski, E.J. Ludwig and W.J. Thompson, Nucl. Phys. A549 (1992) 223
92WO1G J.M. Wouters, X.L. Tu, X.G. Zhou, D.J. Vieira, H.L. Sekfert, K.E.G. Löbner, Z.Y. Zhou, V.G. Lind and G.W. Butler, IOP Conf. Ser. 132, Proc. of the Sixth Int. Conf. on Nucl. Far From Stability and the Ninth Int. Conf. on At. Masses and Fundamental Constants, Bernkastel-Kues, Germany, 19-24 July, 1992 (1993) 25
92YU1A B.S. Yuldashev, M.A. Alimov, M.L. Allaberdin, Kh.Kh. Artykov, S.O.Edgorov, Sh.V. Inogamov, A.V. Khaneles, S.L. Lutpullaev, N. Rasulov, T.P. Rodionova et al, Phys. Rev. D46 (1992) 45
92ZA10 L. Zamick and D.C. Zheng, Phys. Rev. C46 (1992) 2106
93AB02 H. Abele and G. Staudt, Phys. Rev. C47 (1993) 742
93AI02 S. Ait-Tahar, R.S. Mackintosh and S.G. Cooper, Nucl. Phys. A561 (1993) 285
93AM08 A. Amusa, Phys. Rev. C48 (1993) 2302
93AOZZ Y. Aoki, M. Masaki, S. Nakagawa, Y. Tagishi, K. Kato and T. Nakamoto, Univ. T-sukuba, Tandem Accel. Center Ann. Rep. 1992 (1993) 29
93AU01 N. Auerbach, D.C. Zheng, L. Zamick and B.A. Brown, Phys. Lett. B304 (1993) 17
93AU05 G. Audi and A.H. Wapstra, Nucl. Phys. A565 (1993) 1
93BAZX N. Bateman, B. Lund, S. Utku and P. Parker, Bull. Amer. Phys. Soc. 38 (1993) 982
93BAZZ S. Barrow, R. Zurmuhle, J. Murgatroyd, N. Wilmer, K. Pohl, Y. Miao, R. Betts, B. Glagola, A. Wuosmaa and M. Freer, Bull. Amer. Phys. Soc. 38 (1993) 926
93BL10 B. Blank, C. Marchand, R. Del Moral, J.P. Dufour, L. Faux, A. Fleury and M.S. Pravikoff, Nucl. Instrum. Methods Phys. Res. A330 (1993) 83
93BO28 H.G. Bohlen, E. Stiliaris, B. Gebauer, W. von Oertzen, M. Wilpert, Th. Wilpert, A. Ostrowski, D.T. Khoa, A.S. Demyanova and A.A. Ogloblin, Z. Phys. A346 (1993) 189
93BR12 B.A. Brown, A.E. Champagne, H.T. Fortune and R. Sherr, Phys. Rev. C48 (1993) 1456
93BY03 A.V. Bystrenko and I.P. Okhrimenko, Phys. At. Nucl. 56 (1993) 601
93CH2C H.S. Cheng, H. Shen, J.Y. Tang and F. Yang, Nucl. Instrum. Methods Phys. Res. B83 (1993) 449
93CL1B N.M. Clarke, S. Roman, C.N. Pinder and P.R. Hayes, J. Phys. G19 (1993) 1411
93CS03 J. Cseh, J. Phys. G19 (1993) L63
93CSZU J. Cseh, ATOMKI Ann. Rep. 1992 (1993) 41
93DA1N K.M. Danielsen, T. Jacobsen, A. Haatuft, A. Halsteinslid, K. Myklebost, J.M. Olsen, F. Balestra, G. Bendiscioli, V. Filippini, A. Rotondi et al, Phys. Scr. 48 (1993) 653
93DA23 S.O.F. Dababneh, K. Toukan and I. Khubeis, Nucl. Instrum. Methods Phys. Res. B83 (1993) 319
93DE32 P. Descouvemont, Phys. Rev. C48 (1993) 2746
93EN03 P.M. Endt, At. Data Nucl. Data Tables 55 (1993) 171

93ES01 M.A. Eswaran, S. Kumar, E.T. Mirgule, D.R. Chakrabarty, V.M. Datar, N.L. Ragoowansi and U.K. Pal, Phys. Rev. C47 (1993) 1418

93ES03 M.A. Eswaran and S. Kumar, Phys. Rev. C48 (1993) 2120

93GA02 D.L. Gay and L.C. Dennis, Phys. Rev. C47 (1993) 329

93HA1D W.C. Haxton, Nucl. Phys. A553 (1993) C397

93HO14 M. Horoi and G. Clausnitzer, Phys. Rev. C48 (1993) R522

93HO1N M. Horoi and G. Clausnitzer, Building Blocks of Nuclear Structure, 4th Int. Spring Seminar on Nucl. Phys., Amalfi, Italy, 18-22 1992 (World Scientific, 1993) 143

93KH09 R.S. Khanchi, S.L. Bansal, S. Aggarwal, S. Khurana and R.K. Mohindra, Indian J.Pure Appl.Phys. 31 (1993) 371

93KU1F K. Kumar, Int. J. Mod. Phys. E2 Supp. (1993) 71

93LA24 G.H. Lang, C.W. Johnson, S.E. Koonin and W.E. Ormand, Phys. Rev. C48 (1993) 1518

93LE1J J.S. Levinger, Phys. At. Nucl. 56 (1993) 988

93LI25 Q.R. Li and Y.X. Yang, Nucl. Phys. A561 (1993) 181

93MI19 G.E. Mitchell, E.G. Bilpuch, C.R. Bybee, J.M. Drake and J.F. Shriner, Jr., Nucl. Phys. A560 (1993) 483

93MI25 G.E. Mitchell, E.G. Bilpuch, C.R. Bybee, J.M. Drake and J.F. Shriner, Jr., Nucl. Instrum. Methods Phys. Res. B79 (1993) 290

93MU1D M.M. Muminov, I. Suvanov and B.S. Yuldashev, Izv. Akad. Nauk Ser. Fiz. 57:4 (1993) 63; Bull. Acad. Russ. Sci. 57 (1993) 634

93NA08 S. Nakamura, K. Muto and T. Oda, Phys. Lett. B311 (1993) 15

93PA14 S.K. Patra, Nucl. Phys. A559 (1993) 173

93PA25 S.K. Patra and C.R. Praharaj, Nucl. Phys. A565 (1993) 442

93PE09 R.J. Peterson, Phys. Rev. C48 (1993) 1128

93PE18 A. Petrovici, K.W. Schmid and A. Faessler, Z. Phys. A347 (1993) 87

93PI1E S. Pittel and P. Federman, Int. J. Mod. Phys. E2 Supp. (1993) 3

93PLZY A.V. Plavko, M.S. Onegin, K. Olmer and P. Schwandt, Prog. & Thesis, Proc. 43rd Ann. Conf. Nucl. Spectrosc. Struct. At. Nucl., Dubna (1993) 206

93PO11 N.A.F.M. Poppelier, A.A. Wolters and P.W.M. Glaudemans, Z. Phys. A346 (1993) 11

93RA1G W.D.M. Rae and A.C. Merchant, Mod. Phys. Lett. A8 (1993) 2435

93REZX Reeder et al, Proc. 6th Int. Conf. Nuclei far from Stability + 9th Int. Conf. Atomic Masses and Fundamental Constants, Bernkastel-Kues, Germany, 19-24 July 1992 (1993) 623

93RO22 S. Roth, F. Grass, F. De Corte, L. Moens and K. Buchtela, J. Radioanal. Nucl. Chem. 169 (1993) 159

93RUZX J. Ruza, T. Guseva, J. Tambergs, O. Katkevicius and J.A. Castilho Alcaras, Program and Thesis, Proc. 43rd Ann. Conf. Nucl. Spectrosc. Struct. At. Nuclei, Dubna (1993) 43

93SA16 H. Sagawa, I. Hamamoto and M. Ishihara, Phys. Lett. B303 (1993) 215

93SA31 S. Sarangi and J.C. Parikh, Pramana J. Phys. 40 (1993) 43

93SO13 O. Sorlin, J. Phys. G19 (1993) S127

93SO19 V.I. Soroka, M.V. Artsimovich, I.Y. Lobach, I.F. Mogilnik, V.N. Pavlovich, V.V. Tokarevsky, E.M. Kudriavtsev and B.N. Romanjuk, Nucl. Instrum. Methods Phys. Res. B83 (1993) 311

93ST10 B. Strohmaier, Ann. Nucl. Energy 20 (1993) 533

93SZ02 A. Szanto de Toledo, E.M. Szanto, M. Wotfe, B.V. Carlson, R. Donangelo, W. Bohne, K. Grabish, H. Morgenstern and S. Proshitzki, Phys. Rev. Lett. 70 (1993) 2070

93TI07 D.R. Tilley, H.R. Weller and C.M. Cheves, Nucl. Phys. A564 (1993) 1

93VA07 K. Varga and J. Cseh, Phys. Rev. C48 (1993) 602

93VO01 P. Vogel and W.E. Ormand, Phys. Rev. C47 (1993) 623

93XU1A X. Xu, J. Guo, Z. Hu, X. Zhou, R. Ma, H. Liu, G. Li and Y. Du, High Energy Phys. Nucl. Phys. 17 (1993) 577

93YA08 Y.X. Yang and Q.R. Li, Europhys. Lett. 21 (1993) 657

93YA18 Y. Yamashita and Y. Kudo, Prog. Theor. Phys. 90 (1993) 1303

93ZA01 V.P. Zavarzina and A.V. Stepanov, Phys. At. Nucl. 56 (1993) 260; Yad. Fiz. 56 (1993) 206

93ZH18 Z. Zhu, Chin. J. Nucl. Phys. 14 (1993) 1

93ZH21 J. Zhang, A.C. Merchant and W.D.M. Rae, Phys. Rev. C48 (1993) 2117

93ZH22 J. Zhang and W.D.M. Rae, Nucl. Phys. A564 (1993) 252

94CA27 J.A. Caballero, T.W. Donnelly, G.I. Poulis, E. Garrido and E.M. Deguerra, Nucl. Phys. A577 (1994) 528

94CI02 O. Civitarese and M. Schvellinger, Phys. Rev. C49 (1994) 1976

94CO12 R. Coszach, Th. Delbar, W. Galster, P. Leleux, I. Licot, E. Lièнard, P. Lipnik, C. Michotte, A. Ninane, J. Vervier et al, Phys. Rev. C50 (1994) 1695

94DR01 J.M. Drake, E.G. Bilpuch, G.E. Mitchell and J.F. Shriner, Jr., Phys. Rev. C49 (1994) 411

94DU09 M. Dufour, P. Descouvemont and D. Baye, Phys. Rev. C50 (1994) 795

94FU01 B.R. Fulton, S.J. Bennett, J.T. Murgatroyd, N.S. Jarvis, D.L. Watson, W.D.M. Rae, Y. Chan, D. DiGregorio, J. Scarpaci, J. Suro Perez et al, J. Phys. G20 (1994) 151

94GO16 J. Görres, J. Meissner, J.G. Ross, K.W. Scheller, S. Vouzoukas, M. Wiescher and D. Hinnefeld, Phys. Rev. C50 (1994) R1270

94HA39 I. Hamamoto, Nucl. Phys. A577 (1994) 19

94HE1A D.M. Headly, R.K. Sheline and I. Ragnarsson, Phys. Rev. C49 (1994) 222

94KU18 S. Kumar, M.A. Eswaran, E.T. Mirgule, D.R. Chakrabarty, V.M. Datar, N.L. Ragoowansi, U.K. Pal and H.H. Oza, Phys. Rev. C50 (1994) 1535

94ME18 A.C. Merchant and W.D.M. Rae, Z. Phys. A349 (1994) 243

94MI05 H.G. Miller, R.M. Quick, R.R. Rossignoli and G.D. Yen, Nucl. Phys. A570 (1994) C217

94OR02 W.E. Ormand, Nucl. Phys. A569 (1994) 63C

94OS05 A. Osman and A.A. Farra, Can. J. Phys. 72 (1994) 175; Erratum, Can. J. Phys. 72 (1994) 686
94PA42 R.D. Page, G. Vancraeynest, A.C. Shotter, M. Huyse, C.R. Bain, F. Binon, R. Coszach, T. Davinson, P. Decrock, T. Delbar et al, Phys. Rev. Lett. 73 (1994) 3066
94RA03 W.D.M. Rae, A.C. Merchant and J. Zhang, Phys. Lett. B321 (1994) 1
94RA04 W.D.M. Rae, S.C. Allcock and J. Zhang, Nucl. Phys. A568 (1994) 271
94SH35 H. Shen, H. Cheng, J. Tang and F. Yang, Nucl. Instrum. Methods Phys. Res. B90 (1994) 593
94TO04 A. Tohsaki, Phys. Rev. C49 (1994) 1814
94VE04 J. Vernotte, G. Berrier-Ronsin, J. Kalifa, R. Tamisier and B.H. Wildenthal, Nucl. Phys. A571 (1994) 1
94ZH03 J.-K. Zhang and D.S. Onley, Phys. Rev. C49 (1994) 762
94ZU1B R.W. Zurmühle, Z. Liu, D.R. Benton, S. Barrow, N. Wimer, Y. Miao, C. Lee, J.T. Murgatroyd, X. Li, V.Z. Goldberg et al, Phys. Rev. C49 (1994) 2549
95BU01 M. Burlein, H.T. Fortune, W.M. Amos, T.L. Ekenberg, A. Kotwal, P.H. Kutt, J.M. O'Donnell, J.D. Silk, B. Boyer, A. Fuentes et al, Phys. Rev. C51 (1995) 88
95IG1A A.V. Ignatenko, V.M. Lebedev, N.V. Orlova and A.V. Spasskii, Yad. Fiz. 58 (1995) 208; Phys. At. Nucl. 58 (1995) 166
95KA1F Y. Kanadaenyo and H. Horiuchi, Prog. Theor. Phys. 93 (1995) 115
95KU1H R. Kunz, A. Denker, H.W. Drotleff, M. Grosse, H. Knee, S. Kuchler, R. Seidel, M. Soine, J.W. Hammer, Proc. SPIE - Int. Soc. Opt. Eng. 2339 (1995) 38
95MA1A Z.Q. Mao, H.T. Fortune and A.G. Lacaze, Phys. Rev. Lett. 74 (1995) 3760
95MI1B F. Michel, G. Reidemeister and Y. Kondo, Phys. Rev. C51 (1995) 3290
95PI03 A. Piechaczek, M.F. Mohar, R. Anne, V. Borrel, B.A. Brown, J.M. Corre, D. Guillemaud-Mueller, R. Hue, H. Keller, S. Kubono et al, Nucl. Phys. A584 (1995) 509
95SU06 T. Sugimitsu, N. Hori, H. Fujita, Y. Funatsu, N. Kato, K. Kimura, M. Matsuo, S. Mitsuoka, T. Mukae, S. Niiya et al, Nucl. Phys. A586 (1995) 190
95TI1C D.R. Tilley, H.R. Weller, C.M. Cheves and R.M. Chasteler, Nucl. Phys. A595 (1995) 1
96RA04 S.Raman, E.K.Warburton, J.W.Starner, E.T.Jurney, J.E.Lynn, P.Tikkanen and J.Keinonen, Phys. Rev. C53 (1996) 616